PNNL-SA-64785

Prepared for the U.S. Department of Energy
under Contract DE-AC05-76RL01830

Multi-Scale Mass Transfer Processes Controlling Natural Attenuation and Engineered Remediation: An IFRC Focused on Hanford's 300 Area Uranium Plume

January 2008 to January 2009

Annual Report to the
DOE Office of Science, Environmental Remediation Sciences Division

Principal Investigator:
John Zachara, PNNL

Co-Principal Investigators:
Bruce Bjornstad, PNNL
John Christensen, LBNL
Mark Conrad, LBNL
Jim Fredrickson, PNNL
Mark Freshley, PNNL
Roy Haggerty, OSU
Glenn Hammond, PNNL
Doug Kent, USGS
Allan Konopka, PNNL
Peter Lichtner, LANL
Chongxuan Liu, PNNL
Jim McKinley, PNNL
Mark Rockhold, PNNL
Yoram Rubin, U of CA, Berkeley
Vince Vermeul, PNNL
Roelof Versteeg, INL
Andy Ward, PNNL
Chunmiao Zheng, U of AL

DISCLAIMER

PACIFIC NORTHWEST NATIONAL LABORATORY
operated by
BATTELLE
for the
UNITED STATES DEPARTMENT OF ENERGY
under Contract DE-AC05-76RL01830

Multi-Scale Mass Transfer Processes Controlling Natural Attenuation and Engineered Remediation: An IFRC Focused on Hanford's 300 Area Uranium Plume

January 2008 to January 2009

Annual Report to the
DOE Office of Science, Environmental Remediation Sciences Division

J.M. Zachara, Principal Investigator

February 2009

Chemical & Materials Sciences Division
Fundamental & Computational Sciences Directorate
Pacific Northwest National Laboratory

Prepared for
the U.S. Department of Energy
under Contract DE AC05 76RL01830

Pacific Northwest National Laboratory
Richland, Washington 99352

Multi-Scale Mass Transfer Processes Controlling Natural Attenuation and Engineered Remediation: An IFRC Focused on Hanford's 300 Area Uranium Plume

Annual Report: January 2008 – January 2009

Principal Investigator:
John Zachara, Pacific Northwest National Laboratory (PNNL) is IFRC Principal Investigator and primary contact with ERSD.

Field Site Manager:
Mark Freshley, PNNL, is field site manager and primary EM contact.

PNNL Co-Principal Investigators and Major Task (FY-08 Funding):
Here we provide a financial synopsis for the Hanford IFRC for FY 08. The synopsis is organized according to reporting categories in the quarterly and annual reports.

FY08 IFRC Financial Summary

FY08 Project Funding:	$	3,500,000
Carryover from FY07:	$	1,291,496
Total FY08 Funding:	$	4,791,496
FY08 Spent:	$	3,936,169
Carryover to FY09:	$	855,327 [9]

Project Management - $ 290,377[1]
John Zachara – ($228,544)[2] - IFRC project manager and lead scientist. Responsible for project success, reporting, financial management, productivity, and scientific accomplishment. Lead on all geochemical issues.
Mark Freshley – ($61,833)[2] - Responsible for well and tracer permitting, field test plan preparations, site operations, sample dispersement, and QA/QC planning and review.
Site Design and Installation - $ 1,844,302[1,3,4]
Vince Vermeul – ($29,032)[2] - Directed all field hydrologic characterization measurements including the electromagnetic borehole flowmeter surveys and constant rate injection tests.
Bruce Bjornstad – ($60,905)[2] - Hanford IFRC site geologist who established plans and specifications for the well-field. Interface between the Hanford IFRC and the Flour-Hanford well drilling team.
Data Management - $ 194,655[1,5]
Field Site Characterization - $ 635,601[1,4,5,10]

Andy Ward – ($259,225)[2,6] - Worked with R. Versteeg (INL) to design, install, and test the geophysical monitoring system for the IFRC well-field. Now directing field geophysical characterization of the site, and the modeling and interpretation of resulting data.
Bruce Bjornstad – ($103,472)[2] - Interpreted all well logs and is developing a site geologic facies model, and comprehensive well completion report that summarizes all measurements and data collected during the well installation campaign.
Jim McKinley – ($112,957)[2,6] - Oversight of sediment and groundwater sampling, and geochemical characterization analyses of all type.
Saturated Zone Experimental Programs - $ 208,242[1]
Vince Vermeul – ($124,812)[2,6] - Oversight and management of all field hydrologic activities and monitoring systems, infrastructure, and injection experiments. Installed and tested groundwater monitoring systems in FY 08 for November 2008 tracer experiment.
Jim McKinley – ($57,618)[2] - Design and oversight of all groundwater geochemical measurements, and monitoring of passive site behavior for characterization and hypothesis evaluation.
Modeling and Interpretation Programs - $ 762,992[1,8]
Mark Rockhold – ($125,760)[2] - Coordinator of the IFRC modeling team. Responsible for data integration and transfer to others, development of the modeling plan, and for modeling the hydrologic characterization data and results of the first tracer experiment.

1. total dollars spent
2. dollars spent by individual and close associates
3. includes Fluor Drilling subcontract
4. includes significant procurements and bargaining unit charges
5. includes Versteeg – INL subcontract
6. includes junior scientist labor
7. includes injection team members
8. includes external subcontracts to UCB, USGS, OSO, UA, LANL and LBNL (see below)
9. carryover to support Nov 2008 and March 2009 tracer experiments
10. includes Golder Associates (Borehole logging) and Univ of Kansas(300 area seismic feasibility test)

FY08 IFRC Procurements

Vendor	Description	TRANS_AMT	BRDN_AMT
B&B Enterprises	IFC Trailer for Field Equip	2,960	3,532
Campbell Scientific, Inc.	IFC Equipment Order	19,518	23,292
Campbell Scientific, Inc.	Purchase-Campbell Scientific	5,799	6,920
Cole-Parmer Instrument Company	IFC Calibration Standards	1,239	1,478
Envirochem Technology Services	Sodium Bromide & Ammonium	2,130	2,542
Instrumentation Northwest, Inc.	CR1000 Datalogger Instructions	1,000	1,193
Instrumentation Northwest, Inc.	Custom Control Panel-Inst NW	13,417	16,012
Instrumentation Northwest, Inc.	Dedicator Pumps - Instrmnt NW	74,343	88,721
Instrumentation Northwest, Inc.	FC Injection monitoring equip	30,793	36,748
Multi-Phase Technologies, LLC	Cable, electrodes, PU Jacket - Field Tests of the ERT system	56,700	67,665
Multi-Phase Technologies, LLC	General Lab Supplies	5,940	7,089
U.S. Sensor Corporation	Supplies including 80ft lead in cable	18,179	21,694
	TOTAL	232,017	276,887

External Co-Principal Investigators and Subcontracts (FY 08 Funding):
[Note dollars spent in FY 08 are summarized by Table immediately following this listing.]

Fluor Hanford was responsible for well installation, sampling, and completion services, and for subcontracting with Stoller for down-hole neutron moisture and spectral gamma logging.

John Christensen and Mark Conrad, Lawrence Berkeley National Laboratory (LBNL) (No FY08 Activity) are responsible for isotopic geochemical research and analyses. Their subcontract will begin in FY 09 as originally planned.

Yoram Rubin, University of California Berkeley (UCB) is responsible for stochastic hydrology research; including conditional simulations of field experiments and developing geostatistical models of the IFRC field site through data integration and inversion.

Roy Haggerty, Oregon State University (OSU) is responsible for research in mass transfer process characterization and modeling.

Douglas Kent, US Geological Survey (USGS) is responsible for the development of a field scale surface complexation model of U(VI) adsorption/desorption and associated reaction parameters and properties dependencies.

Peter Lichtner, Los Alamos National Laboratory (LANL) is responsible for geochemical modeling of uranium reactive transport processes with the FLOTRAN code, and for collaborations with UCB on large scale data inversions of transport and reaction parameters using PFLOTRAN and other SciDAC capabilities.

Roelof Versteeg, Idaho National Laboratory (INL) is responsible for geophysical research/monitoring in collaboration with Andy Ward, and the IFRC data management program.

Chunmiao Zheng, University of Alabama (UA) is responsible for mass transfer, reactive transport, and hydrologic modeling using the MT3DMS, PHT3D, MODFLOW suite of codes.

FY08 IFRC Subcontracts

Vendor	Description	TRANS_AMT	BRDN_AMT
Oregon State University	Roy Haggerty	154,000	169,440
Los Alamos National Laboratory	Peter Lichtner	99,844	99,844
US Geological Survey - LA	Doug Kent	100,000	110,026
University of California Berkeley	Rubin Newton	125,000	137,533
University of Alabama	Chunmiao Zheng	100,000	110,026
Battelle Energy Alliance, LLC (BEA)	AW - Roelof Versteeg	51,527	51,527
Battelle Energy Alliance, LLC (BEA)	JZ - Roelof Versteeg	188,953	188,953
Fluor Hanford	300 Area IFC Field Service Sup	4,733	4,733
Fluor Hanford	IFC Well Drilling Supplement	1,417,027	1,417,027
Fluor Hanford	RMIS (IDMS) Users Database	69	69
Univeristy of Kansas	Shallow Seismic Feasibility Test	14,256	17,013
Golder Associates, Inc. - GA	Borehole Logging Services	37,369	44,596
Hertz Equipment Rental Corporation	Generator Rental for IFC Work	774	924
Instrumentation Northwest, Inc.	Custom Control Panel (Control Box)	5,530	6,599
Multi-Phase Technologies, LLC	Perform Field Tests of the ERT system	1,000	1,193
Washington Closure Hanford, LLC	Sub to WHC for Power Drop	13,095	13,095
Williams Scotsman, Inc.	Conex Rental	724	864
Williams Scotsman, Inc.	Office Trailer	1,438	1,716
	TOTAL	2,315,339	2,375,179

Key Collaborations:

Harvey Bolton, John Zachara, Jim Fredrickson, Tim Scheibe, Chongxuan Liu, Alan Konopka (PNNL) and other PNNL, national laboratory and university principle investigators collaborate through the PNNL SFA focused on Hanford-inspired subsurface science issues and role of microenvironments and transition zones on contaminant migration. Using IFRC site sediments, SFA investigators are: quantifying and modeling key microscopic reaction and transport processes (adsorption/desorption, precipitation/dissolution, mass transfer), measuring sediment properties required for robust geophysical interpretation (K-U-T isotopic content of different size fraction, and electrical and thermal properties), and characterizing microbiological distributions and function. The SFA team is also developing pore-scale biogeochemical reaction models of IFRC site sediments, and planning in-situ microcosm experiments in IFRC site wells. SFA research is consequently providing significant microscopic basis for IFRC site reactive transport models, and geophysical characterization approaches.

John Fruchter, Dawn Wellman, and Vince Vermeul (PNNL) collaborate through the EM-20 Polyphosphate Demonstration Project, which performed one injection experiment in the saturated zone. The results of the injection test indicated that remediation of the uranium plume via autunite precipitation was unlikely to be feasible at the necessary scale. The current focus of the EM-20 effort has been to conduct a laboratory testing to evaluate infiltration of polyphosphate to remediate uranium in the vadose zone and capillary fringe.

John Fruchter, Dawn Wellman, and Vince Vermeul (PNNL) and Jane Borghese [CH2M Hill Plateau Remediation Contract (CHPRC)] collaborate through the DOE-Richland Operations Office-funded 300-FF-5 CERCLA project. This project has assumed responsibility for the field-scale infiltration test of the polyphosphate remediation technology at a site near the footprint of the North Process Pond adjacent to the location where the saturated zone injection polyphosphate injection test was conducted.

John Christensen and Mark Conrad (LBNL) collaborate on isotopic measurements of uranium in the 300 Area and other locations on the Hanford Site with ERSP funding to assist in source term delineation and flux quantification between environmental compartments (e.g. sediment/water, groundwater/river). Funding was provided in FY 2009 to assist with selection of a source of water for injection experiments with the same isotopic composition as the IFRC well field.

Haluk Beyenal (Washington State University) and Jim Fredrickson (PNNL) collaborate on the study of redox-controlling microorganisms in the 300 A unconfined aquifer. During CY 09 this team will inoculate flow cells and microcosms with in-situ microorganisms by pumping IFRC site groundwater through these cells in the field, in an attempt to initiate biofilm formation. The mature of the biofilms will be characterized by various microscopic methods and their influence on mineral and water biogeochemistry investigated.

Lee Slater (Rutgers University), Roelof Versteeg (INL), Andy Ward (PNNL), Fred Day-Lewis, and John Lane (USGS), and Andrew Binley (Lancaster University, UK) collaborate on geophysical characterization and monitoring strategies for quantifying hydrologic transport processes in the hyporheic zone at the 300 Area with ERSP funding. This team established a temperature monitoring network along the Columbia River shoreline immediately east and downgradient of the IFRC site in CY 08. The network will allow flux measurements of groundwater to the river useful to the calibration of IFRC transport models.

ABSTRACT

The Integrated Field-Scale Subsurface Research Challenge (IFRC) at the Hanford Site 300 Area uranium (U) plume addresses multi-scale mass transfer processes in a complex hydrogeologic setting. A series of forefront science questions on mass transfer are posed for research which relate to the effect of spatial heterogeneities; the importance of scale; coupled interactions between biogeochemical, hydrologic, and mass transfer processes; and measurements/approaches needed to characterize and model a mass-transfer dominated system. The project was initiated in February 2007, and CY 2007 progress was summarized in last year's annual report.

CY 2008 has been a very productive year for the Hanford IFRC and this progress is summarized in the pages that follow. The first half of CY 2008 was devoted to design completion and installation of our saturated zone experimental site within the footprint of the South Process Pond. The design phase of site installation resulted in two planning documents that described sampling protocols and approaches, and well completion criteria and specifications that were posted on the web-site. The site was installed between May and August and included a deeper borehole for microbiologic characterization that sampled the entire thickness of the unconfined 300 A aquifer. Each well bore was logged with 5 different geophysical measures, yielding a 35-well experimental site and over 1000 sediment samples for characterization and subsequent research. All wells except the deep microbiology borehole (that was completed as a biogeochemistry study site) were completed with a robust monitoring system containing downhole thermistors, electrical resistance tomography electrodes, ion selective electrodes, and dedicated pumps. Select wells along the site periphery were also instrumented with pressure transducers for continuous head monitoring. A computerized data collection, logging, and storage system has been installed at the site. An extensive well completion report has been completed and posted on the web-site.

The second half of CY 2008 was dedicated to field characterization of the IFRC site, and laboratory characterization of samples collected during the site drilling campaign. A site characterization plan was written to guide this activity that was posted on the web. An extensive hydrologic testing campaign was completed that included electromagnetic borehole flowmeter surveys of all wells, constant rate injection tests in 14 wells, and a large non-reactive tracer injection experiment of 160,000 gallons in November 2008. The results display and quantify the hydrologic complexity of the site, but also define the presence of variable hydraulic conductivity zones condusive to the evaluation of our mass transfer scientific theme. A site geophysical survey employing cross-hole electrical resistance tomography using our downhole electrode arrays is nearing completion that will provide information on sediment properties and structures over the 10 m distances between wells. A large series of laboratory characterization measurements is well underway on grab and core samples from the site to define physical, chemical, and electrical/geophysical properties as necessary to construct a 3-D geostatistical model of the IFRC experimental domain.

The project modeling team has united around a series of defined responsibilities leading to the initial development of a robost hydrologic site hydrogeologic model that can be expanded to include mass transfer, geochemical and biogeochemical processes, and site-wide properties distributions as documented. Studies of uranium adsorption/desorption and mass transfer have been initiated with contaminated sediments from the site to parameterize process-specific modules for field-scale application. Collaborative modeling activities are underway that exploit attributes of the different project codes for experiment premodeling and design, and experiment interpretation. The project moves into CY 2009 with ambitious plans for a series of well-planned saturated zone field experiments.

PROJECT STATUS: A FIVE-YEAR PERSPECTIVE

Project funding was received in February 2007. Efforts during the first year (described in last years annual report) primarily involved assembling the project team; designing the field site and associated monitoring and injection systems; planning the experimental, modeling, and interpretational activities; creating management systems (documents and data) and controlling documents for the project; and obtaining permits for injection wells and proposed experiments.

Year two (CY 2008) has been a most productive year for the Hanford IFRC with the following identified as major accomplishments:

1.) The Hanford IFRC saturated zone experimental site and integrated monitoring system was installed. This included the wiring and testing of over 1400 thermistors and ERT electrodes installed in wells of the site.
2.) Over 1000 sediment samples from the vadose zone and saturated zone were collected during well installation. The boreholes and completed wells were logged with five different downhole geophysical measurement techniques.
3.) A separate deep borehole spanning the entire unconfined aquifer at this location in the 300 A was installed next to the IFRC site for microbiologic characterization. High quality intact core samples were provided to PNNL's Scientific Focus Area researchers for microbiological studies. Intriguing and interesting results are emerging.
4.) A hydrologic and geochemical characterization plan detailing both laboratory and field measurements was completed for the IFRC experimental site that is now being followed.
5.) Laboratory measurements of physical and geochemical properties has begun on 200 sediment subsamples collected from the well field boreholes. These measurements will support a geostatistical model of sediment properties in the experimental site.
6.) Field hydrologic characterization of the IFRC site, that culminated in a large non-reactive tracer experiment, was completed. Many important new insights were obtained on the site hydrology, including a significant decrease in the estimated groundwater flow velocity from 50'/day to ~10'/day.
7.) Groundwaters from all 35 wells have been sampled and analyzed three times providing the beginnings of a seasonal water quality data base for the experimental site.
8.) Field geophysical characterization of the IFRC experimental domain is actively underway using both surface and cross-hole geophysical techniques.
9.) Our five-member modeling team is actively engaged in a.) premodeling proposed experiments for design optimization, b.) devising effective and robust means for integrating and inverting large IFRC characterization data sets for parameterization and stoichastic analyses, c.) developing field-scale descriptors of geochemical reaction and mass transfer properties and parameters, and d.) interpreting our field experiments that involve complex groundwater-river coupling.
10.) Planning is well underway for our spring experimental campaign that will include a multiple non-reactive tracer injection experiment with chilled groundwater to assess groundwater flow heterogeneity, and a passive experiment to monitor groundwater compositional changes in the IFRC well field that accompany the spring high water river stage and intrusion of low ionic strength river water.

There have been no significant changes to the project scope or objectives during calendar year 2008. However, we have decided to postpone all development of the vadose zone infiltration site until after the Hanford IFRC mid-term peer review in CY 2010. Our 5-year timeline in **Figure 1** has been revised to reflect that decision, and to better coordinate with the task structure adopted for our quarterly reports. Most research dollars in FY09 and early FY10 will be used for subsurface characterization, the saturated zone experimental program, and associated modeling. Our goal is to make a strong and mature scientific contribution from the saturated zone site before moving to the vadose zone. The vadose zone is not necessarily being ignored. Vadose zone samples are being included in the laboratory characterization program (e.g., **Figures 13 and 14**), and U fluxes from the lower vadose zone to groundwater during periods of high river stage and high water table (the primary hypothesized pathway for U recharge to groundwater) will be investigated during a passive saturated zone experiment planned for the spring of CY 2009 as described later in this report.

As a new development, the Hanford IFRC has been establishing strong collaborations with PNNL's Scientific Focus Area (SFA) research team that began new research in FY 09. A summary of SFA research can be found at pnl.gov/biology/sfa. SFA research is addressing the characterization and biogeochemical study of subsurface microenvironments and transition zones, and has a strong emphasis on microscopic reaction and transport processes, and their modeling. They following SFA activities are being performed in collaboration with the Hanford IFRC: i.) uranium reactive transport laboratory experiments and modeling using intact sediment cores from the IFRC saturated zone; ii.) installation of down-well microcosms, coupons, and flux meters to investigate in-situ biogeochemical processes in the IFRC well-field, and iii.) development of pore scale reactive transport models including surface complexation and mass transfer for microscopic to megascopic scaling studies at the IFRC.

Hypothesis/Experiment Year	FY 2007 Year 1				FY 2008 Year 2				FY 2009 Year 3				FY 2010 Year 4				FY2011 Year 5			
Quarter	1	2	3	4	1	2	3	4	1	2	3	4	1	2	3	4	1	2	3	4
Establish Field Site																				
Select site, establish field plot, define drilling specifications																				
Well drilling and saturated site completion																				
Plan for vadose zone site																				
Vadose zone site installation																				
Characterization																				
Characterization plan																				
Field hydrology																				
Groundwater composition																				
Field geophysics																				
Laboratory phys./chem. measurements																				
Saturated Zone Experiments																				
Experimental plan																				
Multitracer/cold water																				
Desorption injection																				
Adsorption injection																				
Passive rising/falling WT																				
Isotopic exchange																				
In-situ microbiologic activity																				
Vadose Zone Experiments																				
Experimental plan																				
Experiment 1																				
Experiment 2																				
Data Management																				
Modeling and Interpretation																				
Updated hydrogeologic model																				
Site geostatistical model																				
Geochemical model																				
Multi-scale mass transfer																				
Conditional simulations																				
Integrated process model																				
Management Activities																				
NEPA documentation & permitting																				
Project documents																				
Project management																				
Reporting																				
	Completed								**In progress**							**Not started**				

Figure 1. 5-Year schedule from proposal (updated 2/9/09).

MAJOR ACCOMPLISHMENTS: LAST 12 MONTHS

For this annual report we describe progress for: Site Design and Installation, Web Site and Data Management, Field Site Characterization, Vadose Zone Experiments, Saturated Zone Experiments, Modeling and Interpretation, and Project Management.

Site Design and Installation

Our site well installation campaign was completed at the end of August 2008. Many pictures from this campaign have been posted on the IFRC web-site. Another 3.5 months (until December 21) were required to finish wiring and testing of the downhole monitoring system of thermistors and electrical resistance tomography electrodes, and completion of monitoring systems for specific conductivity and head along the well-field periphery. These activities have yielded a world-class experimental facility for the dynamic and challenging hydrologic conditions that exist for our linked groundwater-river system. It is a showcase field facility for BER/ERSD that will yield important new fundamental insights on mass transfer, coupled hydrologic-biogeochemical processes, and groundwater microbiology. The well drilling, borehole/core sampling, and associated geophysical logging activities required careful scheduling and logistical control to minimize budget overruns while allowing measurements and materials collection for maximum future scientific payoff. These goals were accomplished without injury or safety issue of any type. The site is well documented on the Hanford IFRC web-site, clearly marked in the field with distinctive signage, and key components of its infrastructure have been tested with outstanding performance. The site is populated with a trailer for meetings and chemical analysis, a smaller trailer housing the well-field manifold system for automated well-water sampling, a small trailer with geophysical data loggers and analogue recorders of different type, and two conex boxes for equipment and sample storage.

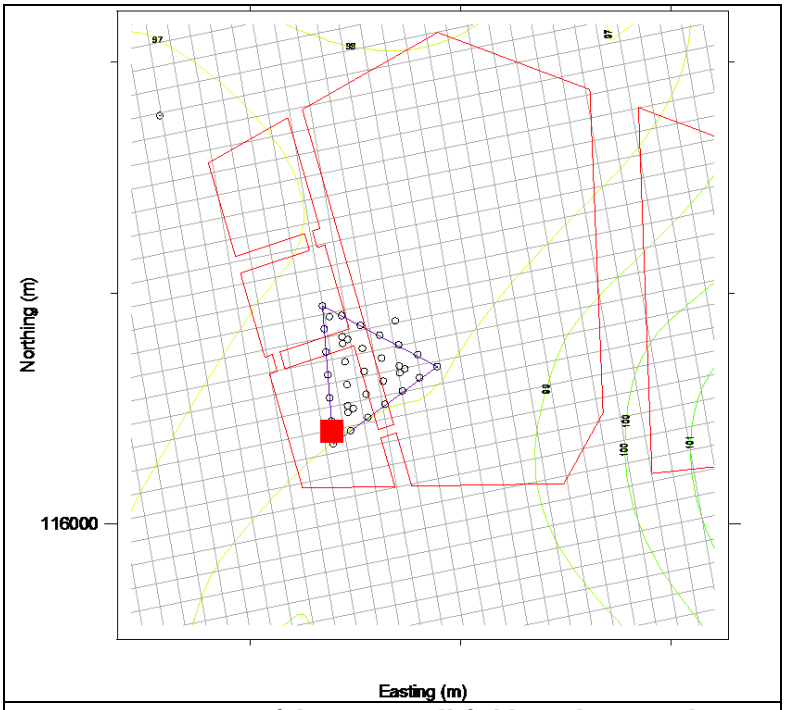

Figure 2. Location of the IFRC well field in relation to the former South Process Pond (red outline). Grid spacing is 10 m. Red square is approximate location of backhoe pit SPP#2 excavated at the base of the remediated South Process Pond in April, 2003. SPP#2 materials have been featured in numerous ERSD publications.

A draft report has been completed that documents the drilling, sampling and construction of the 35 new wells installed within the IFRC footprint (**Figure 2**). During the drilling campaign, undertaken in the summer of 2008, a total of 2,318 feet of hole was drilled and over 1,100 geologic samples were collected that are described in an inventory file on the IFRC web-site. The summary report titled “Borehole Completion and Hydrogeology of the 300-Area IFRC (Integrated Field Research Challenge) Well Field, Hanford Site” is authored

by PNNL scientists B.N. Bjornstad, J.A. Horner, D.C. Lanigan, and P.D. Thorne and is planned for release in early February, 2009. Within the document is also a discussion and summary of the field-geologic characteristics and conceptual hydrogeologic model of the site. In appendices at the end of the report will be copies of all the raw data including:

- Well-Site Geologist Logs
- Sample Inventory Sheets
- Field-Activity Reports
- Well-Development and Testing Data Sheets
- Well-Summary Sheets
- Downhole Geophysical Logs
- Survey Reports
- Chip-Tray Photographs

An integration of all these data are summarized into a Compilation Borehole Summary Log for each of the 35 new wells (**Figure 3**). These shall be presented in a separate appendix. On this one-page log is all the pertinent hydrogeologic, sampling, geophysical, and well-construction information gathered in the field for each well. Summarizing all the data in this way will aid in the comparison and interpretation of subsequent geologic, hydrologic, geochemical, and microbiological analyses.

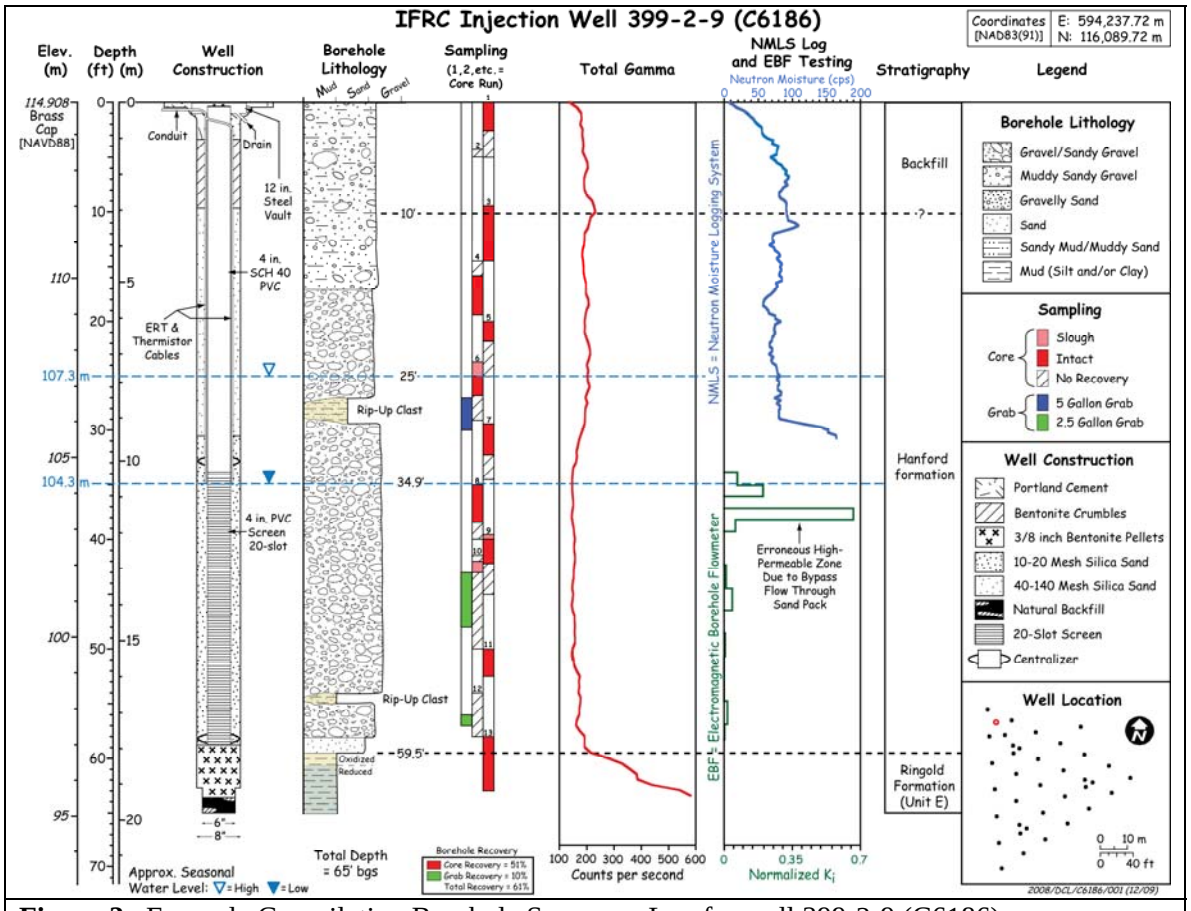

Figure 3. Example Compilation Borehole Summary Log for well 399-2-9 (C6186).

In February 2008, 27 of the IFRC wells were registered with the Washington State Department of Ecology as Class V Underground Injection Control (UIC) Wells as part of our well-permitting activity. All of the wells, except the three-well clusters, were registered as potential injection wells to allow flexibility in planning and implementing field experiments given the complexities of river stage effects. We are currently in the process of updating the UIC registration to include the cluster wells to increase flexibility for future experiments, including direct injection or push-pull experiments over select depth intervals.

Data Management and Data Base

The Hanford IFRC website (http://ifchanford.pnl.gov/) is operational and contains comprehensive background information about the 300 A uranium plume; information on project participants; background and project scientific publications; IFRC documents including required project documents and the field site characterization plan; field site design, drilling specifications, and completion reports; pictures of the field site installation and inventories of samples available to project participants and ERSD investigators. Experimental and modeling plans; and schedules, objectives, and descriptions of planned field campaigns are forthcoming. A password protected link for project participants and ERSD management to the IFRC data base at INL has been activated.

Over the past year the design for the web accessible database for the IFRC was completed. The database has been populated with the currently available data from the IFRC (well data, sample data, geological and geophysical logs), and new measurments and results are being added to the database as it becomes available. Data models are being implemented for new types of data [for instance, experimental data associated with on-going reactive U(VI) transport experiments with intact cores from the well-field], and tools are being put in place to allow for researchers to quickly locate, access and visualize data from all project participants. All data is stored in a MySQL database, with the frontend being implemented through a mix of PHP and Javascript. Visual data access uses the Google Maps Api.

In CY 2009 activities will focus on the integration of modeling results from different IFRC project participants in the website. Currently, modeling results are available through canned animations (mpg or avi). In the next year we will import all the modeling results into a standard format so that end user can access different snapshots, representations and cross sections of modeling results. Such capabilities are essential for both effective field experimental designs as modeling is a critical element of this, and for interpretation and scientific hypothesis evaluation. Additional efforts will be devoted to importing all geological log data from the well installations into industry standard format. Currently, the well logs are only available as electronic scans of the well site logs, limiting their usefulness. All logs will be imported into a standard AGS format, which will provide the ability to make cross sections and perform statistical analysis on the tools. Lastly, the data management team will interact with project participants to identify and provide a useful compliment of analytical and visualization tools for data access and manipulation.

Field Site Characterization

A Hydrologic and Geochemical Characterization Plan for the Hanford IFRC experimental site was drafted and posted to the Hanford IFRC web-site (*Hydrologic and Geochemical Characterization Plan for the Hanford IFRC Well-Field*). Characterization is actively proceeding according to the strategy and methodology of the report.

A. Hydrologic Characterization

The first major phase of the IFRC hydrologic testing program was completed in December 2008. Its objectives were to characterize the field-scale hydraulic and conservative transport properties for the site, and provide a measure of the spatial variability in these properties. Information obtained from these initial characterization activities will be used to plan for and design subsequent field-scale reactive tracer and uranium mass transfer experiments. Hydrologic characterization activities completed to date include 1) electromagnetic borehole flowmeter (EBF) profiling in each fully screened monitoring well within the well field, 2) constant-rate injection tests in 14 fully screened monitoring wells distributed throughout the well field, and 3) a conservative tracer injection and drift experiment.

During the first EBF profiling campaign, measurements were collected at ~30 to 60 cm (1 to 2 ft) depth increments throughout each test interval under both ambient and dynamic flow (i.e., pumping) conditions. **Figure 4** provides an example effective hydraulic conductivity (K_{eff}) plot that can be derived from the EBF profile results (see **Appendix 1** for remaining measurements). These data, in conjunction with depth averaged K results from the constant rate injection tests (**Figure 5**), will be used to develop a vertically discrete K distribution at each well location. These distributions, in turn, will be one of a number of primary data sets that will be integrated into the IFRC site geostatistical model by Murray, Rubin, and others. Collectively, that EBF data from all wells indicate the hydraulic conductivity in the central third of the saturated zone is significantly lower than the top and bottom thirds. This observation was consistently observed in over 75% of the wells.

A second EBF campaign is now underway to better characterize the temporal variability in ambient vertical flows for IFRC site monitoring wells, and determine whether these observed flows can be correlated with river stage fluctuations. These measurements involve the installation of the flowmeter at a given well location and depth, and the monitoring of flow continuously over a multi-day time period.

Constant-rate injection tests were conducted to measure depth averaged hydraulic properties at 14 fully screened well locations distributed throughout the well field (**Figure 5**). Test analyses were focused on early-time pressure response in the closest available monitoring wells, which provides for the most representative estimates of formational properties in the vicinity of the stress well. In addition to later-time data and more distal monitoring well locations being impacted by a larger radial extent of the permeability field, these data also have a larger potential for being impacted by boundary effects (e.g., the river, supply well discharge, distal changes in formation permeability), and are more likely to be impacted by water-level change associated with variability in Columbia River stage.

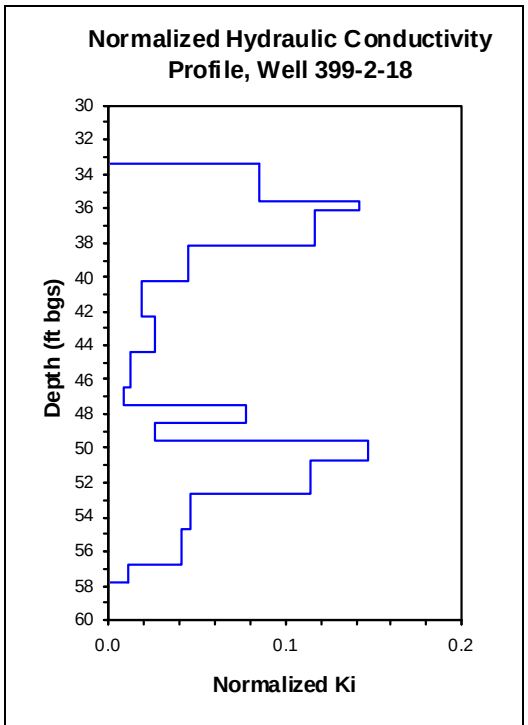

Figure 4. Effective hydraulic conductivity with depth at monitoring well 399-2-18. Similar profiles were collected for all other wells. See **Appendix 2**.

Groundwater was pumped from a distal location (well 399-3-20) and injected into each individual test well at a constant rate of ~ 315 gpm. The test duration required to reach radial flow conditions was determined based on diagnostic plots of pressure response data from an initial longer-duration (5.5 hr) test in IFRC well 399-2-9. These data indicated that radial flow conditions were established within the first five minutes of the test. Based on these results and the desire to keep the tests as short as possible (to provide for more localized estimates of hydraulic properties), a test duration of 20 minutes was selected for subsequent tests. The water supply well, which is located about 800 ft from the southern edge of the IFRC well field, was selected based on its location (close enough to stay within overland piping limitations, far enough to minimize impacts of pumping on injection response) and uranium isotopic signature (as close as possible to that observed in IFRC site wells).

Results from the 14 different constant-rate injection tests indicate spatial variability in hydraulic conductivity (K; K = T/b) estimates across the IFRC well field, as illustrated in **Figure 5**. Values of estimated hydraulic conductivity range from 15,000 to 36,000 ft/day. These values are within the expected range for the highly-transmissive Hanford formation in the 300 Area. For a given stress well, there were generally consistent responses in nearby (radius < 40 ft) observation wells. There was also a degree of consistency between the estimated hydraulic conductivities between neighboring stress wells. The highest values occur on the western side and eastern point of the triangular-shaped IFRC well field, while the lowest values were generally located in a swath through the central/eastern portion of the well field.

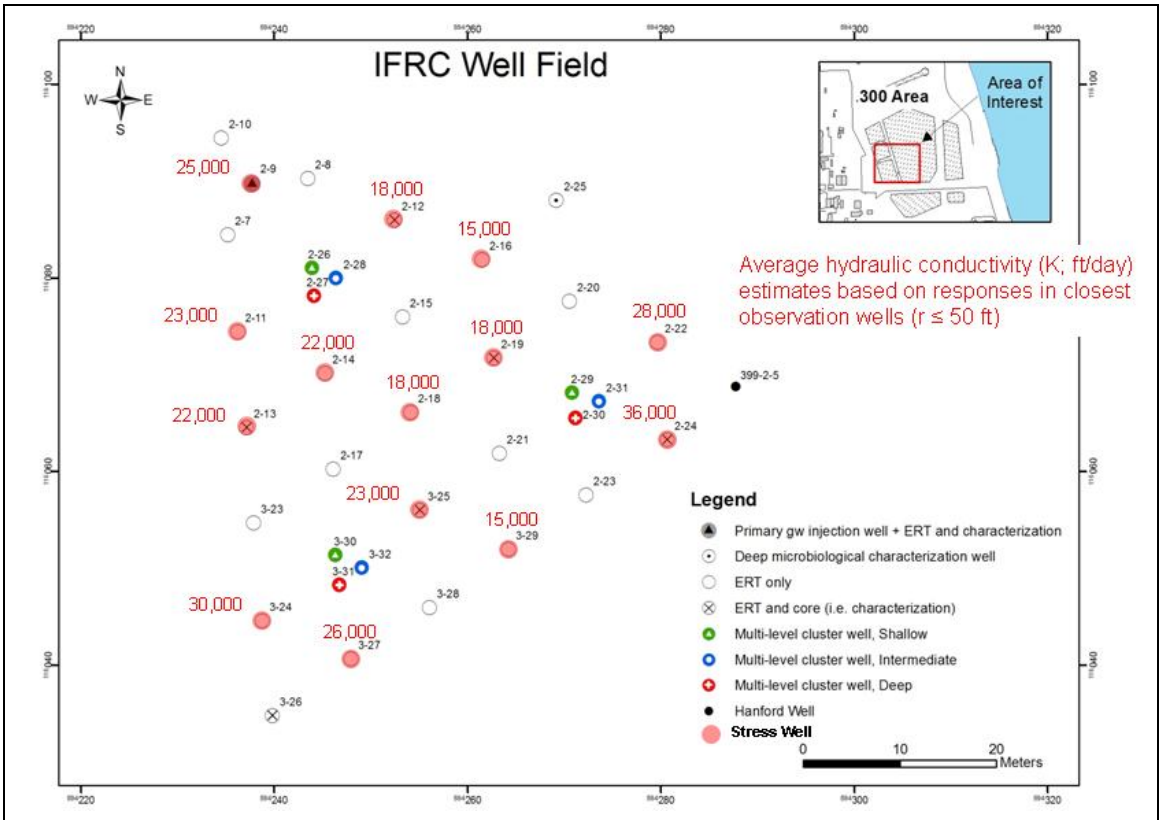

Figure 5. Map showing hydraulic conductivity estimates from short-duration tests performed in selected IFRC wells.

An initial IFRC non-reactive tracer experiment was conducted in November 2008 to: i) rigorously test field experimental infrastructure and operational procedures for large-scale injection experiments in the saturated zone, ii) assess transport processes, rates, and formational heterogeneities present in the saturated zone, and iii) further refine the site conceptual hydrologic model. This initial tracer experiment in the saturated zone was the first characterization activity that provided information on the effective porosity of the aquifer at the IFRC site and arrival times at the monitoring wells. Results from this experiment will be used to determine the injection volume and sampling frequency requirements for subsequent field-scale reactive tracer and uranium mass transfer experiments planned for FY 09.

For this initial test, a solution containing a conservative tracer (~56 mg/L Br^-) was injected into a single injection well (399-2-9, see **Figure 5**) and tracer arrival was monitored in surrounding wells. The test was run for a sufficient duration to fully describe the arrival response at the three closest monitoring wells, at which time the injection was stopped and the tracer plume was allowed to drift under natural gradient conditions (note that gradients are significantly impacted by river stage variability). The location of the injected tracer plume within the well field was tracked by sampling selected monitoring wells over time and monitoring with ion selective electrode (ISE) downhole probes. Bromide concentrations were measured in pumped well waters in the laboratory trailor using ISE in a bench-top flow-through cell. Archive samples were collected and submitted to PNNL laboratories for verification of Br^- concentration by ion chromatography.

During the experiment, ~160,000 gal of tracer solution was injected at a rate of 180 gpm, for a total injection phase duration of ~900 minutes (15 hrs). Tracer concentrations were monitored for several weeks following the injection. **Figure 6** shows snapshots of the tracer plume at different elapsed times. Fluctuations in river stage were fairly dramatic, ranging from ~104.2 to ~106 m elevation during the first two weeks of monitoring. The average river stage increased during the first 3.5 days of the experiment which resulted in more westward (left) drift of the tracer plume than was anticipated for this time of year when the river stage is usually relatively low and constant. The plume drifted out and back into the well

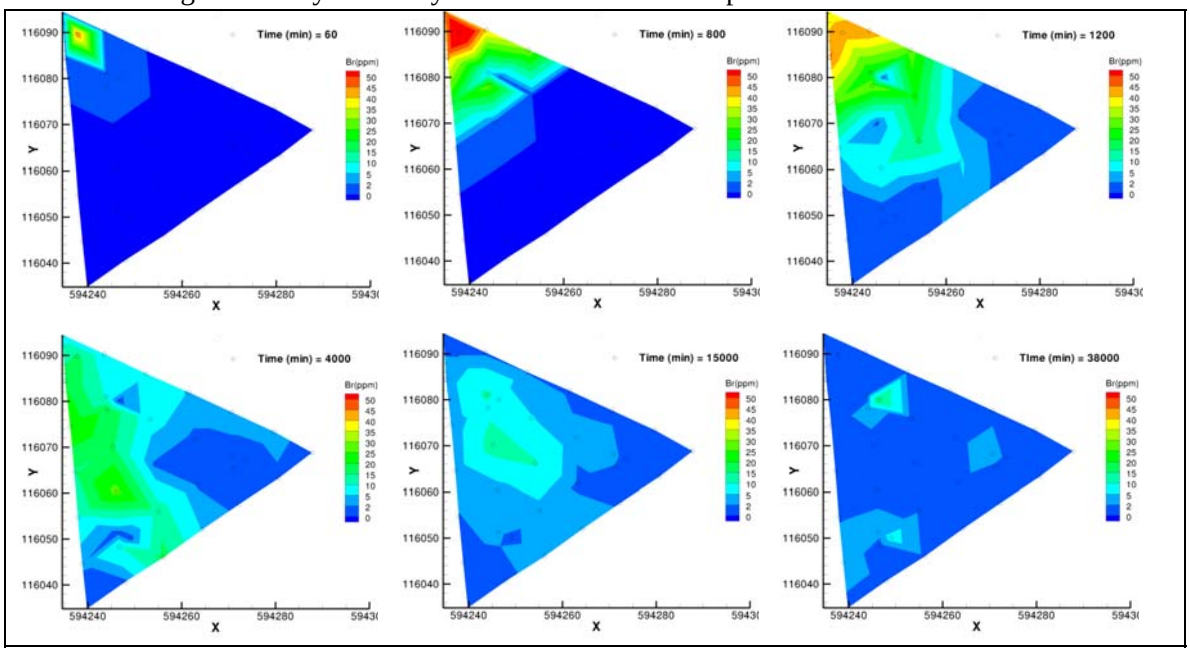

Figure 6. Snapshots of bromide plume at selected elapsed times during the initial tracer test at the Hanford 300 Area IFRC site. Tracer injection period was from zero to 900 min.

field during the experiment. After most of the tracer had drifted beyond the monitoring domain, residual Br was primarily observed in the medium depth wells of the three well clusters (2-28, 2-31, 3-32). The results of the tracer experiment have allowed us to downgrade the estimated groundwater travel time from an initial estimate of 50' per day (based on the polyphosphate experiment) to ~10' day. This travel time estimate will be further refined in a March 2009 low river flow tracer experiment.

Tracer concentrations in the three wells comprising the northern-most multi-level well cluster (2-26, 2-28, 2-27) indicated that arrival in the middle zone monitoring well was significantly lagged with respect to the upper and lower depth intervals and that concentrations remained elevated in this zone throughout the monitoring period, as tracer elution occurred in the upper and lower zones (**Figure 7**). This response is consistent with a general (although non-uniform) depth varying hydraulic conductivity distribution, as indicated by the EBF profiles (**Appendix 1**), characterized by lower permeability materials over the middle portion of the aquifer at many of the well locations. Also worth noting is a relatively strong tracer response to river stage variability observed in the upper zone relative to that observed in the lower zone. This observed difference in connectivity to the Columbia River, and lower permeability over the middle portion of the aquifer, likely explains the strong ambient flow measurements observed in many of the fully penetrating wells during the EBF testing program. These observations have major implications to our saturated zone experimental campaign.

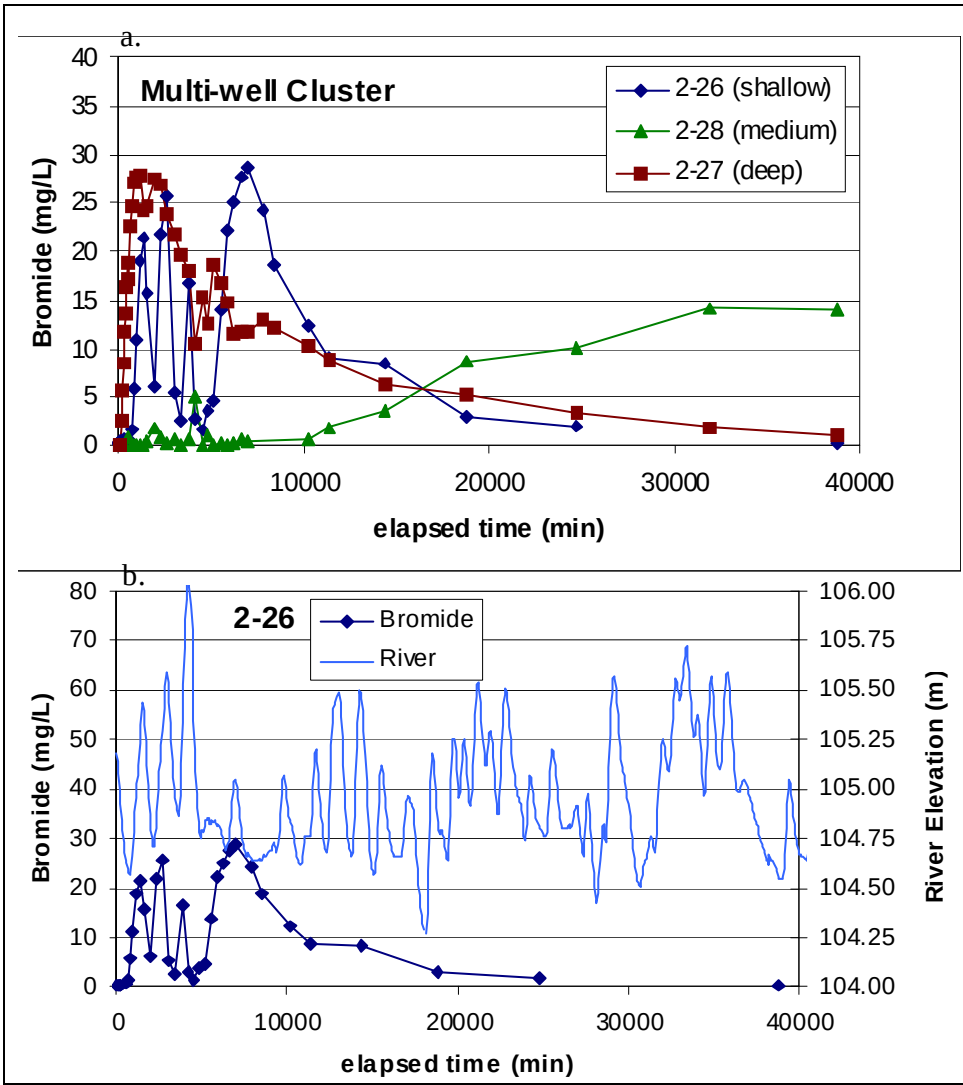

Figure 7. a.) Bromide arrival in NW multi-level well cluster. Note lag in arrival in 2-28 and the significant differences between shallow and deep wells. b.) Bromide concentrations in shallow well 2-26 show some correlation with complex river stage changes over the experiment duration.

B. Geophysical Characterization

A number of investigations have shown that the most important textural properties of natural clastic sediments affecting transport (mass and energy) properties can be expressed in terms of five quantities. These are (i) grain size, (ii) sorting, (iii) particle shape, (iv) roundness (angularity), and (v) packing. Of these five, only the first four are measureable. We hypothesize that the fifth component, packing, plays a major role in facies expression and can be inferred from multi-scale geophysical measurements and their correlation to the other four quantities. During the last year, efforts focused on three activities, (i) completion of instrument installation (resistivity electrodes and thermistors) and integration into an autonomous monitoring network, (ii) characterization of fundamental sediment properties, and (iii) collection of field geophysical data aimed site characterization. The resulting data are being used to generate 3-D facies model that are needed to develop robust transport models for predicting uranium transport in the 300 Area.

Monitoring Network. In the latter part of CY 2008, the entire resistivity electrode array and the thermistor array were wired into fully autonomous monitoring networks for use in monitoring tracer and other interference tests. Of the 672 thermistors, only 13 (2%) appear to be non-functional and as such should not impact monitoring capabilities. Analyses of the calibration data have been completed and a regression equation developed for each thermistor to convert voltage to temperature in degrees Celsius. At present, the monitoring system takes about 2 minutes to scan the entire set of thermistors. For each thermistor, the temperature averaged over a 1-minute interval is recorded every 30 minutes. The control program is such that data reporting can be increased or decreased as needed during injection experiments. Changes in temperature in the boreholes are consistent with changing water levels and the response is instantaneous with a resolution on the order of 0.1 ^{o}C. During the latter part of CY2008, all of the vertical resistivity electrode arrays were also connected into a central location to permit easy selection of different well combinations during the monitoring phase of the study.

Sediment Analyses. Particle size distributions have been completed on71 samples from wells C6212 [2-28], C6216 [2-29], and C6213 [3-30], i.e. one well from each of the 3-well clusters for depths ranging from 0 to 58 ft. Particle size analyses were performed using a combination of dry and wet sieving and laser diffraction, and textures assigned based on the USCS system. Particle densities have been completed on the < 2 mm fraction for a subset of these samples and all show particle densities > 2.65 g/cm^3. **Figure 8** shows particle size distributions of representative textures from the three wells. Poorly graded gravel is well represented in the three boreholes and is present at depths ranging from the surface to 33 ft. Poorly graded gravel with sand accounts for 27% of the samples; 23% were classified as poorly graded gravel with silt and sand; whereas silts accounted for only 8%. A number of samples were essentially cobbles with coatings of fine-textured materials. For example, one sample from 22.5-25 ft in well C6213 (3-30) was 98.43% > 30 mm with the remaining 1.47% comprised of clay. Attempts to characterize the size distribution of these fines using laser diffraction show significant differences in the size distribution of fines by gravel size, which could impact adsorption and electrical properties of the different size fractions.

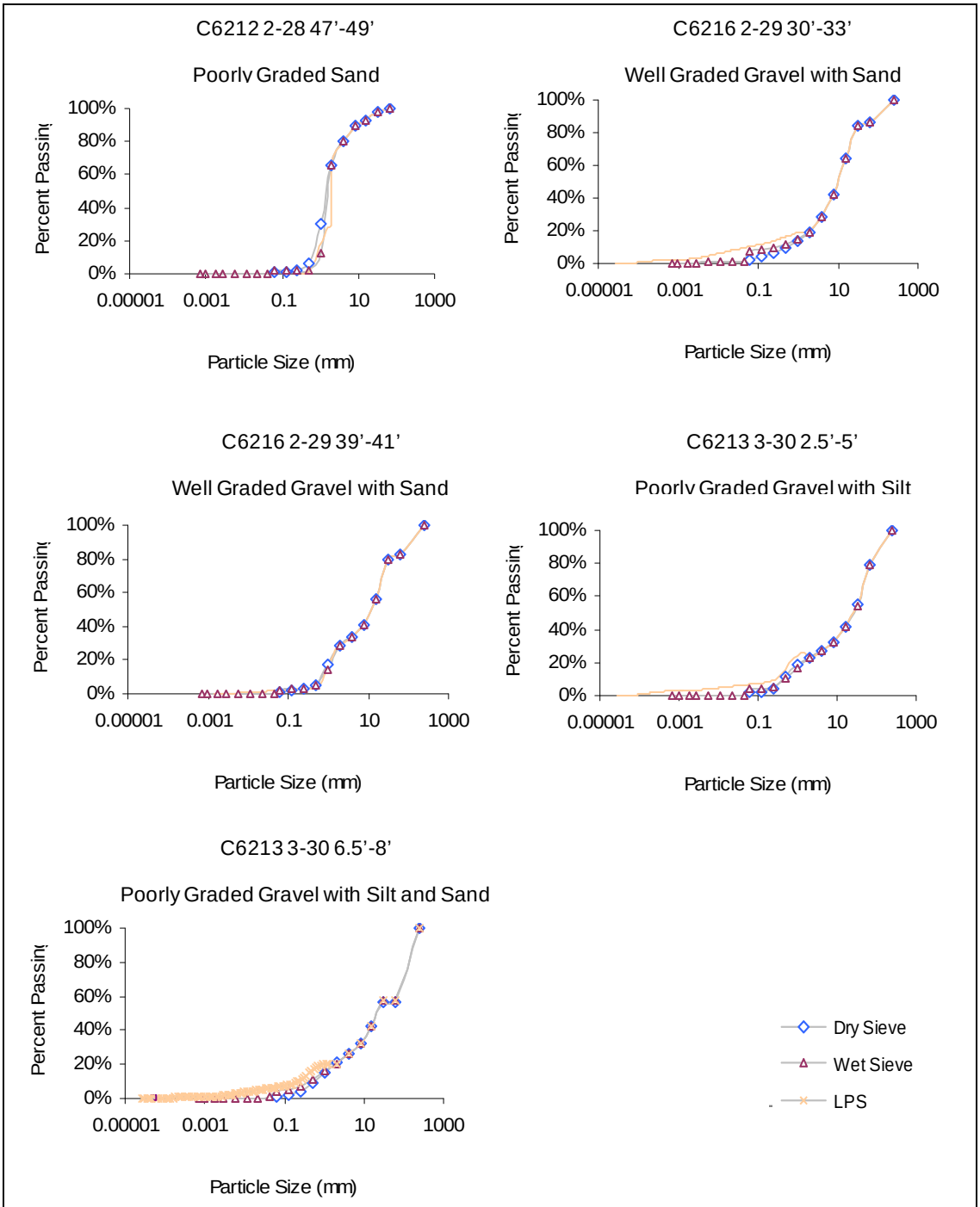

Figure 8. Particle-size distributions derived from a combination of dry sieve, wet-sieve, and laser diffraction and the resulting textural classifications.

Electrical Resistivity. A total of 28 wells were instrumented with electrodes for electrical resistivity tomography (ERT) with an average of 30 electrodes in each well for a total of 840 electrodes. Data collection for characterization was initiated with a single-channel ERT system (Multiphase Technologies) that allows the interrogation of only 4 wells per survey. A 3-D roll-along strategy, consisting of 13

surveys was designed to initiate the characterization while awaiting delivery of a multichannel ERT System that was ordered with BER capital funds. Each survey requires roughly three days to complete and, as of February 3, 2009, eight surveys have been completed. Inversion of these data is progressing in a piecewise manner as new data become available from each survey. After one four well survey is completed, data are collected on the next four well sequence, with at least two wells overlapping between surveys to provide data for error analysis prior to inversion. Resistivity inversions are currently being performed using a parallel finite-element forward/inverse ERT code developed at the Idaho National Laboratory. As new data become available, they are added to the complete data set and inverted to produce an updated image including the next four-well sequence (**Figure 9**).

To date, a total of 8 four-well inversion blocks have been collected and modeled to produce the inversion results shown in **Figure 10**. After filtering, the current inversion consists of approximately 80,000 resistivity measurements taken over 459 electrodes. The current inversion mesh consists of approximately 410,000 elements. The regularization constraints for the inversion results shown in **Figure 10** specify first spatial derivative smoothness constraints on the estimated conductivity field, with a ratio of 10:1 (horizontal to vertical) weighting, which provides lateral continuity between boreholes. Inversions using 1: 1 smoothness constraints show similar layered features, suggesting these features are necessary to fit the ERT data (i.e. they are not regularization artifacts). The data are fit to a root mean square error of approximately 25%. The shallow high conductivity structure to the west is consistent with a

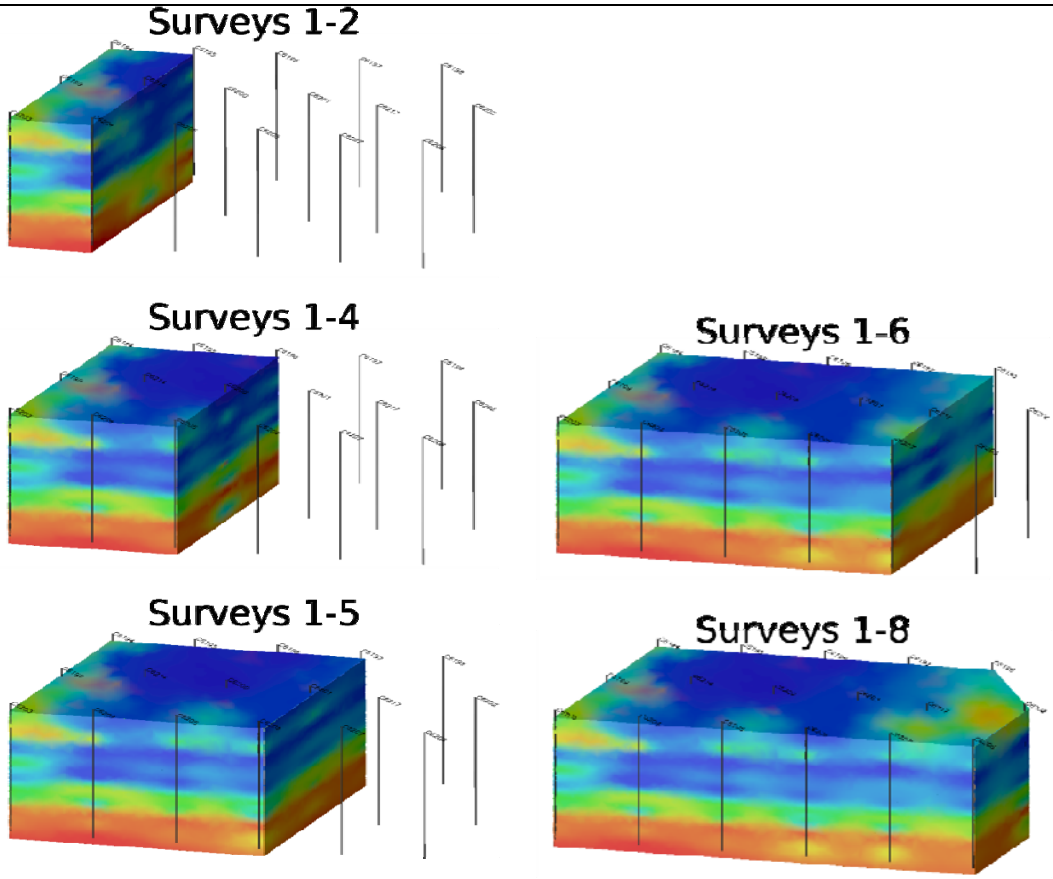

Figure 9. Demonstration of ERT data processing sequence. As a four-well data set becomes available it is added to the total data set and inverted to produce and updated bulk conductivity estimate.

high conductivity structure observed in the surface surveys using ERT and electromagnetic induction (EM-31) during the site selection phase. This anomaly was attributed to a possible unexcavated trench. However, these images provide a much better indication of the lateral extent and depth of the presumed trench. Laboratory measurements are beginning to characterize the electrical properties of the IFRC sediments to allow extrapolatable correlations between sediment physical properties such as particle size distribution, and the electrofacies shown in **Figure 10**.

Borehole Logs. As described above, the current approach to inversion of the resistivity data is based on a smoothness-constrained method that assumes the subsurface resistivity varies in a smooth manner as it attempts to minimize the changes in resistivity in a least-squares sense. In cases where the subsurface consists of homogeneous regions with a sharp interface between them, inversion can be improved and resolution increased with prior information such as borehole logs. To this end, the boreholes were logged in CY 2008 under contract by Golder Associates. A total of 35 wells were logged using acoustic televiewer, electromagnetic induction, borehole deviation, cross-borehole ground penetrating radar (GPR), and gross natural gamma activity. Two Mount Sopris Instruments borehole logging systems were used for this investigation as well as a Mala Geoscience cross-hole radar system and a Sensors and Software cross-hole radar system. A Sensors and Software modular borehole GPR system was used successfully at the Area 300 wells. GPR measurements were made using a 100 MHz antennas in zero-offset profiling (ZOP) configuration (step size = 0.125 m).

An important lesson learned in this survey was that the standard 30-volt GPR system resulted in a very low signal to noise ratio and produced data of very poor quality between the wells spaced at 10 m. A high power transmitter assembly (1000 V) provided superior signal to noise ratio, and as a result, all surveys were completed with the high power transmitter. As expected, electrical conductivity measurements in the vadose zone were quite sensitive to cables and metallic sensors and produced data of low quality. However, data quality in the saturated zone where the cables and sensors are removable was significantly better. All of the borehole data are currently being processed to develop information needed to constrain resistivity inversions and to identify vertical variations in stratigraphy, water content (in the vadose zone), and porosity (in the saturated zone). In addition, the data are being analyzed to identify anomalous zones between the boreholes, particularly in well completion that might influence transport.

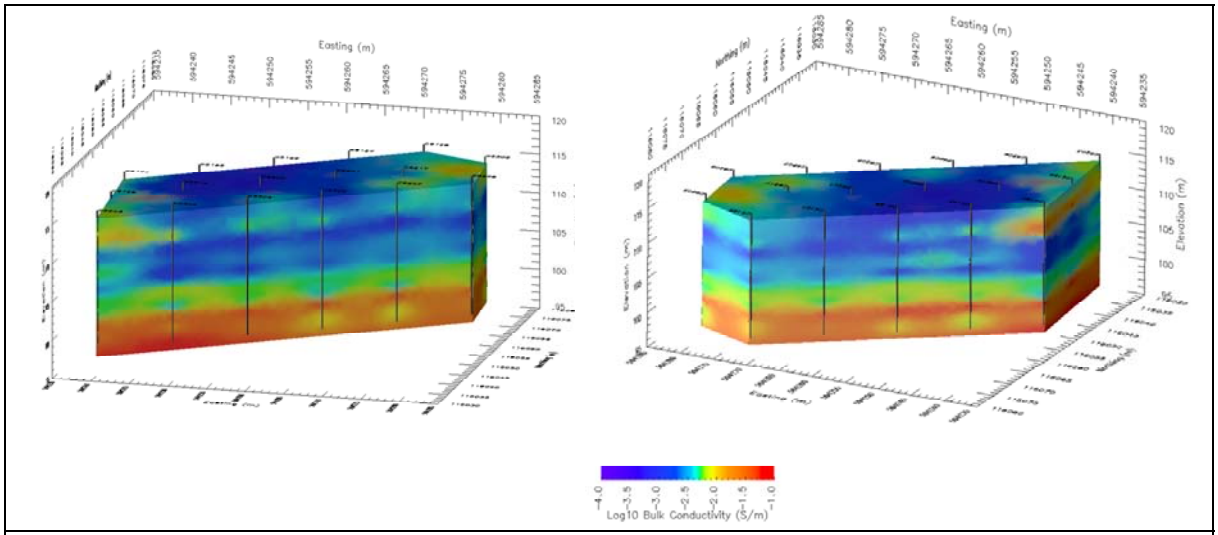

Figure 10. IFRC ERT inversion results as of 02/04/09. Top, view from southeast to northwest. Bottom, view from northwest to southeast.

C. Groundwater Characterization

A routine groundwater sampling methodology was established to collect samples from the full well array, as described in **Appendix 2**. The field array permitted rapid (single-day) collection of groundwaters using pumps permanently installed in the aquifer, midway with respect to each well's screened interval. In 2008, the field was sampled three times, on September 2, October 7, and on December 31. During October to December, the well field was subjected to extensive hydrologic testing, precluding groundwater sampling.

Wells were sampled in the sequence suggested by the results tabulations (**Appendix 3**), beginning with Well 399-2-9 and ending with Well 399-2-5. Sampling included the deep borehole finished in the Ringold Formation, the nine wells comprising the three, three-well clusters completed at shallow, intermediate, and deep zones within the saturated Hanford formation, and 25 wells screened throughout the saturated Hanford Formation. During sampling, water was pumped into the surface laboratory and purged for the periods shown in **Appendix 2**, typically at a flow rate of 8 L per minute for 5 minutes, sufficient for temperature, conductivity, etc., readings on laboratory instruments to stabilize. In-laboratory measurements are tabulated under the heading "Field Measurements". After sample collection, the samples were split, filtered, acidified if indicated (**Appendix 2**), and stored under refrigeration until analyzed.

Means and one-sigma standard deviations of analytical measurements, by inductively coupled plasma – atomic emission spectroscopy (ICP-AES) for cations, by kinetic phosphorescence analyzer (KPA) for U, and by ion chromatography (IC) for organic and inorganic carbon, are listed in **Table 1**. These results indicated that while some components remained at essentially constant concentration over the period from early September to late December (e.g., DIC, conductivity), other components varied significantly, particularly between October and December. The concentration of U dropped 25%, from 50 µg/L to 37 µg/L. Temperature decreased 3 degrees, from 19 ºC to 16 ºC, and dissolved oxygen increased from ca. 5.8 mg/L to ca. 8.2 mg/L. The anionic components decreased significantly also. These changes could reflect the infiltration of colder water from the Columbia River.

The variation within a single sampling event for each of the components presented a relatively flat parametric surface, illustrated by the plots of temperature across the well site in **Figure 11** for September and December. (In these plots, the results for the deep well and the nine discrete-depth wells were omitted.) In September, the mean of temperature measurements was 18.66 ºC, with a 1-sigma value of 0.65 ºC. In December, the mean temperature had decreased to 16.05 degrees, with a 1-sigma value of 0.96. Systematic variation in data for either date was not pronounced. When the differences between temperatures in September and December were plotted (**Figure 11**, "Difference"), a systematic variation was observed, which suggested that colder water was intruding the site from the southwest. The effects of surface temperatures on measured groundwater temperatures have not been evaluated; when data from the thermistor array is available, these observations can be tested.

Since pumped samples represent a weighted average of groundwater over the screened interval of the aquifer, wells screened at discrete intervals over the vertical extent of the aquifer provide an estimate of compositional variation in the aquifer. Temperature and uranium analyses illustrate the variations over time and vertical position within the aquifer (**Table 2**, **Figure 12**). In September and in December, the measured temperatures were approximately equal at all three depths, and showed the same variation as

the pumped samples, i.e., a drop in temperature from ca. 18.5 ºC to ca. 16.1 ºC. The distribution of U, however, changed significantly between September and December. In September, the U concentrations, shallow-intermediate-deep, were 75, 60, and 52 µg/L. The shallow and deep wells were not sampled in October, but the intermediate concentration remained unchanged at 50 µg/L. In December, the shallow U concentration had dropped to approximately match the intermediate concentration – both were 54 µg/L – and the deep concentration of U had dropped to 30 µg/L. The latter value compares to the mean for pumped samples overall (37 µg/L in December, **Table 1**), but the concentrations above it were significantly higher than the site's mean in December.

The results represent early points over a longer-term series of measurements. They provide information to guide experimentation at the field site. Specifically, the changes and apparent gradient in temperatures suggest that the passive monitoring of the thermistor array will reveal a three-dimensional view of groundwater-surface water interaction. The broad variation in concentrations for major-ion solutes suggests that the aquifer is heterogeneous. This hypothesis will be tested in more detail during passive aquifer sampling using a dialysis cell sampler. The variation of U, an endogenous component of the aquifer, suggests that its supply and influx to the aquifer change with the seasons. This is a central hypothesis to be tested during the Spring transition to a higher water table. If U is contributed to the aquifer by 'capture' from the vadose zone during the Spring transition, then sampling at the aquifer surface will show a rise in U concentrations. The results of that sampling will be put in context with scheduled, repeated sampling of the pumped-sample network.

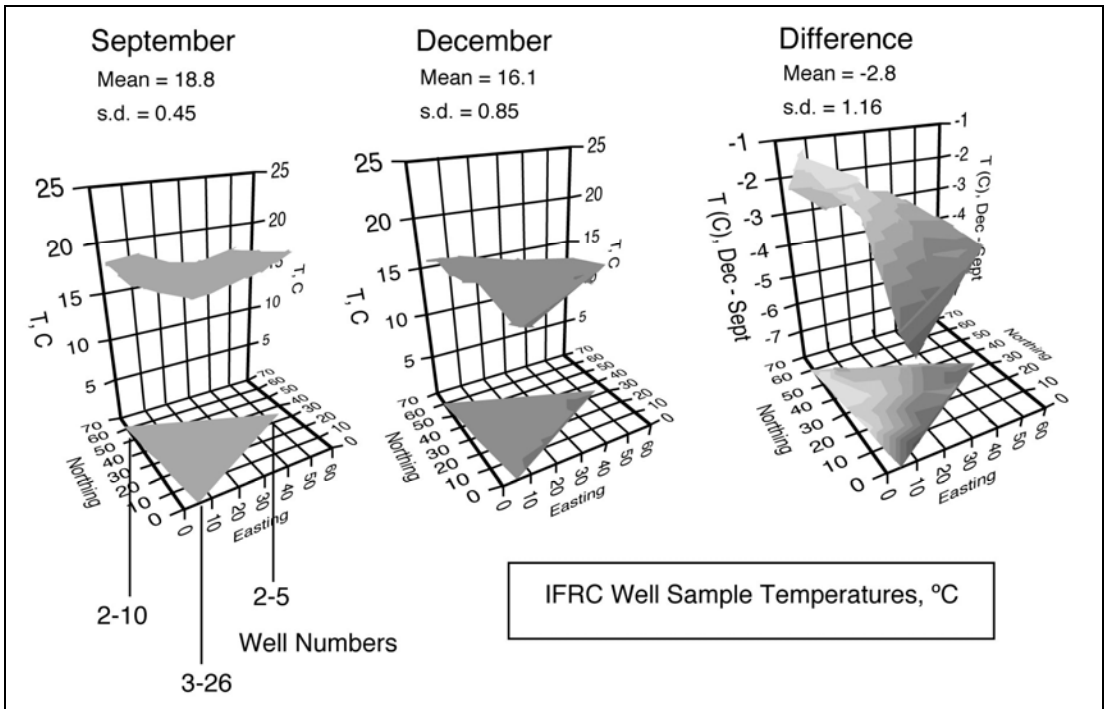

Figure 11. Lateral temperature variations for pumped samples plotted as three-dimensional surfaces. The difference between single points measured in September and December suggests encroachment of colder water at the south of the well field.

Table 1. Compositional Means for Baseline Groundwater Samplings in September, October, and December, 2008 Blank values were below detection. ICP analyses for cation samples collected in December have not yet been released from QA assessment.

Well Name	BL1		BL2		BL3	
	Sept. 2,		Oct. 7,		Dec. 31,	
Sample ID	2008	*s.d.*	2008	*s.d.*	2008	*s.d.*
U (ug/L)	50.73	*15.88*	46.10	*6.10*	37.03	*8.98*
DIC (mg/L)	30.82	*0.81*	31.50	*0.95*	32.75	*1.16*
S (ug/L)	19089	*664*	17273	*704*	Not Measured at January 2009	
P (ug/L)	224	*235*				
Ba (ug/L)	57	*6*	51	*4*		
Fe (ug/L)	109		91			
Si (ug/L)	13984	*1331*	15669	*602*		
Mn (ug/L)	15	*14*				
Cr (ug/L)	8	*2*	5	*0*		
Mg (ug/L)	12232	*374*	11140	*354*		
Ca (ug/L)	48362	*1287*	43785	*1329*		
Na (ug/L)	23628	*1451*	22655	*782*		
K (ug/L)	5811	*546*	5744	*139*		
Sr (ug/L	248	*9*	223	*8*		
F (ug/L)	389	*35*	379	*21*	355	*13*
Cl (ug/L)	24416	*1225*	22938	*333*	18563	*441*
SO4 (ug/L)	61139	*1860*	55794	*1474*	46888	*1050*
NO3 (ug/L)	29215	*861*	27459	*400*	22100	*903*
Br (ug/L)					724.56	*598.75*
Temp. (degrees C)	18.66	*0.65*	19.09	*0.82*	16.05	*0.85*
Cond. (mS/cm)	0.47	*0.02*	0.45	*0.01*	0.43	*0.01*
Diss. Ox. (mg/L)	5.60	*0.47*	5.76	*0.47*	8.22	*0.26*
pH	7.36	*0.28*	7.60	*0.09*	7.64	*0.09*
ORP (mv)	96.57	*26.65*	Not Measured		93.71	*4.96*

Table 2. Composite results for cluster wells, blank values were not collected.

DATE		U, µg/L	1-sigma s.d.	T, ºC	1-sigma s.d.
9/2/08	Shallow	75.2	10.65	18.6	0.8
10/7/08					
12/31/08		53.95	5.8	16.1	1.3
9/2/08	Intermediate	59.3	8.9	18.9	7
10/7/08		58.9	6.75	19.1	0.9
12/31/08		53.62	7.4	16	0.96
9/2/08	Deep	51.9	1.65	18.8	0.6
10/7/08					
12/31/08		30.4	1.4	16.3	0.93

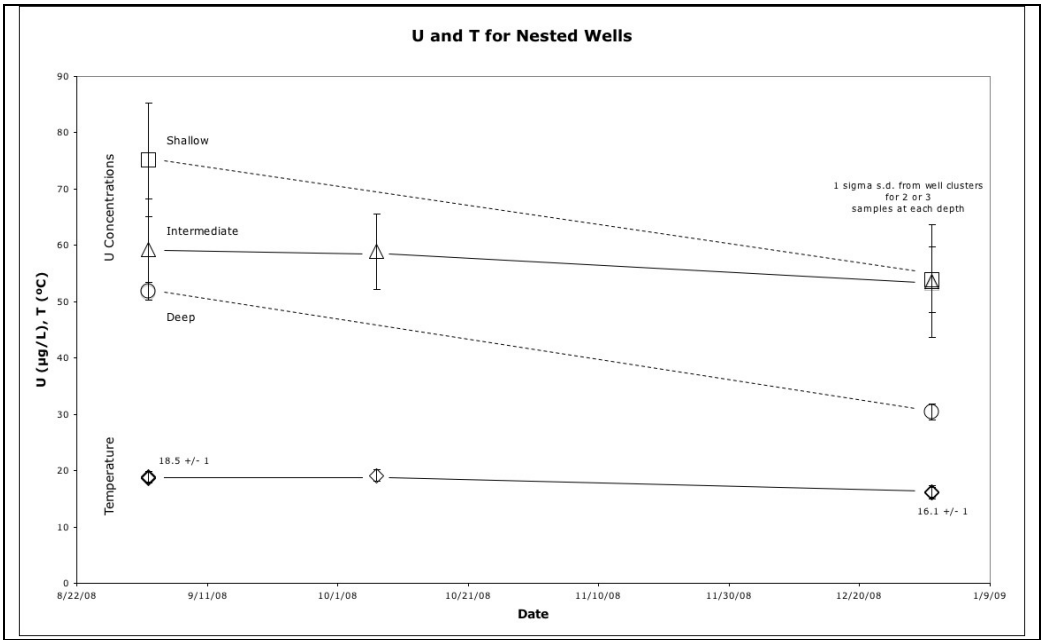

Figure 12. Aqueous U(VI) concentration and temperature in the multi-level wells sampled in September, October and December, 2008.

C. Laboratory Characterization

Laboratory chemical and mineralogic characterization is being performed on the < 2.0 mm size fraction of air-dried "grab samples" from the well boreholes. The initial phase of laboratory characterization is measuring particle size distribution, total uranium (U), bicarbonate extractable U, U-K_d, and ammonium oxalate extractable Fe(III) on 100, < 2.0 mm grab samples taken from the 3 well clusters (strategy described in "Characterization Plan"). Surface area/mineralogy will be determined on 50/25 of these samples that vary in silt and clay content. A second series of 100 samples has been selected for characterization based on geostatistical considerations. Analyses on this second sample set

will be initiated after the consistency of the first data set is evaluated through correlation analyses of different properties.

The chemical characterization measurements that have been completed to date include total U, bicarbonate extractable U, and groundwater soluble U in preparation for U-K_d measurerments. These results have been recently received and are considered preliminary as they have not had QA review. As expected, the results show the presence of significant heterogeneity in U concentration distribution within the site, with higher U concentration observed in SE well 2-30 that is located toward the interior of SPP (**Figure 13**). Point-to-point heterogeneity in U concentration is markedly greater in the vadose zone, while uniform concentrations were observed within the core of the saturated zone (35'-55'). Within this heterogeneity, total U and bicarbonate U display strong correlation (**Figure 14**), with occasional exceptions, and clear generalizations hold: i.) U is highest in the deeper vadose zone (e.g., 10'-20' bgs) below backfill and above the saturated zone; ii.) U concentrations in the saturated zone appear highest at the top (e.g., near the water table) and bottom (e.g., near the Ringold contact) of the transmissive aquifer section; and iii.) where noted, high U concentrations in the saturated zone are associated with meter-scale, silt-textured rip-up clasts. The chemical results also suggest a that a secondary maximum in adsorbed U occurs in the "smear" zone (25' – 35' bgs) that is seasonally saturated by water fluctuations (**Figure 13**). A future analytical campaign in early FY 10 will measure total and bicarbonate extractable U in all "smear" zone samples collected from the well field to provide a 3-D concentration map of this important zone. These recently obtained analyses have important implications to our experimental planning.

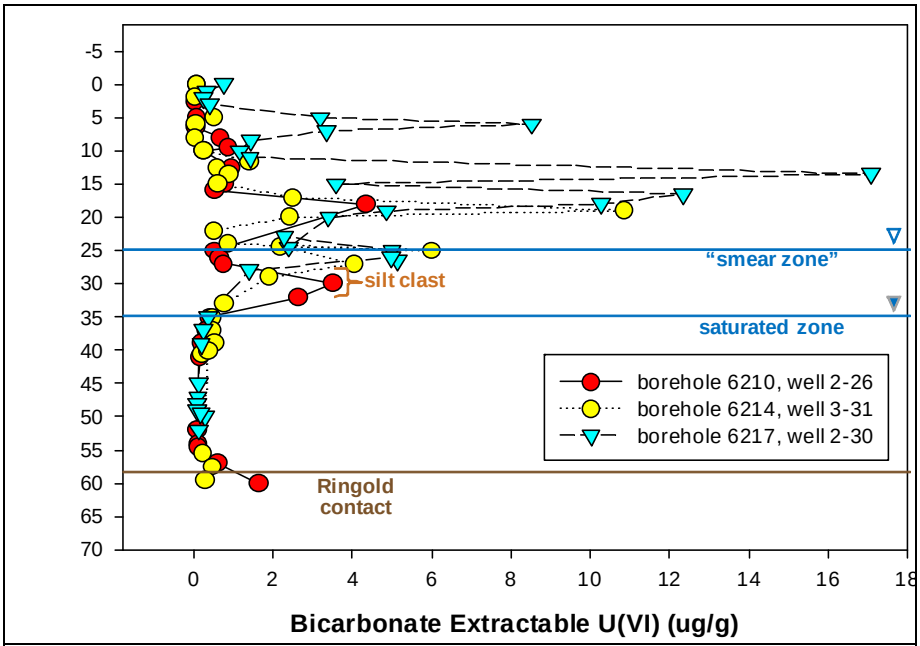

Figure 13. Bicarbonate extractable U(VI) in grab samples from three IFRC boreholes associated with the three well clusters. The extractions were performed for 1000 h, and approximate the adsorbed U(VI) concentration in the sediments. These results have been corroborated by other analyses performed at the USGS on samples from nearby boreholes. USGS is developing a surface complexation model for adsorbed contaminant U(VI) based on these and other measurements.

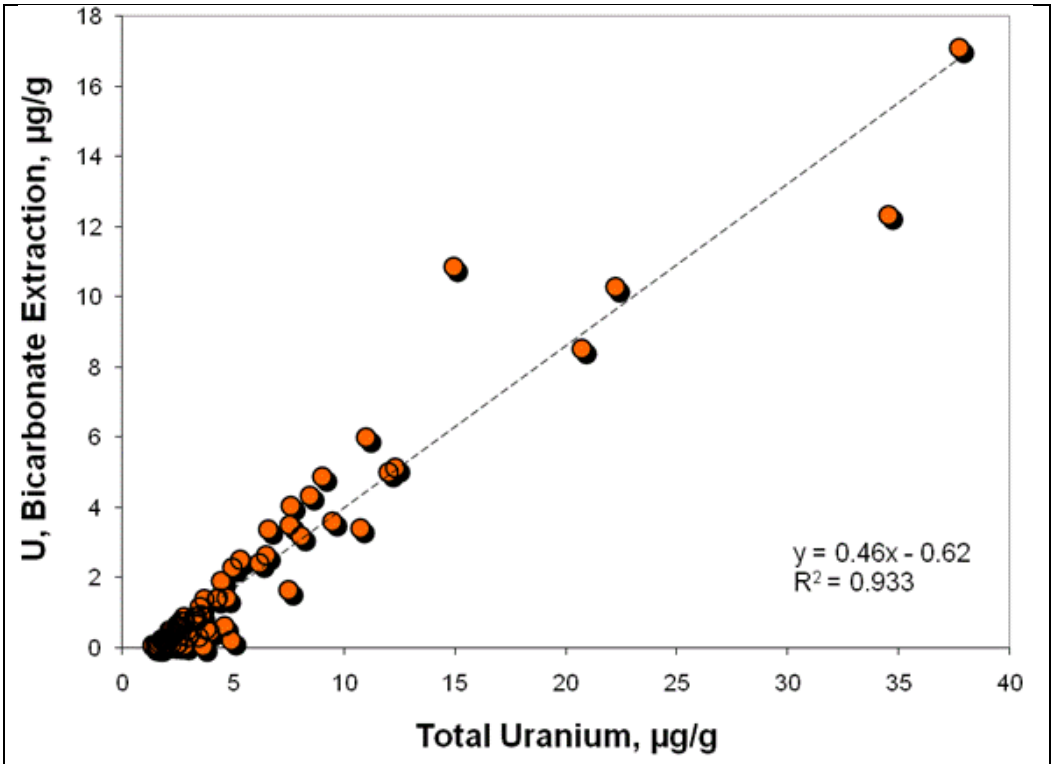

Figure 14. Relationship of total U (by fusion and complete dissolution) to 1000 h bicarbonate extractable U(VI) in grab samples from IFRC wells 2-26, 3-31, and 2-30. The results imply an average, insoluble background U concentration of 1.35 µg/g; and an average adsorbed, exchangeable concentration that is approximately 46% of the total. Other regressions of this nature are being formulated.

Vadose Zone Experiments

As shown in **Figure 1**, we have decided to postpone the vadose zone experimental program until FY 09. There are three reasons for this. First, we thought it prudent to make the best scientific use out of our significant infrastructure investments in the saturated zone site prior to our mid-term project review in 2010. Second, a passive saturated zone experiment planned for FY 09 (described below) will evaluate U fluxes from the lower vadose zone to groundwater providing important insights on critical objectives for future vadose zone experimentation. Third, EM has funded a vadose zone polyphosphate treatability study for FY 09 and FY 10 (see preliminary schedule in **Appendix 4**). This experiment will be performed well north of the IFRC well field near the 316 process trench and will involve one tracer infiltration experiment (June to August 2009) and one polyphosphate experiment (March to May, 2010). We believe that our vadose zone program could be more impactful if it took their results into due consideration during experimental design. We intend to develop a vadose zone site design and associated field experiment plan in the first half of FY 10 to present at the mid-term review.

Saturated Zone Experiments

Now that a large scale injection experiment has been successfully completed to test infrastructure performance and evaluate site hydrologic behavior (e.g., **Figure 6**), a full sequence of saturated zone field experiments has been planned for FY 09 and FY 10. These experiments are briefly described below. These are subject to change and refinement as new information becomes available characterization activities underway, and from each progressive experimental campaign.

1.) Multi-tracer, cold water injection (March, 2009)

This experiment will further characterize the hydrology and heterogeneity of the IFRC site during a period of stable hydrologic conditions in the river. A suite of non-reactive tracers of varying aqueous diffusivity and susceptibility to anion exclusion (Br^-, D_2O, and PFBA) will be injected into groundwater (~17^o C) in chilled site groundwater (~12^o C). Depth discrete breakthrough will be monitored by continuous monitoring of the down-hole thermistor arrays in all arrival wells at approximate 1' increments, while average well concentrations of tracers will be analyzed by ISE (Br) and subsequent laboratory analyses (all tracers). The experiment will accurately define vertical heterogeneities in flow paths and the implications of these on well-averaged tracer concentrations.

2.) Passive during rising and falling water table (May-July, 2009)

An important site hypothesis is that U(VI) is mobilized from the deep vadose zone during seasonal periods of high water table (high river stage), and that this mobilized U(VI) is the source of persistent groundwater contamination. A passive, robust monitoring experiment will be performed to evaluate this hypothesis. The experiment will utilize the robust riverside river stage and IFRC water level and electrical conductivity monitoring arrays, and the down-well thermistors to record the arrival of the spring snowmelt pulse in the Columbia River and its depth discrete intrusion into the IFRC experimental domain (clearly evident by temperature and electrical conductivity differences) at hourly time steps. During this period, and at strategically selected time points, well waters at different well depths will be pumped for total and isotopic U and compositional analyses. D_2O will be released to the deep vadose zone in two select wells to follow the migration path of solubilized U(VI).

3.) Desorption injection (September, 2009)

A critical hypothesis for the IFRC science program is that slow-mass transfer of adsorbed U(VI) in intra-grain and finer-textured sediment domains retards U(VI) desorption in the saturated zone, and contributes to long term plume persistence. This experiment will inject up-gradient, low U(VI), high bicarbonate groundwater with appropriate non-reactive tracers into the IFRC site to induce a desorption plume. The advancing and retreating plume fronts will be tracked through the site to provide data on the kinetics of the field desorption process, and relationships to site hydrology (e.g., variable hydraulic conductivity and porosity zones) as defined by the temperature tracer study. Current plans include for three sequential, but time staggered injections along a common flow-path to monitor the adsorption desorption process as site ground-waters return with higher U(VI).

4.) Adsorption injection (March, 2010)

Accurate prediction of plume persistence and the development of an effective, long-term remediation strategy requires that retardation capacity of the saturated zone for U(VI) and its spatial variability be quantitatively understood and incorporated into a robust 3-D simulation capability. This experiment will inject site waters with higher U(VI) concentration (at least 2X) and appropriate non-reactive tracers into the IFRC experimental domain to follow the retardation of a U(VI) plume as it migrates through the experimental domain, and its desorption as lower IFRC site waters mix with groundwater and sediments containing elevated U. We will attempt to interrogate different flow-paths through the IFRC well field by performing multiple injections at different river stage, and in different injection wells.

5.) Passive during rising and falling water table (May-July, 2010)

This experiment will replicate and improve on the Spring 2009 experiment. Specific time periods during transient hydrologic and geochemical conditions will be targeted for intense temporal and depth discrete sampling.

6.) In-situ microbiologic activity (August, 2010 – February 2011)

The nature of this experiment is dependent on the findings of currently ongoing PNNL SFA research on the identity, functionality, and community structure of micro-organisms in upper unconfined aquifer (Hanford formation). The experiment is not expected to be a stimulatory one as performed at the other IFRC sites. Our goal will be to probe the in-situ activity of a target community by injection of low, but detectable concentrations of specific reactive tracers that are assimilated, metabolized, or bio-utilized in different ways [e.g., electron donors, carbon substrates, or other nutrients (e.g., P or N)]. Multiple reactive tracers will likely be used and tracer detection may be accomplished by direct analysis or isotopic labeling techniques. Trial experiments will determine whether localized, push-pull experiments of this nature are feasible in the lower conductivity zone that is believed to exist in the central region of the Hanford formation saturated zone.

7.) Isotopic exchange (March 2011)

Uranium isotopic analyses of IFRC site ground-waters and others from the overall U plume, and 300 A have revealed a significant isotopic gradient from the south to the north ends of the plume. This apparently results from differences in the U isotopic composition of wastes that were released to the SPP, NPP, and process trenches over time. SPP, the location of the IFRC, is the oldest disposal location and received no U containing ^{236}U. Wastes disposed to the other locations had increasing amounts of this isotope with time. We recognized these important isotopic differences soon after well installation and have performed all hydrologic testing in a manner that preserves the isotopic integrity of the site. This planned experiment will inject waters of similar total U concentration, but different isotopic signature, from the northern end of the site into the IFRC experimental domain. The inclusion of non-reactive tracers with similar diffusivity to U(VI) carbonate species will allow us to track the injectate flowpath. Isotopic analyses of plume waters will define the rate and extent of isotopic exchange that will provide unique insights on the in-situ lability and rate of exchange of

adsorbed U. An experiment of this nature has never been performed in the field. It is, however, likely to perturb the isotopic status of the site for some time.

We should note that we are now considering the feasibility smaller scale experiments using variable temperature water injection to better characterize flow paths between proximate wells and different hydraulic conductivity zones, and push-pull type experiments in the apparently lower hydraulic conductivity region in the center of the saturated zone. Modeling calculations are underway to assess the viability of these smaller scale experiments, with feasibility tests planned for the spring and summer of 2010.

Modeling and Interpretation

Progress is described here for four external IFRC P.I.s working in the Modeling and Interpretational Program.

1.) Mass Transfer Processes - Dr. Roy Haggerty (OSU)

Due to fluctuation of the Columbia River stage, at some times of the year the interface between Columbia River water and Hanford groundwater oscillates with an amplitude of many meters per day. U(VI) transport is significantly different on either side of this interface, with much greater sorption in Columbia River water. We hypothesize that mass transfer traps and irreversibly mixes significant quantities of both waters on the opposing side of the interface, complicating U(VI) transport from the Hanford formation to the Columbia River. We are conducting a series of column and larger intermediate scale experiments with transient (i.e., oscillating) flow to develop and test mass transfer and geochemical theory of U(VI) transport in a controlled environment similar to the IFC site. The experiments will help to build a more accurate U(VI) transport model that can be used to describe the U(VI) plume transport in the Hanford 300 Area.

To date, four column experiments have been conducted to study the effects of transient flow on conservative tracer (Br) transport. Sediments collected from the Hanford formation and 12/20-mesh Accusand were used as testing materials, representing flow domains with and without immobile zones. Steady-state and transient flow were used in both materials. The solute transport experiments were modeled with a solute transport and multirate mass transfer model, STAMMT-L [*Haggerty and Reeves*, 2002; *Haggerty*, in preparation]. For the Hanford sediments, a slightly increased dispersivity was found with transient flow. This effect, however, was not observed in the transient flow experiment using Accusand. Both results are consistent with theory already in the literature that suggests that dispersion increases with mass transfer under transient flow, and that the increase is a function of oscillation frequency and amplitude. The results suggest that the transient flow conditions in the field (e.g., hydraulic gradient change due to the river stage change) increases dispersion and mixing, and that the size of the effect will be influenced by the frequency and duration of the Columbia River stage changes. Based on the literature review, this increased dispersivity can be predicted given the characteristics of the transient flow condition.

Figure 15 shows breakthrough curves for steady-state and transient flow experiments for the two materials. Quantified parameters (e.g., slightly increased dispersivity) show that the effects of the transient flow can only be reflected in the system where immobile domain exists.

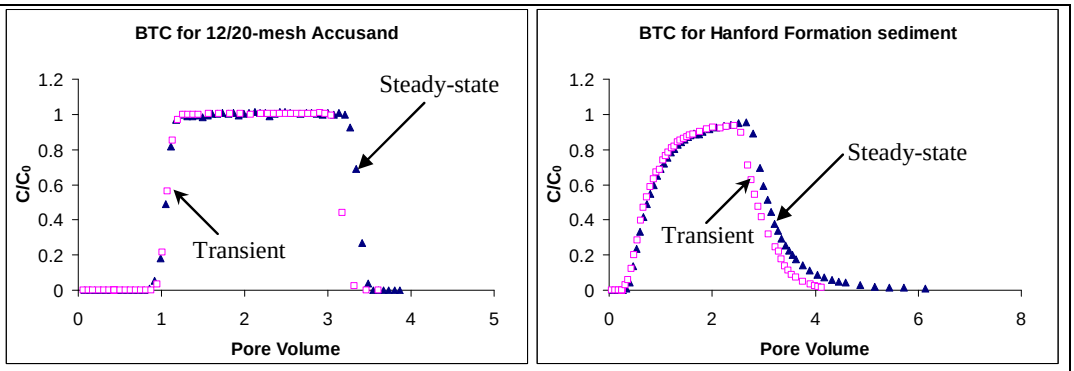

Figure 15. Breakthrough curves for steady-state and transient flow experiments in Accusand (no mass transfer) and Hanford Formation sediment (significant mass transfer). Differences between the breakthrough curves in each sediment are subtle and masked by different pore-volumes, but transient flow in the Hanford Formation has slightly higher dispersion than steady-state flow.

CY 09 Objectives:

- Conduct steady-state and transient flow experiments using IFRC smear-zone composite sediment as well as the 12/20-mesh Accusand with Br and uranium
- Quantify and simulate the effects of transient flow on U(VI) transport in IFRC Hanford formation sediments using the PNNL solute transport and geochemistry model STOMP.
- Develop a theory to predict effective parameters due to transient flow
- Design the intermediate scale flow apparatus and begin conducting meter-scale experiments
- Develop a 3D conceptual model using the developed theory through the column experiments and apply this conceptual model to the 3D flume experiment
- Coordinate with the IFRC modeling team to model flume results and test various multi-scale mass transfer models that may be applied to the IFRC experimental field site.

2.) Developing the Site Geostatistical Model - Dr. Yoram Rubin (UCB)

The UCB modeling team is developing a new numerical approach to integrate multiple data sets of different type from the IFRC site to establish 3-D geostatistical models of hydrologic properties (hydraulic conductivity and porosity); U distribution, surface complexation model parameters (binding constant, site concentration), and mass transfer parameters (e.g., statistical distribution of first order rate constants). Their first milestone objective is to establish the 3-D model for the site saturated zone flow properties.

Over the past year an approach was devised for hydrogeological and geochemical site characterization through inverse modeling (or inversion, in short). The approach is called the Method of Anchored Distributions (MAD) and is described in **Appendix 5**. MAD was tested with two synthetic case studies, with good results. After this, our team began organization and mapping the of the initial data base that we would need as input for MAD for the development of the flow-field model. This includes careful evaluation of the range of data types that are being acquired by the IFRC field team, in terms of their potential benefit for inversion; setting criteria for prioritization; and identifying key personnel associated with each of data type that could provide technical expertise needed for

interpretation. During the latter portion of the calendar year we began collaborations with Lichtner (LANL) and Hammond (PNNL) of the IFRC modeling team who will be assisting in the linkage of PFLOTRAN with MAD for large scale forward projections of the influence on hydrologic properties distributions on the known or measured hydrologic behaviors of the 300 A IFRC site.

CY 09 Objectives:

- Implement MAD at the IFRC site, with a primary focus on hydrogeology.
- Develop a three-dimensional image of the IFRC field site in terms of geology and flow variables including conductivity and porosity.
- Establish a computational infrastructure to support a large-scale MAD application through collaboration with Peter Lichtner and Glenn Hammond. The focus will be on developing a scheme that integrates MAD with PFLOTRAN into a powerful computational platform.
- Work with the PNNL and INL researchers to organize the field and laboratory characterization measurements in the required form for MAD-based inversion
- Establishing the physical and mathematical underpinning of the various data types and their inter-relationships. For example, there were numerous constant rate injection tests that were conducted during hydrologic characterization. The tests vary in space and time scales, and thereby offer different perspectives on hydraulic conductivity. Integrating these results to provide a coherent image of the subsurface is one of our main challenges for the coming year.

3.) Hydrologic and Transport Modeling with PFLOTRAN - Dr. Peter Lichtner (LANL)

Work activities during 2008 included a 3D site-scale model of migration of a tracer at the Hanford 300 Area, and development of a simple 1D geochemical flow and transport model to better understand the role of mineral dissolution, adsorption, and river stage fluctuations on U(VI) mobility at the site. These preliminary activities will aid in identifying key processes for incorporation in a 3D multicomponent field-scale model of U(VI) transport at the IFRC site.

The 3D tracer model was based on a variably saturated model of the 300 Area incorporating fluctuations of the Columbia River stage and inland head measurements to fix the upgradient time-dependent boundary conditions. The tracer was released from the IFRC site in the model

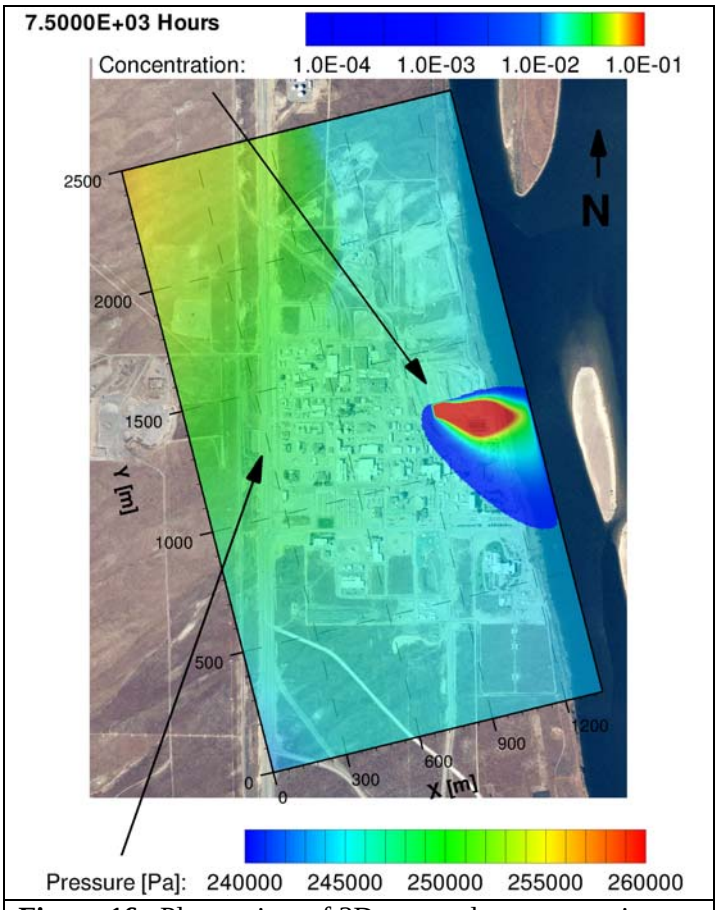

Figure 16. Planar view of 3D tracer plume emanating from the IFRC.

(see **Figure 16**). The computational domain consisted of a rectangular box measuring 1350 x 2500 x 20 meters (x, y, z) with orientation aligned with the Columbia River at 14 degrees west of north. Three different grid resolutions were used in the simulations and the results compared for convergence of piezometric heads and flow velocities. The coarsest grid used (dx = dy = 20 m, dz = 1 m) resulted in 170,000 nodes. An intermediate grid (dx = dy = 10 m, dz = 0.5 m) resulted in 1,350,000 nodes. And the finest grid (dx = dy = 5 m, dz = 0.25 m) consisted of 10,800,000 nodes. Calculations were carried out for approximately 10 months using available contiguous data sets for head and river fluctuations. For the 170k node scenario, 128 processor cores on ORNL's Jaguar XT3 Cray supercomputer required 50 minutes to complete the 7500 hour simulation. Simulations involving 1.35M and 10.8M nodes used 1024 and 600 processor cores and ran for 2.3 and 16 hours, respectively.

Excellent agreement was found between the predicted heads and observations at several wells. All three grid resolutions produce nearly identical piezometric heads that slightly overestimated the observed head and were more oscillatory. Although no data is available to compare the predicted flow velocities, slower convergence of the velocities was observed in the simulations compared to the heads as is to be expected. The coarse grid model underestimated the peak velocities by as much as 60% compared to the fine grid model. The velocities are more consistent for the 1.35M and 10.8M node simulations, although it was not clear that velocities fully converged. The high-resolution simulations predicted peak flow velocities at the IFRC site of over 15,000 m/y, a magnitude that may require care in scheduling/setting up field experiments at the site. Even during low river stage periods of the year, the predicted flow velocities were well in excess of 5000 m/y. In spite of these predictions, we note that the November 2008 tracer experiment displayed much slower velocities, and we await updated hydrologic measurements from the PNNL team to refine the site hydrologic model that is now overly simplistic.

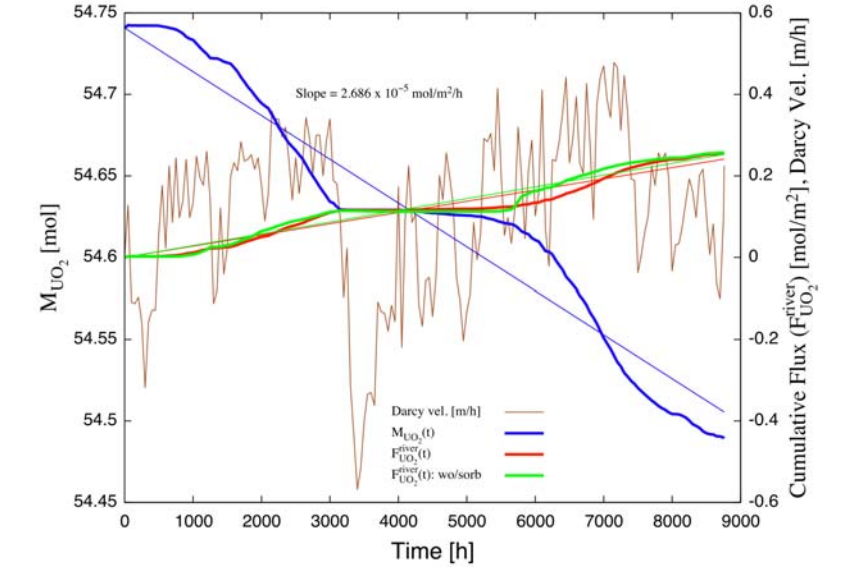

Figure 17. 1D model showing the effect of Columbia River stage fluctuations on the release of U(VI) into the river as a function of time. The thin brown curve shows the Darcy velocity imposed on the system. The red and green curves give the flux of U(VI) with and without sorption. The blue curve is the total moles of U(VI) remaining in the system and the magenta curve demonstrates conservation of total mass in the system balancing the total amount of U(VI) in the system against the amount flowing into and out of the system. Metatorbernite is used as the source of U(VI).

In support of the PFLOTRAN simulations of the 300 Area, conceptual model development tools (written in Python and C++) were developed to automate the mapping of stratigraphy, and boundary and initial conditions to the model domain and expedite the generation of large, transient input decks

(piezometric head, river stage) for any user-defined region within the 300 Area. These preprocessing tools will greatly ease the often tedious task of conceptual model development and improve simulation turnaround in the future.

In preparation for incorporating uranium chemistry into the 3D field site model, a 1D model was constructed that included river stage fluctuations with a multicomponent description of groundwater and river chemistry. The model domain was 500 m long with river fluctuations imposed at the right boundary and a constant pressure at the left boundary adjusted to give a mean flux of 1 km/y into the river. In the model, metatorbernite (a copper-uranium-phosphate precipitate) was used as a source of U(VI) localized in a region 50-100 m from the left boundary, with an effective dissolution rate constant to represent multiscale release mechanisms. This precipitated U(VI) phase has been observed in the vadose zone above the U groundwater plume. Ongoing IFRC characterization measurements are expected to rigorously define the source term character and behavior for more robust future modeling activities.

Although the 1D model can provide considerable insight into the processes taking place at the 300 Area site, there are several limitations where the model does not capture processes present in a full 3D model. First, in the 1D model flow is strictly linear along a fixed streamline, when in actuality streamlines will form a complex pattern changing position with time with both horizontal and vertical flow. Secondly, rather than a steady release rate of U(VI) from the source region as occurs in the 1D model, in the 3D model the release is correlated with fluctuations in the watertable as caused by river stage fluctuations. The aqueous solution was represented by 18 primary species with 150 aqueous complexes. Adsorption reactions were described by surface complexes $>SOUO_2OH$ and $>SOHUO_2CO_3$ parameterized by other IFRC researchers. In addition, reaction of calcite was included in the model. Time t=0 was taken to represent present-day conditions (as opposed to time of waste emplacement) with surface complexation sites within the computational domain initially equilibrated with U(VI).

Two significant findings were obtained from this preliminary 1D modeling exercise: (i) the flux of U(VI) into the river was independent of the surface complexation reactions (see **Figure 17**), in spite of a U(VI) distribution coefficient for the dimensionless ratio of sorbed to aqueous concentration on the order of several hundred; and (ii) the approximate independence on smoothing of river fluctuations over time periods of one day, one week, and one month (see **Figure 18**), indicating that

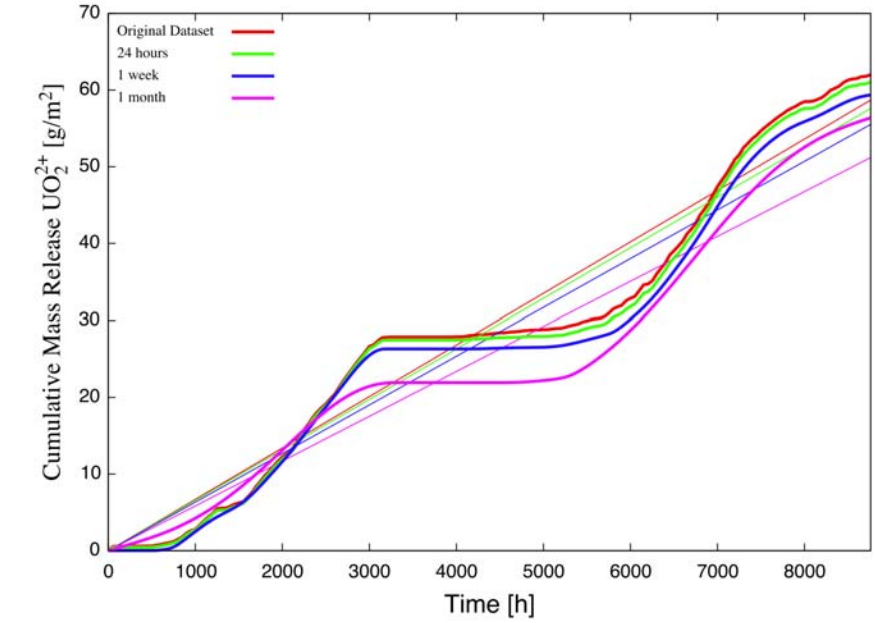

Figure 18. Comparison of flux of U(VI) into the Columbia River as a function of time for different smoothing intervals of river stage fluctuations as indicated in the figure.

seasonal variation may be most important. Adsorption reactions are expected to be of primary significance to flux during and after periods of transient water chemistry that induce desorption and adsorption events. .

CY 09 Objectives

- Work with IFRC experimental geochemists to incorporate and parameterize the most current and robust models for U(VI) source terms in the lower vadose, smear, and saturated zones.
- Develop and add isotopic exchange routine to PFLOTRAN
- Carry out 3D simulations of U(VI) migration with multicomponent chemistry using a site-scale model of the 300 A.
- Refine grid resolution using adaptive mesh refinement
- Simulate U(VI) fall 2009 desorption injection experiment and compare with experimental observations
- Support parallel implementation of MAD to allow for computation of hundreds of thousands of realizations
- Include the Columbia River boundary in IFRC site model in order to better understand role of mixing of river water and groundwater

4.) Hydrologic and Transport Modeling with MODFLOW and MT3DMS – Dr. Chunmiao Zheng (UA)

The main objectives of our research activities in the past year were to develop a sound conceptual model for the flow and reactive transport processes at the IFRC experimental site, design and test appropriate spatial and temporal discretization schemes for the numerical model based on MODFLOW and MT3DMS, define and test appropriate boundary conditions, and set up the numerical model for flow and reactive transport with measured hydrogeologic, transport and geochemical properties. We did not formally start the research project until we received the funding in April 2008.

From April to May 2008, we focused on testing the applicability of the MODFLOW/MT3D/PHT3D suite of codes to the Hanford IFRC site by applying MODFLOW/MT3D/PHT3D to a hypothetical model with idealized, but relevant parameters. The test demonstrated the importance of hydrodynamics and surface complexation processes on the fate and transport of uranium. In June and July 2008, we set up a small-scale IFRC site model using the head solution from the regional 300A flow model (described in the report PNNL-16396) as the boundary conditions. We only simulated the groundwater flow and conservative trace transport with an one-month stress period length from 1997 to 2004 because the same stress period length was used in the regional flow model. We found the one-month stress period length was not appropriate for the IFRC site due to the highly dynamic nature of river stage fluctuation. Thus the simulated tracer plume behavior based on an one-month stress period length would be unrealistic.

In August, pre-modeling began for the conservative tracer (November 2008) and heat transport experiments (March 2009) planned for the IFRC site later in the year. Using the existing head data outside of the IFRC plot measured between January and June 2008, we interpolated the boundary conditions and simulated hypothetical conservative tracer and heat experiments during that data period. We tried several models each lasting one month in total simulation time. The models show the effects of changing flow directions on a 1-hour interval in response to significant water level fluctuations induced by the Columbia River. With hourly boundary conditions, we found that the tracer plume lingered within the IFRC domain for a much longer time than it would under constant boundary conditions. Based on the same flow model,

we also tried a heat transport simulation. The heat plume moves slower but dissipates more rapidly than a conservative plume.

Since August, we have been pursuing a hypothesis-driven study of two-dimensional reactive transport along a cross-section through the IFRC site. The two-dimensional reactive transport model is based on the actual site hydrogeology. The cross sectional model extends the eastern boundary to the Columbia River to account for changes in aqueous chemistry from mixing of river water and groundwater. Measured hourly water levels in well 399-3-19 and at river gage SWS-1 were used for the prescribed piezometric head boundary conditions at the western end of the domain and for the river boundary at the eastern end, respectively. To account for the full complexity of the uranium transport processes observed at the 300A site, we changed from the previously tested equilibrium surface complexation model (SCM) to a multi-rate kinetic SCM based on Liu et al. (2008), and investigated its application to the cross-section. The simulations were used to assess the hypothesized importance of multi-rate processes on the fate and mobility of uranium at the 300A site, and to more generally evaluate the effect of variable chemical conditions caused by dynamic river stage fluctuations.

In the scenario used for equilibrium and multi-rate kinetic SCM model comparison, a U(VI) bearing solution was introduced as a short-term point source about 160 m from the river. The reactive transport simulation indicated that with both the multi-rate kinetic SCM and the equilibrium SCM, the U(VI) plume was strongly adsorbed by aquifer sediments and does not arrive at the river for close to 20 years. In both models river water intrusion results in complex spatio-temporal variations of water chemistry, leading to a decrease in the carbonate content of groundwater near the river, and a corresponding increase in adsorption and decrease in uranium mobility. U(VI) migration was more dynamic when controlled by the multi-rate kinetic SCM and was more coupled with the groundwater flow field. Even though the general extent of the U(VI) plume does not change significantly after one year, the plume's high concentration zone is still fairly dynamic. However, in the simulations with the equilibrium SCM, the plume shows very limited seasonal movement (**Figure 19**). Overall the results from the multi-rate SCM were more consistent with the field observations. For both models, U(VI) transport was largely constrained within the highly permeable Hanford Formation and penetration into the less permeable underlying Ringold Formation was limited. During the simulation period, adsorbed U(VI) concentrations increased in the upper Ringold Formation, thus indicating its potential role as a long-term source during desorption in the future. The effect of boundary conditions on transport with hourly, weekly and monthly water level changes was also tested using thins model. The simulation results were quite different with different frequencies of water level changes imposed on the boundary conditions. Thus, accounting for hourly variations in boundary conditions is necessary to accurately describe (VI) reactive transport at the IFRC site.

We have also been testing the unsaturated flow and transport capabilities of MODFLOW using two existing unsaturated flow packages, VSF and UZF. Given the results found, we are now collaborating with the principal author of the UZF package, Rich Niswonger of the USGS, to develop a seamless link between UZF and MT3DMS/PHT3D.

In addition to successfully incorporating the conceptual dual-domain, multi-rate surface complexation model proposed by Liu et al. (2008)[1] into the existing multi-component reactive transport model PHT3D, we have also investigated (a) whether the processes that are important at the laboratory scale are similarly important at larger spatial and temporal scales and (b) whether model complexity adequate for the laboratory scale needs to be preserved or can be simplified for field-scale investigations.

The investigation was accomplished by analyzing parameter sensitivities for different spatial and temporal scales, and by varying model complexity. Parameter sensitivities characterizing the calibrated lab-scale model of Liu et al (2008) and those for a corresponding field-scale model were calculated and compared to different objective functions (mass fluxes, cumulative mass fluxes and concentrations). For the field-scale model, additional parameter sensitivities needed to be calculated for the 1st and 2nd spatial moments.

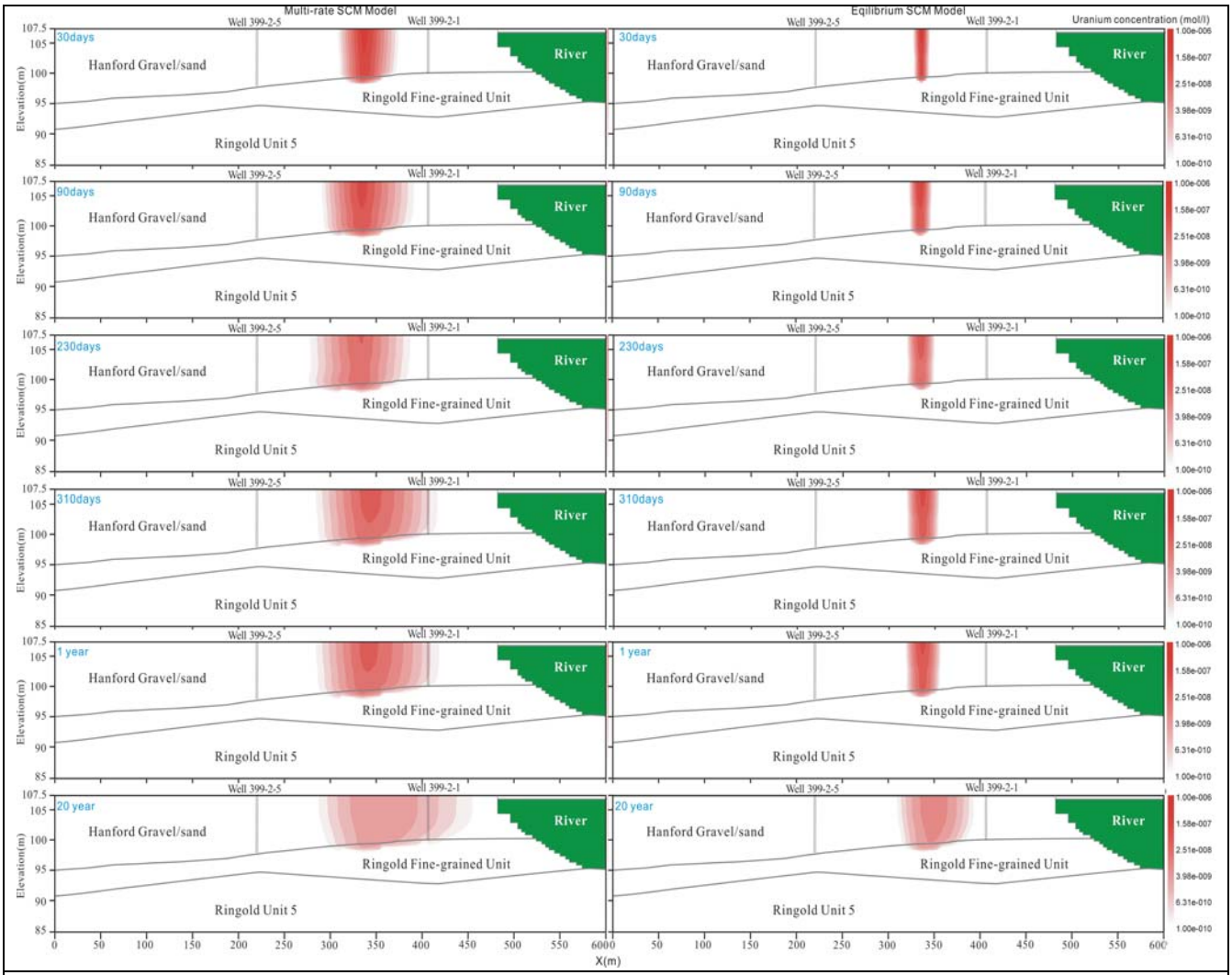

Figure 19. Comparison of uranium plumes simulated with multi-rate kinetic SCM model (left) and equilibrium SCM model (right) at different times.

[1] Liu, C., Zachara, J.M, Qafoku, N.P., Wang, Z. (2008), Scale-dependent desorption of uranium from contaminated subsurface sediments, *Water Resour. Res.*, 44, W08413, doi:10.1029/2007WR006478.

Preliminary results indicated that the composite scaled sensitivities calculated from the different objective functions are very similar (**Figure 20**). For the sensitivity analyses of the field scale model, a 1-dimensional, groundwater flow and reactive transport model was set up for a 500m long aquifer section (East-West direction). The model integrates a highly dynamic groundwater flow regime for a 1 year simulation period. The computation of the parameter sensitivities and variations of model complexities are currently in progress.

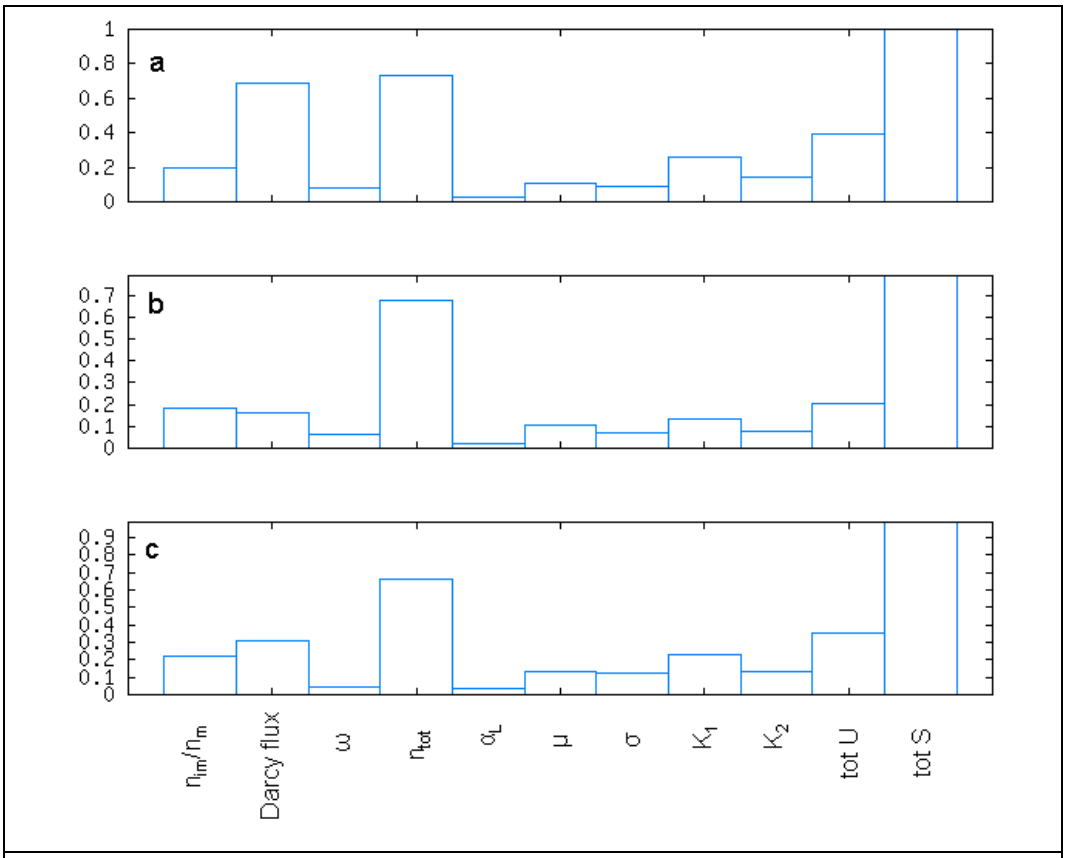

Figure 20. Composite scaled sensitivities calculated from (a) effluent U(VI) concentrations, (b) mass flux and (c) cumulative mass flux at the column outlet for the lab scale model.

CY 09 Objectives:

- Complete the addition of variably saturated flow conditions to MT3DMS and PHT3D so they can be applied to simulate multi-species/multi-component reactive transport in both vadose and saturated zones.
- Update the hydrologic model for the IFRC plot with measured filed data. Calibrate the flow and transport model using experimental data from the completed tracer test, including temperature measurements and concentration data. Explore the role of small-scale preferential flow paths in multi-scale mass transfer processes.
- Verify the applicability of the PHT3D reactive transport code to model U(VI) fate and multi-rate mass transfer processes at the IFRC experimental site using both laboratory and field data.

Implement multi-rate mass transfer as linked to and controlled by both physical heterogeneity and aqueous chemistry in the MT3DMS and PHT3D codes with due consideration of scale issues.

- Apply MT3DMS and PHT3D to the March 2009 multiple tracer saturated zone experiment, and to the fall 2009 U(VI) desorption experiment to explore, validate and/or otherwise modify the central hypothesis concerning the effects of small-scale preferential flow paths on multi-scale mass transfer processes and their implications for U(VI) fate and transport.
- Complete the investigation on scale dependent sensitivities of key parameters in the dual-domain multi-rate kinetic surface complexation model.

Project Management

Management and operations of the Hanford IFRC have proceeded without major problems during CY 08. To large extent this has resulted from active oversight by the P.I. who is committed to the success of this project, and who is familiar and experienced in working with a multidisciplinary team with different perspectives. There have been some challenging issues over the past year that were successfully resolved. These have included:

1.) Completing the well field within budget without compromising technical requirements, while dealing with a testy and difficult subcontractor.

2.) Initiating meaningful collaborations between investigators and getting all to share new unpublished data between project participants for mutual and project benefit.

3.) Uniting a modeling team containing members with vested interests in three different reactive transport models.

Site completion, lab/field characterization, laboratory experimentation, modeling, and project spending has proceeded as planned. The project overall is on schedule with milestones, although there is delay in the completion of two important project planning documents: the Hanford IFRC Modeling Plan and the Hanford IFRC Experimental Plan. The modeling plan is nearing completion and has been delayed by its complexity, and the fact that it involves many of our external collaborators that use different models. The experimental plan has been delayed by the need for substantive hydrologic and geochemical characterization data from the site. This information is now becoming available, and will allow plan completion by the ERSD contractors meeting in April. Characterization results obtained to date have both affirmed, and changed past conceptual models of the site in ways that will revise previous scientific plans. Fortunately these changes to the site conceptual hydrologic and geochemical models increase the scientific merit of the IFRC.

RESEARCH PLANS: NEXT 12 MONTHS

The following are important research activities that will be conducted over the next 12 months:

- Porosity and density geophysical logging of all wells will be performed by the USGS in March or April 2009.

- Phase I laboratory measurements of physical and chemical properties will be completed and results subject to geostatistical and multivariate statistical analysis.
- Preliminary uranium surface complexation and mass transfer models will be developed, parameterized for IFRC site sediments, and incorporated into IFRC reactive transport models.
- Cross-hole, electrical resistance tomography (ERT) measurements will be completed on all 745 electrodes in the IFRC well field, and measurements inverted using INL's FE code. The results will define the 3D distribution of electrofacies for the experimental site.
- Laboratory measurements will be completed on the K/U/T isotope and electrical properties of IFRC vadose zone and saturated zone sediments (through PNNL SFA) to allow the derivation of correlations between a.) spectral gamma logging results and b.) electrofacies defined by ERT and other measurements with sediment particle size distribution.
- Laboratory reactive transport experiments will be completed and modeled that use intact IFRC sediment cores and that investigate the desorption kinetics of contaminant U(VI), and the adsorptive retardation of spiked U(VI) at concentrations relevant to IFRC site groundwaters (through PNNL SFA). The data and model parameters so derived will enable accurate premodeling of U(VI) desorption and adsorption field experiments.
- Three major saturated zone experiments will be completed including: multi NR tracer, cold water injection (March, 2009); passive during rising and falling water table (May-July, 2009); and desorption RT injection (September 2009). Each of these will require significant premodeling to optimize experimental design.
- Numerous physical, geologic, geophysical, and hydrogeologic data sets will be assimilated and integrated within MAD, the primary IFRC inversion model developed by UCB, to define a 3-D site model for hydraulic conductivity and other flow parameters. Numerical manipulations of the large data sets will be facilitated by Lichtner and Hammond through a combination of IFRC and SciDAC support.
- Comprehensive transport analyses and modeling will be performed of the saturated zone experiments by various members of the IFRC modeling team.
- Trial push-pull type experiments for small-scale, in-situ microbiologic and kinetic reaction studies in the lower K zone will be performed during the spring and summer of 2009 to assess their potential utility in the experimental program.
- Trial, small scale cold-water injection type experiments will be tested in the spring and summer of 2009 for their ability to probe variations in hydrologic properties between groupings of nearby wells.
- In collaboration with the PNNL SFA, a variety of different type of in-situ experimental cells (containing various redox sensitive minerals, basalt coupons, and other colonization surfaces) will be deployed in select IFRC wells for the study of aquifer biogeochemical processes.

OUTREACH ACTIVITIES

During the past year, the IFRC has provided information for proposal preparation and statements of "collaboration intent" or "sample availability for a number of new proposals submitted to ERSD's FY 08 university calls. We have also agreed to provide intact IFRC core materials to Gilles Bussod of New England Nuclear in support of his Phase II SBIR proposal on core-scale imaging. Bussod spent two days visiting in October 2008 where we discussed possible applications of his core-scale imaging and

processing capabilities to IFRC cores. IFRC sediments were provided to: i.) Ken Kemner for ANL Scientific Focus Area (SFA) research, ii) Frank Loffler of Georgia Tech. University for PNNL SFA research, and iii.) Brad Tebo of Oregon Health and Science University for proposed ERSP research. A full inventory of IFRC sediments collected during the drilling campaign, including those from the deep microbiology borehole, has been posted on the web. Many of these samples are available to ERSD investigators, should they request them.

The LBNL isotope geochemistry group (Christensen and Conrad) has been extremely helpful and responsive in performing rapid turn-around, high precision U isotopic measurements of IFRC well waters. Their measurements allow us to protect the isotopic integrity of groundwater within the IFRC well field for future high-impact isotopic exchange experiments. They have begun as IFRC-funded project participants in FY 09.

The IFRC project continues its interactions with DOE EM-20 and DOE Richland Operations focused on investigation and remediation of the 300 Area plume. The IFRC project participates in routine monthly meetings with other PNNL staff, CHPRC, DOE Richland Operations, and the local Environmental Protection Agency office regarding activities in the 300 Area. In particular, DOE Richland Operations awaits the results from IFRC characterization measurements and field experiments to update the conceptual models of aquifer hydrology and uranium resupply and transport in the 300 Area. The Hanford site remediation contractor (CHPRC) has assumed responsibility for a field-scale infiltration test of the polyphosphate remediation technology at a site near the footprint of the North Process Pond adjacent to the location where the saturated zone injection polyphosphate injection test was conducted (see **Appendix 4**). Results from this field test will be useful for planning future IFRC vadose zone experiments.

On September 17, the IFRC project team worked with DOE Richland Operations and the BER-ERSD team to issue a press release and hold a media event at the completed IFRC field site. At the time of the event, a number of activities were underway and several local TV stations, the local newspaper, and National Public Radio participated. Interviews were aired on local TV and NPR as well as published in the Tri City Herald. The release was featured in over 20 venues (list sent to ERSD) and the feedback was uniformly positive.

Site tours and discussions were given to Dr. Anna Palmisano of BER and several student-professor groups from Washington State University, Montana State University, and the University of Montana. During the last quarter, the IFRC project hosted another TV interview crew from PBS who were preparing a documentary film on groundwater at Hanford. This site visit included Matt McCormick, the DOE Richland Operations Associate Manager for Central Plateau. Linkages between the IFRC project and remediation activities in the 300 Area were discussed. We were told the clip would air after January 1, 2009, but we have not heard a final date.

During January, 2009, several presentations on the IFRC project were made to the Hanford Advisory Board, CHPRC management, DOE Richland Operations management, and the Washington State Department of Ecology. These groups represent the Hanford Site stakeholder community, both internal to DOE and external, including Native American Tribes and public interest groups. The presentations were well received, and again, the feedback was positive. Another briefing is planned for Hanford 300 A remediation contractors and regulators (U.S. EPA and WA-DOE) on February 24, 2009.

CHALLENGES/OPPORTUNITIES/CONCERNS

Challenges

The Hanford IFRC has four primary challenges for CY 2009.

1.) Maximizing Internal Project Collaborations and Joint Publications: Since its inception, the Hanford IFRC was viewed as a collaborative project, where an interactive team would develop and characterize a state of the art field site, design and perform unique and sophisticated field experiments, and interpret and model the field results to yield new scientific insights on field scale subsurface processes with emphasis on mass transfer. Over the past year we have had problems realizing this spirit of advanced collaboration that is essential for project success. However, significant progress has been made in resolving this issue after elevating it to primacy with all Hanford IFRC principles. While we now have momentum in our collaborations and planned joint publications, it is clear that continued vigilance is necessary to nurture this important project aspect.

2.) Designing the most rigorous and scientifically advanced field experiments possible in the face of hydrologic complexity: Our first tracer experiment was very successful, but it did reveal the presence of considerable hydrologic complexity resulting from hourly and daily river stage variations. Such variations appear to have unexpected influences on the migration behavior of U(VI) within the aquifer. While we expected this, and have developed rigorous modeling approaches using different codes to describe this dynamic hydrologic system, questions remain on the nature, identity, and design of saturated zone experiments that should be performed at the Hanford IFRC site that will yield the highest scientific payoff. We will be discussing this important issue with ERSD, and may propose a workshop during the summer of CY 09 to review our experimental plan, and the different motivating research questions and designs for saturated zone experiments.

3.) Determining need for additional infrastructure developments: During CY 08 we completed installation and testing of our saturated zone experimental site. While it is a world-class facility; some additional and limited infrastructure improvements may be needed. These could include additional wells screened over specific depth intervals to improve depth specific resolution; or new line of wells at larger distances from the injection source. This issue presents challenge as the well installation process at Hanford is lengthy and expensive. We will report on our evaluation of this need at the end of CY 09 after completion of multiple non-reactive and reactive tracer field experiments. Hopefully, no further well installation will be needed.

4.) Improving coordination with EM, and EM-supported PNNL investigators: An important goal for the Hanford IFRC is to transfer fundamental ERSD science advances made at the 300 A site to EM for improved site remediation. However, in spite of multiple attempts to do so, we have had limited success in engaging with our EM-funded counterparts both at PNNL and the broader Hanford site. There are a number of reasons for this. During CY 2009 we will continue our: i.) proactive solicitations for meaningful collaboration and science transfer with EM, and ii.) active and open communication policy and willingness to share results and advances with all reasonable Hanford interest groups. Maybe we will report success in next year's annual report.

Opportunities

Given its infrastructure and site attributes, the Hanford IFRC has a unique opportunity within the world-wide scientific community to investigate and understand a complex linked groundwater-river system with dynamic, coupled hydrologic, geochemical, and microbiologic processes. Opportunities exist to identify the best and most effective ways to characterize inaccessible subsurface systems with transients in hydrologic and geochemical conditions at scales in excess of 50 m, and to model them in the most robust manner that accounts for multiple process interactions, properties and processes uncertainties, and heterogeneities of different sort. The Hanford IFRC functions as a unique laboratory to assess how well documented microscopic geochemical and transport processes manifest themselves in a complex field setting; and to evaluate, refine, and improve upon geophysical methodologies and inversion modeling for extended 3D subsurface properties characterization. Moreover, well-conceived field experiments will provide lasting and robust field measurements and extensive data sets to test the most advanced new models of reactive chemical transport and biogeochemical interactions and contaminant transformations.

Hanford Columbia River corridor sites have marked similarities and great complexities in hydrologic, geochemical, and microbiological processes; and are the final discharge points for Hanford contaminants to the Columbia River where contact with human and ecologic receptors may occur. If properly conceptualized and performed, Hanford IFRC science and resulting field-scale models could lead to significant cost savings in remediation, and much improved long term reductions in risk. With proper planning, this positive impact to site closure can be achieved while simultaneously making strong and lasting fundamental scientific contributions via publication and accessible field experiment data sets for understanding of coupled mass transfer, geochemical, biogeochemical, and transport processes in subsurface environments. Achieving these important multiple and synergistic impacts is a primary project goal.

PRESENTATIONS

Zhang, Z., H. Murakami, W. Nowak, and Y. Rubin. 2008. Data assimilation for stochastic site characterization and conditional simulation. Presented at the 3rd Annual DOE-ERSP PI Meeting, Lansdowne, VA.

Zhang, Z., and Y. Rubin. 2008. Gaussian random field inverse modeling with the method of “anchored distributions” (MAD) in statistical issues in monitoring the environment. A Workshop on Environmetrics, NCAR, Boulder, CO.

Zhang, Z., and Y. Rubin. 2008. MAD: A new method for inverse modeling of spatial random fields with applications in hydrogeology. Presented at the AGU Fall Meeting, December 2008, San Francisco, CA.

Rubin, Y. 2009. The MAD concept and its applications in hydrogeology. Invited seminar, Chevron Research Center, San Ramon, CA.

Ma, R., C. Zheng, H. Prommer, J. Zachara, C. Liu, and M. Rockhold. 2008. Modeling uranium fate and transport at the Hanford Integrated Field Challenge Site. Presented at the “MODFLOW and More 2008” International Conference, Golden, CO.

Zheng, C. and M. Rui. 2008. Modeling uranium fate and transport at the Hanford site: An integrated field challenge. Invited keynote talk at the International Groundwater Forum 2008, Changchun, China.

Ma, R., C. Zheng, H. Prommer, J. Greskowiak, C. Liu, J. Zachara, and M. Rockhold. 2008. A Preliminary assessment of the effects of river water dynamics and chemistry on uranium fate and transport at the Hanford 300A site. Presented at AGU Fall Meeting, San Francisco, CA.

Ma, R., C. Zheng, H. Prommer, and J. Greskowiak. 2008. A Preliminary assessment of the effects of river water dynamics and chemistry on uranium fate and transport at the Hanford 300A site, 0850, AGU Fall Meeting, San Francisco, CA.

Ma, R., C. Zheng, H. Prommer, J. Greskowiak, C. Liu, J. Zachara, M. Rockhold. 2009. Modeling field-scale multi-rate surface complexation reactions to quantify their impact on uranium mobility at the Hanford site. Abstract accepted for ModelCARE 2009 (The 7th International Conference on Calibration and Reliability in Groundwater Modeling "Managing Groundwater and the Environment").

Greskowiak, J., H. Prommer, C. Liu, V.E.A. Post, R. Ma, C. Zheng, J. Zachara. 2009. Scaling effects on parameter sensitivities in a dual-domain, multi-rate reactive transport system. Abstract accepted for ModelCARE 2009.

Hammond, G. and P. Lichtner. 2008. Massively parallel ultrascale subsurface simulation. Computational Methods in Water Resources XVII July 6-10, 2008.

Hammond, G. E., P. C. Lichtner, R. T. Mills, and C. Liu. 2008. Toward petascale computing in geosciences: Application to the Hanford 300 A – art. No.012051. *Journal of Physics Conference Series*, 125:12051-12051.

Versteeg, R. 2008. Web centric data management for the Hanford 300 Area IFC. *Eos Trans. AGU*, 89(53), Fall Meet. Suppl, Abstact IN23B-1083.

Yin, J., R. Haggerty, and J. D. Istok. 2008. Experimental investigation of the effect of transient groundwater flow on dispersion, *Eos Trans. AGU*, 89(52), Fall Meet. Suppl., Abstract H41C-0888.

Zachara, J. M., J. Davis, J. McKinley, D. Singer, J. Stubbs, G. E. Brown, Z. Wang, and J. –F. Boily. 2008. Frontiers in environment remediation research. Presentation given at the Synchrotron Environmental Science IV Conference, San Francisco, CA.

Zachara, J. M., M. Rockhold, J. K. Fredrickson, V. Vermeul, A. Ward, C. Liu, J. McKinley, B. Bjornstad, M. Freshley, R. Haggerty, D. Kent, P. Lichtner, Y. Rubin, R. Versteeg, and C. Zheng. 2008. Hanford's 300 Area Integrated Field Research Challenge Site. Poster given at the American Geophysical Union Fall Meeting, San Francisco, CA.

PUBLICATIONS

Liu, C., J. M. Zachara, N. P. Qafoku, Z. Wang. 2008. Scale-dependent desorption of uranium from contaminated subsurface sediments. *Water Resour. Res*., 44, W08413, doi:10.1029/2007WR006478.

Liu, C., S. Shi, and J.M. Zachara. 2009. Kinetics of uranium (VI) desorption from contaminated sediments: Effect of geochemical conditions and model evaluation. *Environmental Science and Technology* (Submitted).

Stoliker, D., J. A. Davis, and J. M. Zachara. 2009. Characterization of metal contaminated sediments: Distinguishing between samples with sorbed and precipitated metal ions. *Environmental Science and Technology* (Submitted).

Singer, D. M., J. M. Zachara, and G. E. Brown. 2009. Uranium speciation as a function of depth in contaminated Hanford Site sediments – A micro-XRF, micro-XAFS, and micro-XRD study. *Environ. Sci. & Technol.*, 43:630-636.

Stubbs, J. E., L. A. Veblen, D. C. Elbert, J. M. Zachara, J. A. Davis, and D. R. Veblen. 2009. Newly recognized hosts for uranium in the Hanford Site vadose zone. *Geochimica et Cosmochimica Acta* (In press).

Versteeg, R., and T. Johnson. 2008. Using time lapse geophysics to monitor subsurface processes. *The Leading Edge*, 27(11):1488-1497.

Um, W., J. M. Zachara, C. Liu, and D. Moore. 2009. Resupply mechanism to a contaminated aquifer: A laboratory study of U(VI) desorption from capillary fringe sediments. *Geochimica et Cosmochimica Acta* (Submitted).

Zhang, Z. and Y. Rubin. 2009. Inverse modeling of spatial random fields using anchors. *Water Resources Research* (Submitted).

Appendix 1

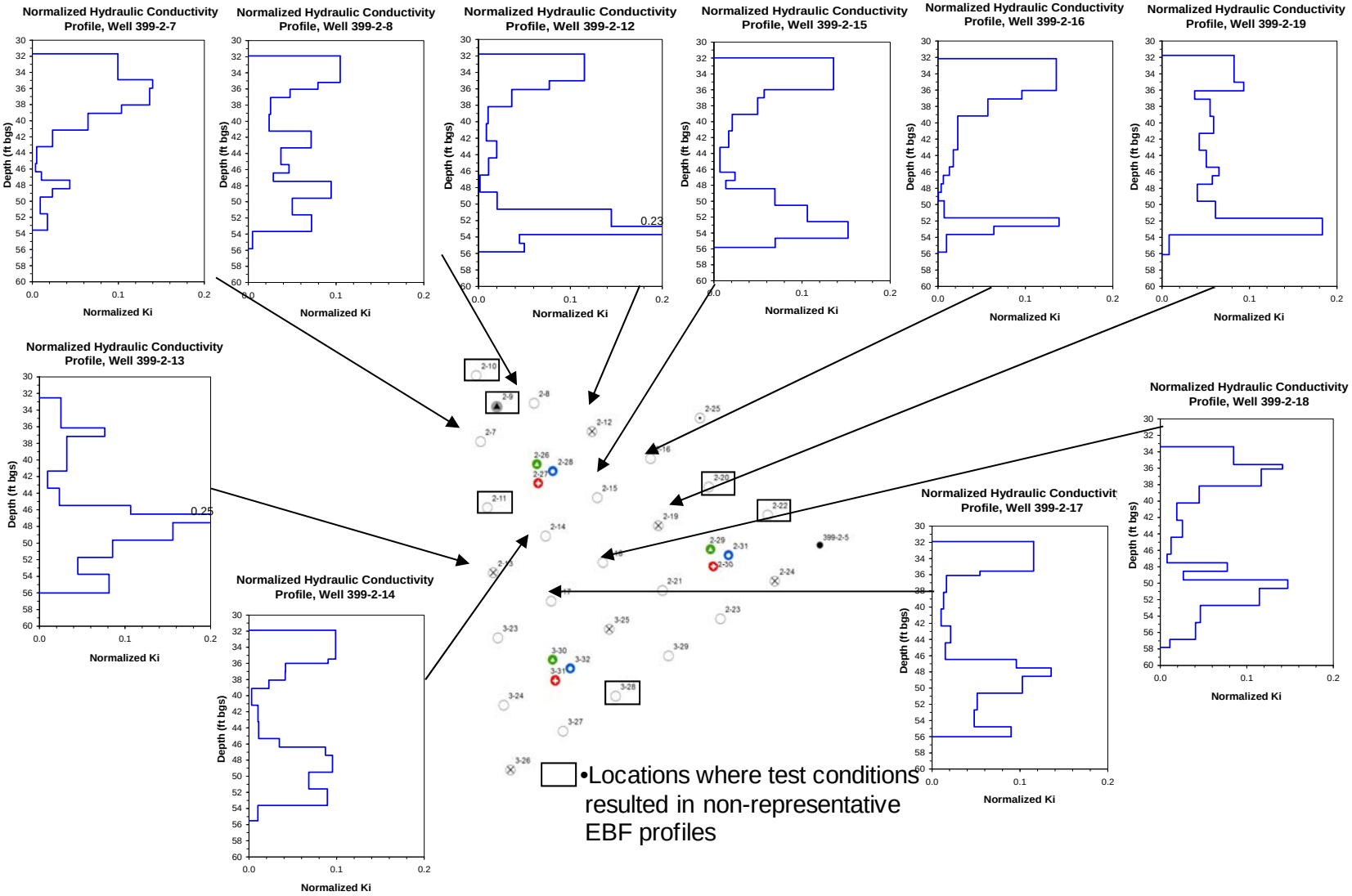

Figure A1-1. EBF profiles.

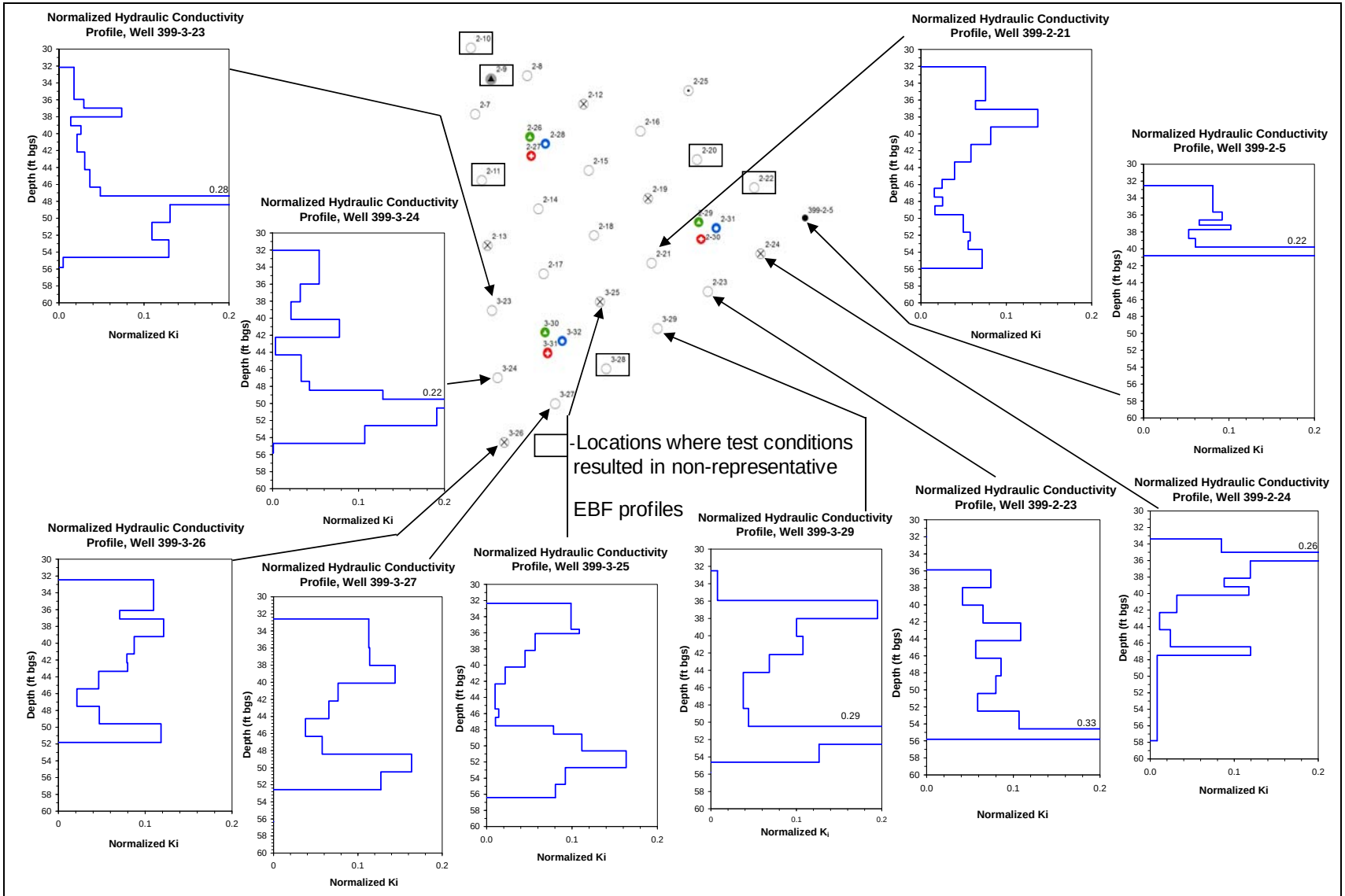

Figure A1-2. EBF profiles.

Appendix 2: Test Plan for IFRC Baseline Groundwater Sampling Using the Central Sampling Laboratory and Automated in Situ Ready-Flow Pumps

IFRC Hanford	Reference: IFRCJPM-003 December 29, 2008
BL3, Baseline Groundwater Sampling, December 31, 2008 Written To File: IFRCJPM003_BL3BaseLineGroundwaterSamplingDecember2008	
Author: J.P. McKinley	

Introduction

This document presents instructions for baseline groundwater sampling and analysis for the Hanford IFRC, for sampling to occur on about December 31, 2008. Tom Resch and Brad Fritz are scheduled to do this work, with assistance from Dave Kennedy.

Work Instructions

A. General quality control:

1.) In the field, collect a sample of de-ionized filtered water (transported from the laboratory) as a field blank (Millipore, Inc, Milli-Q grade de-ionized water).
2.) Use filters that have been qualified as previously described by serial filtration of a known U-spiked synthetic groundwater. (If necessary, for each batch of (Millipore Teflon IC Millex-LG, cat # SLLGC25NS, lot # R8MN19634) filters received, conduct a serial dilution, with sub-sampling at each step, of 20 ml of U-spiked synthetic groundwater solution. This step is to assure the absence of U loss to the filters.) Document results with test results, including filter name and lot number.
3.) Designate samples BL-3 for reference.

B. Field sampling:

1.) Sample the full suite of IFRC wells using the central sampling manifold at the site.
2.) Sample each well as before.
3.) For isotopic measurements: filtered samples in plastic wide mouth 125ml high density polyethylene bottles (Nalgene cat # 2104-0004) rinsed 3X with Milli-Q deionozed water and filled with minimal head space.
4.) For Cation analyses: filtered, HNO_3-acidified samples. Use sterile 15 mL polypropylene screw capped centrifuge tubes (Corning cat # 430766) containing 0.3 milliliters of 70% double distilled

nitric acid, GFS Chemicals, Inc, cat # 621, lot # P889768. Fill with minimal head space. Fill with minimal head space.

5.) For anion analyses: filtered, unacidified samples. Use sterile 15 mL polypropylene screw capped centrifuge tubes (Corning cat # 430766). Fill with minimal head space.
6.) For U(VI) KPA analysis: Use nitric acid acidified filtered cation sample. In addition, take an unacidified filtered U(VI) sample using sterile 15 mL polypropylene screw capped centrifuge tubes (Corning cat # 430766). Fill with minimum headspace. Check difference of acidified verses unacidified U(VI) sample by KPA analysis.
7.) For carbon analyses: carbon analyzer autosampler vials. Use 40 mL VOA QA level 1 clear glass vials with Teflon septum caps, EP Science Products, cat # 140-40C/DB, lot # B8141130. Fill with minimal head space.
8.) For microbiological experimentation, collect unfiltered samples in provided sterile, polypropylene 50 ml corning tubes (Fisher Scientific #05-539-9) with 1ml 50% glutaraldehyde, Electron Microscopy Sciences, Ft. Washington, PA, cat# 16316, lot # 540218. Fill to 50ml mark for 1% glut fixation.
9.) Measure and record pH in the field.

C. Laboratory Analyses

1.) Store samples under refrigeration.
2.) Immediate analyses, using ICP, IC, C analyzer, KPA, microbial characterization, and isotopic methods at LBL, will be limited to samples from the following wells:
    a. 2-26, 2-27, 2-28, and 2-10
    b. 2-29, 2-30, 2-31, and 2-5
    c. 3-30, 3-31, 3-32, and 3-26
    d. Analyze field blank and ASGW-1
3.) Other analyses will be done as results indicate. If the stored samples are of little interest, they will be discarded 60 days after sampling.

D. Microbiology Samples

Transfer gluteraldehyde-fixed samples to Dave Kennedy.

Source Information/References

Synthetic groundwater formulation, WTF: IFRCJPM-002.

Appendix 3

BL1-300 Area IFC pumped water samples taken September 2, 2008
Samples rerun ion chromatograph and on ICP-OES Oct 25 through Oct 27th 2008.

		Acidified HNO3		Acidified HNO3 ICP-OES		
Well Name	Sample ID	KPA U (ug/L)	Inorganic carbon (mg/L)	S (ug/L)	P (ug/L)	Ba (ug/L)
399-2-2	BL1-2-2	109.76	29.38	18899	252	62
399-2-3	BL1-2-3	61.63	30.45	19935	180	62
399-1-7	BL1-1-7	65.59	29.51	18900	878	49
399-2-1	BL1-2-1	90.65	29.08	17755	< 100	75
399-3-18	BL1-3-18	99.12	29.01	18386	204	75
399-3-20	BL1-3-20	69.62	31.47	19129	155	65
399-3-12	BL1-3-12	39.71	29.08	16697	< 100	47
399-2-9	BL1-2-9	43.62	31.21	18520	< 100	50
399-2-10	BL1-2-10	40.40	30.81	18444	130	50
399-2-8	BL1-2-8	43.73	30.74	19008	132	51
399-2-7	BL1-2-7	45.41	30.69	19186	< 100	49
399-2-11	BL1-2-11	43.63	30.78	18848	< 100	50
399-2-26	BL1-2-26	56.13	32.65	18705	< 100	55
399-2-27	BL1-2-27	42.47	31.27	19387	< 100	53
399-2-28	BL1-2-28	52.29	31.45	19384	< 100	63
399-2-12	BL1-2-12	42.05	30.42	18646	< 100	55
399-2-16	BL1-2-16	44.73	30.58	18958	< 100	54
399-2-15	BL1-2-15	44.68	30.80	19061	< 100	56
399-2-14	BL1-2-14	52.37	31.84	19282	101	57
399-2-13	BL1-2-13	41.85	30.74	19063	101	54
399-3-23	BL1-3-23	41.50	30.63	19287	106	56
399-2-17	BL1-2-17	40.88	30.78	18778	< 100	55
399-2-18	BL1-2-18	49.63	31.68	19391	< 100	59
399-2-19	BL1-2-19	40.60	30.79	19036	< 100	56
399-2-20	BL1-2-20	48.79	31.93	19525	< 100	60
399-2-22	BL1-2-22	40.23	30.78	19140	< 100	56
399-2-31	BL1-2-31	39.78	32.27	21557	< 100	62
399-2-29	BL1-2-29	60.23	31.36	18983	< 100	63
399-2-30	BL1-2-30	41.32	30.76	19316	< 100	59
399-2-21	BL1-2-21	43.74	31.07	19107	< 100	56
399-3-25	BL1-3-25	42.61	30.91	19317	< 100	58
399-3-31	BL1-3-31	41.99	31.11	19073	< 100	54
399-3-30	BL1-3-30	64.79	32.04	19025	< 100	62
399-3-32	BL1-3-32	48.89	31.21	19455	< 100	66
399-3-24	BL1-3-24	42.55	30.06	18727	< 100	53
399-3-26	BL1-3-26	44.30	30.30	19425	< 100	52
399-3-27	BL1-3-27	41.77	30.29	19267	< 100	55
399-3-28	BL1-3-28	40.96	30.46	19481	< 100	57
399-3-29	BL1-3-29	42.94	30.93	19106	< 100	58
399-2-23	BL1-2-23	44.25	30.49	19739	< 100	60
399-2-24	BL1-2-24	48.37	31.46	19183	< 100	59
399-2-5	BL1-2-5	51.17	31.13	19606	< 100	62

BL1-300 Area IFC pumped
Samples rerun ion chroma

Well Name	Sample ID	Fe (ug/L)	Si (ug/L)	Mn (ug/L)	Cr (ug/L)	Mg (ug/L)
399-2-2	BL1-2-2	< 50	10975	< 5	< 5	12013
399-2-3	BL1-2-3	< 50	11893	< 5	< 5	12080
399-1-7	BL1-1-7	< 50	12769	< 5	< 5	12158
399-2-1	BL1-2-1	< 50	9226	8	< 5	11209
399-3-18	BL1-3-18	< 50	10316	< 5	< 5	11577
399-3-20	BL1-3-20	< 50	13631	< 5	9	12051
399-3-12	BL1-3-12	< 50	15142	32	< 5	11196
399-2-9	BL1-2-9	< 50	14927	< 5	6	12028
399-2-10	BL1-2-10	< 50	14944	< 5	6	11975
399-2-8	BL1-2-8	< 50	14877	< 5	7	12360
399-2-7	BL1-2-7	< 50	15012	< 5	7	12336
399-2-11	BL1-2-11	< 50	14416	< 5	7	12211
399-2-26	BL1-2-26	< 50	14003	< 5	7	12523
399-2-27	BL1-2-27	109	14525	6	8	12531
399-2-28	BL1-2-28	< 50	13612	< 5	10	12104
399-2-12	BL1-2-12	< 50	14612	< 5	6	12164
399-2-16	BL1-2-16	< 50	14842	< 5	6	12349
399-2-15	BL1-2-15	< 50	14850	< 5	7	12653
399-2-14	BL1-2-14	< 50	14149	< 5	7	12273
399-2-13	BL1-2-13	< 50	14838	< 5	9	12201
399-3-23	BL1-3-23	< 50	15083	< 5	9	12365
399-2-17	BL1-2-17	< 50	15023	< 5	8	12363
399-2-18	BL1-2-18	< 50	14133	< 5	9	12567
399-2-19	BL1-2-19	< 50	14724	< 5	7	12377
399-2-20	BL1-2-20	< 50	13986	< 5	12	12994
399-2-22	BL1-2-22	< 50	14408	< 5	7	12377
399-2-31	BL1-2-31	< 50	12014	< 5	6	11498
399-2-29	BL1-2-29	< 50	13089	< 5	10	11782
399-2-30	BL1-2-30	< 50	14522	< 5	6	12470
399-2-21	BL1-2-21	< 50	14413	< 5	9	12602
399-3-25	BL1-3-25	< 50	14763	< 5	9	12572
399-3-31	BL1-3-31	< 50	14654	< 5	9	12279
399-3-30	BL1-3-30	< 50	13747	< 5	7	12073
399-3-32	BL1-3-32	< 50	13572	< 5	10	12087
399-3-24	BL1-3-24	< 50	14623	< 5	8	12080
399-3-26	BL1-3-26	< 50	14926	< 5	9	12244
399-3-27	BL1-3-27	< 50	15000	< 5	9	12212
399-3-28	BL1-3-28	< 50	14810	< 5	8	12517
399-3-29	BL1-3-29	< 50	14564	< 5	9	12472
399-2-23	BL1-2-23	< 50	14295	< 5	9	12840
399-2-24	BL1-2-24	< 50	13411	< 5	12	12490
399-2-5	BL1-2-5	< 50	14017	< 5	10	12505

BL1-300 Area IFC pumped
Samples rerun ion chroma

Well Name	Sample ID	Ca (ug/L)	Al (ug/L)	Na (ug/L)	K (ug/L)	Sr (ug/L
399-2-2	BL1-2-2	48241	< 50	22364	4325	254
399-2-3	BL1-2-3	46873	< 50	23057	4631	255
399-1-7	BL1-1-7	47440	< 50	23328	4568	255
399-2-1	BL1-2-1	47180	< 50	19989	4100	236
399-3-18	BL1-3-18	47313	< 50	20755	4389	237
399-3-20	BL1-3-20	50386	< 50	23529	5754	261
399-3-12	BL1-3-12	45255	< 50	21007	6091	218
399-2-9	BL1-2-9	47230	< 50	23428	5969	235
399-2-10	BL1-2-10	45982	< 50	23559	5998	234
399-2-8	BL1-2-8	47274	< 50	24179	5990	244
399-2-7	BL1-2-7	48221	< 50	23469	6023	246
399-2-11	BL1-2-11	46816	< 50	23007	5907	233
399-2-26	BL1-2-26	49161	< 50	23999	5750	254
399-2-27	BL1-2-27	49205	< 50	24022	6149	250
399-2-28	BL1-2-28	48542	< 50	23558	5815	254
399-2-12	BL1-2-12	46759	< 50	23675	6020	239
399-2-16	BL1-2-16	46898	< 50	23680	6191	239
399-2-15	BL1-2-15	48947	< 50	24098	6121	249
399-2-14	BL1-2-14	49077	< 50	23426	5843	248
399-2-13	BL1-2-13	48516	< 50	23626	6076	243
399-3-23	BL1-3-23	48598	< 50	23843	6111	244
399-2-17	BL1-2-17	48187	< 50	23896	6144	242
399-2-18	BL1-2-18	49744	< 50	24635	6052	251
399-2-19	BL1-2-19	47580	< 50	23813	6135	241
399-2-20	BL1-2-20	51154	< 50	25173	6148	265
399-2-22	BL1-2-22	48012	< 50	23516	6084	247
399-2-31	BL1-2-31	49822	< 50	30663	5733	265
399-2-29	BL1-2-29	49681	< 50	23776	5599	266
399-2-30	BL1-2-30	47282	< 50	23676	6062	245
399-2-21	BL1-2-21	48469	< 50	23806	6095	248
399-3-25	BL1-3-25	48464	< 50	23494	6118	249
399-3-31	BL1-3-31	48094	< 50	23264	6090	247
399-3-30	BL1-3-30	49175	< 50	23450	5839	257
399-3-32	BL1-3-32	50339	< 50	23278	5807	255
399-3-24	BL1-3-24	47475	< 50	23543	6066	242
399-3-26	BL1-3-26	48698	< 50	23449	6084	246
399-3-27	BL1-3-27	48029	< 50	23624	6040	247
399-3-28	BL1-3-28	48285	< 50	23888	6122	248
399-3-29	BL1-3-29	48381	< 50	23598	6068	251
399-2-23	BL1-2-23	49857	< 50	23811	6167	254
399-2-24	BL1-2-24	49948	< 50	23802	5904	256
399-2-5	BL1-2-5	50611	< 50	24618	5890	257

BL1-300 Area IFC pumped
Samples rerun ion chroma

IC unpreserved sample

Well Name	Sample ID	F (ug/L)	Cl (ug/L)	SO4 (ug/L)	NO3 (ug/L)	NO2 (ug/L)
399-2-2	BL1-2-2	370	20757	60098	31866	< 750
399-2-3	BL1-2-3	399	22603	62975	29812	< 750
399-1-7	BL1-1-7	412	21611	61006	30354	< 750
399-2-1	BL1-2-1	365	20969	57112	28719	< 750
399-3-18	BL1-3-18	353	22466	59319	29251	< 750
399-3-20	BL1-3-20	371	25307	61365	30935	< 750
399-3-12	BL1-3-12	378	23452	53760	27486	< 750
399-2-9	BL1-2-9	443	24167	60758	29015	< 750
399-2-10	BL1-2-10	435	23764	60758	29015	< 750
399-2-8	BL1-2-8	376	24150	60596	28529	< 750
399-2-7	BL1-2-7	443	24171	60566	28405	< 750
399-2-11	BL1-2-11	390	24128	60076	28534	< 750
399-2-26	BL1-2-26	421	24707	61688	29062	< 750
399-2-27	BL1-2-27	359	24447	61103	28276	< 750
399-2-28	BL1-2-28	337	25241	61464	29456	< 750
399-2-12	BL1-2-12	374	23798	60354	28348	< 750
399-2-16	BL1-2-16	377	24243	61239	28703	< 750
399-2-15	BL1-2-15	366	24520	61502	28796	< 750
399-2-14	BL1-2-14	434	24554	61094	29024	< 750
399-2-13	BL1-2-13	381	25026	61094	28970	< 750
399-3-23	BL1-3-23	428	25007	61055	29065	< 750
399-2-17	BL1-2-17	369	24790	61379	28986	< 750
399-2-18	BL1-2-18	347	24967	61514	29283	< 750
399-2-19	BL1-2-19	429	24137	61081	28653	< 750
399-2-20	BL1-2-20	388	26108	62684	30883	< 750
399-2-22	BL1-2-22	367	24664	61313	28827	< 750
399-2-31	BL1-2-31	448	25750	67833	28135	< 750
399-2-29	BL1-2-29	351	25344	62142	29780	< 750
399-2-30	BL1-2-30	368	24154	61838	28285	< 750
399-2-21	BL1-2-21	361	25017	61776	29312	< 750
399-3-25	BL1-3-25	362	24676	61342	28973	< 750
399-3-31	BL1-3-31	379	24947	61189	29210	< 750
399-3-30	BL1-3-30	353	24421	59900	28551	< 750
399-3-32	BL1-3-32	304	26137	61718	30202	< 750
399-3-24	BL1-3-24	437	24542	60376	28656	< 750
399-3-26	BL1-3-26	454	25000	60987	29222	< 750
399-3-27	BL1-3-27	382	25113	61461	29641	< 750
399-3-28	BL1-3-28	407	24766	61369	29307	< 750
399-3-29	BL1-3-29	414	24667	61654	29225	< 750
399-2-23	BL1-2-23	428	25007	61055	29065	< 750
399-2-24	BL1-2-24	396	26404	62910	30682	< 750
399-2-5	BL1-2-5	372	25768	63320	30548	< 750

BL1-300 Area IFC pumped
Samples rerun ion chroma

Well Name	Sample ID	not rerun *PO4 (ug/L)	Br (ug/L)	Temp (degrees C)	Sp. Cond (mS/cm)	dissolved oxygen (mg/L)
399-2-2	BL1-2-2	< 5000	< 750	18.0	0.438	ND
399-2-3	BL1-2-3	< 5000	< 750	17.0	0.454	ND
399-1-7	BL1-1-7	< 5000	< 750	17.9	0.407	ND
399-2-1	BL1-2-1	< 5000	< 750	17.3	0.433	ND
399-3-18	BL1-3-18	< 5000	< 750	17.2	0.441	ND
399-3-20	BL1-3-20	< 5000	< 750	19.5	0.470	ND
399-3-12	BL1-3-12	< 5000	< 750	18.5	0.434	ND
399-2-9	BL1-2-9	< 5000	< 750	18.0	0.469	6.1
399-2-10	BL1-2-10	< 5000	< 750	18.7	0.466	6.0
399-2-8	BL1-2-8	< 5000	< 750	19.3	0.471	6.1
399-2-7	BL1-2-7	< 5000	< 750	18.3	0.471	6.0
399-2-11	BL1-2-11	< 5000	< 750	18.1	0.470	5.9
399-2-26	BL1-2-26	< 5000	< 750	17.8	0.484	5.9
399-2-27	BL1-2-27	< 5000	< 750	18.1	0.477	5.7
399-2-28	BL1-2-28	< 5000	< 750	18.1	0.482	5.7
399-2-12	BL1-2-12	< 5000	< 750	18.6	0.468	5.7
399-2-16	BL1-2-16	< 5000	< 750	18.4	0.470	6.0
399-2-15	BL1-2-15	< 5000	< 750	18.5	0.475	6.0
399-2-14	BL1-2-14	< 5000	< 750	18.3	0.475	5.9
399-2-13	BL1-2-13	< 5000	< 750	18.4	0.474	6.1
399-3-23	BL1-3-23	< 5000	< 750	18.8	0.475	6.0
399-2-17	BL1-2-17	< 5000	< 750	19.0	0.474	5.6
399-2-18	BL1-2-18	< 5000	< 750	18.7	0.480	5.4
399-2-19	BL1-2-19	< 5000	< 750	19.0	0.471	5.5
399-2-20	BL1-2-20	< 5000	< 750	19.4	0.488	5.4
399-2-22	BL1-2-22	< 5000	< 750	19.8	0.475	5.5
399-2-31	BL1-2-31	< 5000	< 750	19.5	0.500	3.5
399-2-29	BL1-2-29	< 5000	< 750	19.4	0.481	5.3
399-2-30	BL1-2-30	< 5000	< 750	19.3	0.471	4.7
399-2-21	BL1-2-21	< 5000	< 750	19.2	0.478	5.6
399-3-25	BL1-3-25	< 5000	< 750	19.3	0.478	5.5
399-3-31	BL1-3-31	< 5000	< 750	19.0	0.475	5.7
399-3-30	BL1-3-30	< 5000	< 750	18.8	0.476	5.3
399-3-32	BL1-3-32	< 5000	< 750	19.1	0.481	5.1
399-3-24	BL1-3-24	< 5000	< 750	19.1	0.471	5.7
399-3-26	BL1-3-26	< 5000	< 750	19.4	0.473	5.6
399-3-27	BL1-3-27	< 5000	< 750	19.2	0.472	5.6
399-3-28	BL1-3-28	< 5000	< 750	19.1	0.475	5.6
399-3-29	BL1-3-29	< 5000	< 750	18.8	0.477	5.5
399-2-23	BL1-2-23	< 5000	< 750	18.8	0.480	5.6
399-2-24	BL1-2-24	< 5000	< 750	18.5	0.487	5.6
399-2-5	BL1-2-5	< 5000	< 750	18.4	0.487	5.6

BL1-300 Area IFC pumped
Samples rerun ion chroma

Well Name	Sample ID	pH	ORP (mv)	purge rate
399-2-2	BL1-2-2	7.3	54	L/min for 5 min
399-2-3	BL1-2-3	7.8	46	L/min for 5 min
399-1-7	BL1-1-7	8.7	19	L/min for 5 min
399-2-1	BL1-2-1	7.8	17	L/min for 5 min
399-3-18	BL1-3-18	7.5	108	L/min for 5 min
399-3-20	BL1-3-20	7.3	133	L/min for 5 min
399-3-12	BL1-3-12	8.0	83	L/min for 5 min
399-2-9	BL1-2-9	7.3	148	L/min fpr 10 min
399-2-10	BL1-2-10	7.4	116	L/min for 10 min
399-2-8	BL1-2-8	7.3	89	L/min for 10 min
399-2-7	BL1-2-7	7.2	109	L/min for 5 min
399-2-11	BL1-2-11	7.2	115	L/min for 5 min
399-2-26	BL1-2-26	7.1	114	L/min for 5 min
399-2-27	BL1-2-27	7.3	89	L/min for 5 min
399-2-28	BL1-2-28	7.1	120	L/min for 5 min
399-2-12	BL1-2-12	7.4	84	L/min for 5 min
399-2-16	BL1-2-16	7.4	88	L/min for 5 min
399-2-15	BL1-2-15	7.3	99	L/min for 5 min
399-2-14	BL1-2-14	7.1	126	L/min for 5 min
399-2-13	BL1-2-13	7.3	130	L/min for 5 min
399-3-23	BL1-3-23	7.3	100	L/min for 5 min
399-2-17	BL1-2-17	7.4	94	L/min for 5 min
399-2-18	BL1-2-18	7.2	119	L/min for 5 min
399-2-19	BL1-2-19	7.4	73	L/min for 5 min
399-2-20	BL1-2-20	7.3	105	L/min for 5 min
399-2-22	BL1-2-22	7.4	77	L/min for 5 min
399-2-31	BL1-2-31	7.4	90	L/min for 5 min
399-2-29	BL1-2-29	7.2	117	L/min for 5 min
399-2-30	BL1-2-30	7.3	110	L/min for 5 min
399-2-21	BL1-2-21	7.3	113	L/min for 5 min
399-3-25	BL1-3-25	7.3	90	L/min for 5 min
399-3-31	BL1-3-31	7.3	108	L/min for 5 min
399-3-30	BL1-3-30	7.1	107	L/min for 5 min
399-3-32	BL1-3-32	7.1	106	L/min for 5 min
399-3-24	BL1-3-24	7.3	103	L/min for 5 min
399-3-26	BL1-3-26	7.3	108	L/min for 5 min
399-3-27	BL1-3-27	7.3	94	L/min for 5 min
399-3-28	BL1-3-28	7.5	93	L/min for 5 min
399-3-29	BL1-3-29	7.3	68	L/min for 5 min
399-2-23	BL1-2-23	7.3	86	L/min for 5 min
399-2-24	BL1-2-24	7.3	101	L/min for 5 min
399-2-5	BL1-2-5	7.3	107	L/min for 5 min

BL2-300 Area IFC pumped water samples taken October 7, 2008
Samples rerun ion chromatograph and on ICP-OES Oct 25 through Oct 27th 2008.

		Acidified		Acidified HNO3 ICP-OES		
Well Name	Sample ID	KPA U (ug/L)	Inorganic carbon (mg/L)	S (ug/L)	P (ug/L)	Ba (ug/L)
399-2-9	NA					
399-2-8	BL2-2-8	40.96	30.37	16685	< 500	49
399-2-7	BL2-2-7	49.51	33.60	16973	< 500	48
399-2-11	BL2-2-11	44.82	32.34	16076	< 500	43
399-2-26	BL2-2-26					
399-2-27	BL2-2-27	46.45	32.36	17815	< 500	53
399-2-28	BL2-2-28	61.86	32.92	17915	< 500	61
399-2-12	BL2-2-12	40.03	30.59	16514	< 500	50
399-2-16	BL2-2-16	41.44	30.52	17191	< 500	48
399-2-15	BL2-2-15	42.05	30.71	16475	< 500	50
399-2-14	BL2-2-14	56.90	33.32	16752	< 500	54
399-2-13	BL2-2-13	49.73	31.94	16763	< 500	51
399-3-23	BL2-3-23	46.51	31.35	17524	< 500	52
399-2-17	BL2-2-17	42.43	30.79	17300	< 500	47
399-2-18	BL2-2-18	47.06	31.83	16848	< 500	52
399-2-19	BL2-2-19	41.74	30.78	17120	< 500	50
399-2-20	BL2-2-20	41.51	30.72	17638	< 500	48
399-2-22	BL2-2-22	40.84	30.69	17076	< 500	48
399-2-31	BL2-2-31	51.16	32.57	19678	< 500	58
399-2-29	BL2-2-29					
399-2-30	BL2-2-30	43.10	31.34	17464	< 500	53
399-2-21	BL2-2-21	42.00	30.89	17875	< 500	49
399-3-25	BL2-3-25	44.96	31.35	17813	< 500	50
399-3-31	BL2-3-31					
399-3-30	BL2-3-30					
399-3-32	BL2-3-32	63.72	33.06	18256	< 500	60
399-3-24	BL2-3-24	44.69	31.30	16733	< 500	49
399-3-26	BL2-3-26	44.81	31.18	16844	< 500	49
399-3-27	BL2-3-27	45.67	31.44	17184	< 500	47
399-3-28	BL2-3-28	45.53	31.22	17661	< 500	50
399-3-29	BL2-3-29					
399-2-23	BL2-2-23	42.65	30.86	17097	< 500	53
399-2-24	BL2-2-24	42.52	30.45	17115	< 500	53
399-2-5	BL2-2-5					

BL2-300 Area IFC pumped
Samples rerun ion chroma

Well Name	Sample ID	Fe (ug/L)	Sl (ug/L)	Mn (ug/L)	Cr (ug/L)	Mg (ug/L)
399-2-9	NA					
399-2-8	BL2-2-8	< 50	16586	< 5	< 5	11480
399-2-7	BL2-2-7	< 50	15851	< 5	< 5	11839
399-2-11	BL2-2-11	< 50	15291	< 5	< 5	10540
399-2-26	BL2-2-26					
399-2-27	BL2-2-27	< 50	16479	< 5	< 5	11177
399-2-28	BL2-2-28	< 50	14956	< 5	< 5	11404
399-2-12	BL2-2-12	< 50	15841	< 5	< 5	11314
399-2-16	BL2-2-16	< 50	15954	< 5	< 5	11444
399-2-15	BL2-2-15	101	15762	< 5	5	11296
399-2-14	BL2-2-14	81	15431	< 5	< 5	11540
399-2-13	BL2-2-13	< 50	15704	< 5	< 5	11187
399-3-23	BL2-3-23	< 50	16000	< 5	5	11600
399-2-17	BL2-2-17	< 50	15747	< 5	4	10875
399-2-18	BL2-2-18	< 50	15762	< 5	< 5	11344
399-2-19	BL2-2-19	< 50	16010	< 5	< 5	11229
399-2-20	BL2-2-20	< 50	15705	< 5	4	10665
399-2-22	BL2-2-22	< 50	15756	< 5	< 5	10730
399-2-31	BL2-2-31	< 50	13434	< 5	4	10724
399-2-29	BL2-2-29					
399-2-30	BL2-2-30	< 50	15914	< 5	< 5	11137
399-2-21	BL2-2-21	< 50	15964	< 5	4	10918
399-3-25	BL2-3-25	< 50	15942	< 5	< 5	11144
399-3-31	BL2-3-31					
399-3-30	BL2-3-30					
399-3-32	BL2-3-32	< 50	14462	< 5	5	10734
399-3-24	BL2-3-24	< 50	15814	< 5	< 5	10936
399-3-26	BL2-3-26	< 50	15472	< 5	< 5	10764
399-3-27	BL2-3-27	< 50	15715	< 5	< 5	10561
399-3-28	BL2-3-28	< 50	15830	< 5	< 5	11191
399-3-29	BL2-3-29					
399-2-23	BL2-2-23	< 50	15846	< 5	< 5	11428
399-2-24	BL2-2-24	< 50	15834	< 5	< 5	11583
399-2-5	BL2-2-5					

BL2-300 Area IFC pumped
Samples rerun ion chroma

Well Name	Sample ID	Ca (ug/L)	Al (ug/L)	Na (ug/L)	K (ug/L)	Sr (ug/L)
399-2-9	NA					
399-2-8	BL2-2-8	43259	< 50	22773	6123	217
399-2-7	BL2-2-7	46681	< 50	23148	5892	239
399-2-11	BL2-2-11	42153	< 50	21725	5558	211
399-2-26	BL2-2-26					
399-2-27	BL2-2-27	45560	< 50	22624	5761	224
399-2-28	BL2-2-28	45283	< 50	23402	5672	232
399-2-12	BL2-2-12	44920	< 50	22574	5803	224
399-2-16	BL2-2-16	43167	< 50	22860	5843	225
399-2-15	BL2-2-15	43373	< 50	22592	5835	218
399-2-14	BL2-2-14	44040	< 50	22916	5607	230
399-2-13	BL2-2-13	44452	< 50	22151	5681	222
399-3-23	BL2-3-23	45981	< 50	23372	5929	234
399-2-17	BL2-2-17	41952	< 50	22503	5753	219
399-2-18	BL2-2-18	44648	< 50	22474	5786	221
399-2-19	BL2-2-19	43735	< 50	22436	5803	222
399-2-20	BL2-2-20	42547	< 50	21852	5692	215
399-2-22	BL2-2-22	41367	< 50	22398	5773	211
399-2-31	BL2-2-31	45307	< 50	25730	5475	247
399-2-29	BL2-2-29					
399-2-30	BL2-2-30	43124	< 50	22749	5769	219
399-2-21	BL2-2-21	41782	< 50	22514	5713	217
399-3-25	BL2-3-25	43229	< 50	22461	5688	219
399-3-31	BL2-3-31					
399-3-30	BL2-3-30					
399-3-32	BL2-3-32	44067	< 50	22247	5467	230
399-3-24	BL2-3-24	43881	< 50	22192	5734	218
399-3-26	BL2-3-26	44121	< 50	21867	5649	216
399-3-27	BL2-3-27	42137	< 50	21530	5605	211
399-3-28	BL2-3-28	43821	< 50	22229	5759	218
399-3-29	BL2-3-29					
399-2-23	BL2-2-23	44327	< 50	23124	5832	225
399-2-24	BL2-2-24	43287	< 50	23242	5879	229
399-2-5	BL2-2-5					

BL2-300 Area IFC pumped
Samples rerun ion chroma

IC unpreserved sample

Well Name	Sample ID	F (ug/L)	Cl (ug/L)	SO4 (ug/L)	NO3 (ug/L)	NO2 (ug/L)
399-2-9	NA					
399-2-8	BL2-2-8	387	22718	54539	27036	< 750
399-2-7	BL2-2-7	382	22569	54900	27434	< 750
399-2-11	BL2-2-11	383	22267	53023	27911	< 750
399-2-26	BL2-2-26					
399-2-27	BL2-2-27	358	23060	56685	27647	< 750
399-2-28	BL2-2-28	348	23291	57739	27999	< 750
399-2-12	BL2-2-12	381	22794	54898	26956	< 750
399-2-16	BL2-2-16	369	22503	54981	27429	< 750
399-2-15	BL2-2-15	366	23080	55282	27549	< 750
399-2-14	BL2-2-14	395	23050	55934	28111	< 750
399-2-13	BL2-2-13	392	22479	53850	27499	< 750
399-3-23	BL2-3-23	386	23257	56936	27443	< 750
399-2-17	BL2-2-17	367	22823	55557	27505	< 750
399-2-18	BL2-2-18	357	22812	55014	26866	< 750
399-2-19	BL2-2-19	368	22640	55129	27100	< 750
399-2-20	BL2-2-20	386	23119	56517	28099	< 750
399-2-22	BL2-2-22	376	22661	55183	27422	< 750
399-2-31	BL2-2-31	437	23684	60762	26703	< 750
399-2-29	BL2-2-29					
399-2-30	BL2-2-30	422	23155	56469	26754	< 750
399-2-21	BL2-2-21	383	22862	55745	27411	< 750
399-3-25	BL2-3-25	355	23192	56044	27404	< 750
399-3-31	BL2-3-31					
399-3-30	BL2-3-30					
399-3-32	BL2-3-32	337	23709	58069	28017	< 750
399-3-24	BL2-3-24	383	22988	55180	27667	< 750
399-3-26	BL2-3-26	392	22810	54545	27257	< 750
399-3-27	BL2-3-27	387	22906	55409	27936	< 750
399-3-28	BL2-3-28	368	23086	56562	27738	< 750
399-3-29	BL2-3-29					
399-2-23	BL2-2-23	380	22851	55705	27306	< 750
399-2-24	BL2-2-24	384	22964	55779	27181	< 750
399-2-5	BL2-2-5					

BL2-300 Area IFC pumped
Samples rerun ion chroma

Well Name	Sample ID	PO4 (ug/L)	Br (ug/L)	Temp (degrees C)	Sp. Cond (mS/cm)	dissolved oxygen (mg/L)
399-2-9	NA					
399-2-8	BL2-2-8	< 5000	< 750	18.7	0.443	5.8
399-2-7	BL2-2-7	< 5000	< 750	17.8	0.459	5.7
399-2-11	BL2-2-11	< 5000	< 750	18.1	0.443	5.9
399-2-26	BL2-2-26					
399-2-27	BL2-2-27	< 5000	< 750	18.1	0.459	5.8
399-2-28	BL2-2-28	< 5000	< 750	18.1	0.458	5.7
399-2-12	BL2-2-12	< 5000	< 750	18.5	0.445	6.3
399-2-16	BL2-2-16	< 5000	< 750	18.9	0.447	6.0
399-2-15	BL2-2-15	< 5000	< 750	18.2	0.447	6.1
399-2-14	BL2-2-14	< 5000	< 750	18.3	0.456	5.9
399-2-13	BL2-2-13	< 5000	< 750	18.5	0.446	5.9
399-3-23	BL2-3-23	< 5000	< 750	18.4	0.454	6.0
399-2-17	BL2-2-17	< 5000	< 750	18.2	0.449	6.1
399-2-18	BL2-2-18	< 5000	< 750	18.8	0.453	6.2
399-2-19	BL2-2-19	< 5000	< 750	19.0	0.450	5.9
399-2-20	BL2-2-20	< 5000	< 750	19.5	0.450	5.9
399-2-22	BL2-2-22	< 5000	< 750	19.8	0.448	5.8
399-2-31	BL2-2-31	< 5000	< 750	19.6	0.469	4.7
399-2-29	BL2-2-29					
399-2-30	BL2-2-30	< 5000	< 750	19.6	0.454	4.1
399-2-21	BL2-2-21	< 5000	< 750	19.4	0.448	5.8
399-3-25	BL2-3-25	< 5000	< 750	19.4	0.452	5.9
399-3-31	BL2-3-31					
399-3-30	BL2-3-30					
399-3-32	BL2-3-32	< 5000	< 750	19.7	0.463	4.9
399-3-24	BL2-3-24	< 5000	< 750	20.1	0.448	5.7
399-3-26	BL2-3-26	< 5000	< 750	20.2	0.446	5.8
399-3-27	BL2-3-27	< 5000	< 750	19.8	0.447	5.8
399-3-28	BL2-3-28	< 5000	< 750	20.6	0.453	5.9
399-3-29	BL2-3-29					
399-2-23	BL2-2-23	< 5000	< 750	19.8	0.450	6.2
399-2-24	BL2-2-24	< 5000	< 750	20.6	0.448	5.8
399-2-5	BL2-2-5					

BL2-300 Area IFC pumped
Samples rerun ion chroma

Well Name	Sample ID	pH	ORP (mv)	purge rate
399-2-9	NA			
399-2-8	BL2-2-8	7.7	ND	L/min for 5 min
399-2-7	BL2-2-7	7.6	ND	L/min for 5 min
399-2-11	BL2-2-11	7.5	ND	L/min for 5 min
399-2-26	BL2-2-26			
399-2-27	BL2-2-27	7.5	ND	L/min for 5 min
399-2-28	BL2-2-28	7.5	ND	L/min for 5 min
399-2-12	BL2-2-12	7.7	ND	L/min for 5 min
399-2-16	BL2-2-16	7.7	ND	L/min for 5 min
399-2-15	BL2-2-15	7.7	ND	L/min for 5 min
399-2-14	BL2-2-14	7.5	ND	L/min for 5 min
399-2-13	BL2-2-13	7.4	ND	L/min for 5 min
399-3-23	BL2-3-23	7.6	ND	L/min for 5 min
399-2-17	BL2-2-17	7.7	ND	L/min for 5 min
399-2-18	BL2-2-18	7.6	ND	L/min for 5 min
399-2-19	BL2-2-19	7.7	ND	L/min for 5 min
399-2-20	BL2-2-20	7.7	ND	L/min for 5 min
399-2-22	BL2-2-22	7.7	ND	L/min for 5 min
399-2-31	BL2-2-31	7.7	ND	L/min for 5 min
399-2-29	BL2-2-29			
399-2-30	BL2-2-30	7.6	ND	L/min for 5 min
399-2-21	BL2-2-21	7.7	ND	L/min for 5 min
399-3-25	BL2-3-25	7.7	ND	L/min for 5 min
399-3-31	BL2-3-31			
399-3-30	BL2-3-30			
399-3-32	BL2-3-32	7.4	ND	L/min for 5 min
399-3-24	BL2-3-24	7.5	ND	L/min for 5 min
399-3-26	BL2-3-26	7.6	ND	L/min for 5 min
399-3-27	BL2-3-27	7.6	ND	L/min for 5 min
399-3-28	BL2-3-28	7.6	ND	L/min for 5 min
399-3-29	BL2-3-29			
399-2-23	BL2-2-23	7.7	ND	L/min for 5 min
399-2-24	BL2-2-24	7.7	ND	L/min for 5 min
399-2-5	BL2-2-5			

BL3-300 Area IFC pumped water samples taken December 31, 2008

		acidified		Acidified HNO3 ICP-OES		
Well Name	Sample ID	KPA U (ug/L)	Inorganic carbon (mg/L)	S (ug/L)	P (ug/L)	Ba (ug/L)
399-2-9	BL3-2-9	36.33	33.91			
399-2-10	BL3-2-10	29.51	32.12			
399-2-8	BL3-2-8	32.67	32.51			
399-2-7	BL3-2-7	33.18	32.38			
399-2-11	BL3-2-11	35.89	34.77			
399-2-26	BL3-2-26	48.05	33.75			
399-2-27	BL3-2-27	31.88	32.89			
399-2-28	BL3-2-28	56.75	36.16			
399-2-12	BL3-2-12	28.12	31.58			
399-2-16	BL3-2-16	28.84	31.35			
399-2-15	BL3-2-15	28.43	31.85			
399-2-14	BL3-2-14	45.54	34.77			
399-2-13	BL3-2-13	39.40	33.53			
399-3-23	BL3-3-23	29.46	31.85			
399-2-17	BL3-2-17	30.41	32.32			
399-2-18	BL3-2-18	35.35	32.25			
399-2-19	BL3-2-19	33.13	31.51			
399-2-20	BL3-2-20	42.12	32.87			
399-2-22	BL3-2-22	30.27	31.36			
399-2-31	BL3-2-31	45.18	32.60			
399-2-29	BL3-2-29	59.66	34.39			
399-2-30	BL3-2-30	30.17	31.78			
399-2-21	BL3-2-21	30.12	31.74			
399-3-25	BL3-3-25	34.57	32.78			
399-3-31	BL3-3-31	29.15	32.15			
399-3-30	BL3-3-30	54.15	34.39			
399-3-32	BL3-3-32	58.93	34.41			
399-3-24	BL3-3-24	35.15	32.83			
399-3-26	BL3-3-26	39.05	32.67			
399-3-27	BL3-3-27	31.66	32.55			
399-3-28	BL3-3-28	33.42	32.71			
399-3-29	BL3-3-29	31.99	32.19			
399-2-23	BL3-2-23	31.35	31.44			
399-2-24	BL3-2-24	37.59	32.05			
399-2-5	BL3-2-5	38.70	31.95			

BL3-300 Area IFC pumped

Well Name	Sample ID	Fe (ug/L)	Si (ug/L)	Mn (ug/L)	Cr (ug/L)	Mg (ug/L)
399-2-9	BL3-2-9					
399-2-10	BL3-2-10					
399-2-8	BL3-2-8					
399-2-7	BL3-2-7					
399-2-11	BL3-2-11					
399-2-26	BL3-2-26					
399-2-27	BL3-2-27					
399-2-28	BL3-2-28					
399-2-12	BL3-2-12					
399-2-16	BL3-2-16					
399-2-15	BL3-2-15					
399-2-14	BL3-2-14					
399-2-13	BL3-2-13					
399-3-23	BL3-3-23					
399-2-17	BL3-2-17					
399-2-18	BL3-2-18					
399-2-19	BL3-2-19					
399-2-20	BL3-2-20					
399-2-22	BL3-2-22					
399-2-31	BL3-2-31					
399-2-29	BL3-2-29					
399-2-30	BL3-2-30					
399-2-21	BL3-2-21					
399-3-25	BL3-3-25					
399-3-31	BL3-3-31					
399-3-30	BL3-3-30					
399-3-32	BL3-3-32					
399-3-24	BL3-3-24					
399-3-26	BL3-3-26					
399-3-27	BL3-3-27					
399-3-28	BL3-3-28					
399-3-29	BL3-3-29					
399-2-23	BL3-2-23					
399-2-24	BL3-2-24					
399-2-5	BL3-2-5					

BL3-300 Area IFC pumped

Well Name	Sample ID	Ca (ug/L)	Al (ug/L)	Na (ug/L)	K (ug/L)	Sr (ug/L)
399-2-9	BL3-2-9					
399-2-10	BL3-2-10					
399-2-8	BL3-2-8					
399-2-7	BL3-2-7					
399-2-11	BL3-2-11					
399-2-26	BL3-2-26					
399-2-27	BL3-2-27					
399-2-28	BL3-2-28					
399-2-12	BL3-2-12					
399-2-16	BL3-2-16					
399-2-15	BL3-2-15					
399-2-14	BL3-2-14					
399-2-13	BL3-2-13					
399-3-23	BL3-3-23					
399-2-17	BL3-2-17					
399-2-18	BL3-2-18					
399-2-19	BL3-2-19					
399-2-20	BL3-2-20					
399-2-22	BL3-2-22					
399-2-31	BL3-2-31					
399-2-29	BL3-2-29					
399-2-30	BL3-2-30					
399-2-21	BL3-2-21					
399-3-25	BL3-3-25					
399-3-31	BL3-3-31					
399-3-30	BL3-3-30					
399-3-32	BL3-3-32					
399-3-24	BL3-3-24					
399-3-26	BL3-3-26					
399-3-27	BL3-3-27					
399-3-28	BL3-3-28					
399-3-29	BL3-3-29					
399-2-23	BL3-2-23					
399-2-24	BL3-2-24					
399-2-5	BL3-2-5					

BL3-300 Area IFC pumped

IC unpreserved sample

Well Name	Sample ID	F (ug/L)	Cl (ug/L)	SO4 (ug/L)	NO3 (ug/L)	NO2 (ug/L)
399-2-9	BL3-2-9	352	17993	45585	21879	< 250
399-2-10	BL3-2-10	361	18913	47998	22924	< 250
399-2-8	BL3-2-8	353	19142	48560	22004	< 250
399-2-7	BL3-2-7	355	18753	47559	23097	< 250
399-2-11	BL3-2-11	345	18235	46543	23030	< 250
399-2-26	BL3-2-26	359	18673	47141	24134	< 250
399-2-27	BL3-2-27	352	18758	47400	22604	< 250
399-2-28	BL3-2-28	341	18214	44729	22247	< 250
399-2-12	BL3-2-12	355	18667	46752	20840	< 250
399-2-16	BL3-2-16	355	18591	46952	21326	< 250
399-2-15	BL3-2-15	355	18596	47022	21166	< 250
399-2-14	BL3-2-14	355	18120	46333	22677	< 250
399-2-13	BL3-2-13	352	17645	46441	23591	< 250
399-3-23	BL3-3-23	359	17870	44802	21214	< 250
399-2-17	BL3-2-17	352	18451	46023	21331	< 250
399-2-18	BL3-2-18	357	18617	47000	21592	< 250
399-2-19	BL3-2-19	352	18678	47266	21401	< 250
399-2-20	BL3-2-20	338	19106	47733	22251	< 250
399-2-22	BL3-2-22	359	18884	47850	21254	< 250
399-2-31	BL3-2-31	366	18935	46948	21798	< 250
399-2-29	BL3-2-29	339	19027	47664	22794	< 250
399-2-30	BL3-2-30	389	18765	47685	20792	< 250
399-2-21	BL3-2-21	359	18766	47373	21062	< 250
399-3-25	BL3-3-25	350	18417	46746	21662	< 250
399-3-31	BL3-3-31	365	18026	45372	21105	< 250
399-3-30	BL3-3-30	362	17812	46572	24293	< 250
399-3-32	BL3-3-32	305	18298	46586	23561	< 250
399-3-24	BL3-3-24	358	18021	45377	22240	< 250
399-3-26	BL3-3-26	363	18374	45542	22414	< 250
399-3-27	BL3-3-27	367	18173	45706	21656	< 250
399-3-28	BL3-3-28	354	18457	46495	21678	< 250
399-3-29	BL3-3-29	361	18962	47861	22236	< 250
399-2-23	BL3-2-23	363	19119	48090	21668	< 250
399-2-24	BL3-2-24	358	19210	48354	22139	< 250
399-2-5	BL3-2-5	371	19456	49030	21859	< 250

BL3-300 Area IFC pumped

Well Name	Sample ID	PO4 (ug/L)	Br (ug/L)	Temp (degrees C)	Sp. Cond (mS/cm)	dissolved oxygen (mg/L)
399-2-9	BL3-2-9	< 400	< 250	16.9	0.435	8.2
399-2-10	BL3-2-10	< 400	< 250	16.7	0.431	8.1
399-2-8	BL3-2-8	< 400	< 250	16.7	0.438	7.9
399-2-7	BL3-2-7	< 400	< 250	17.2	0.431	7.9
399-2-11	BL3-2-11	< 400	< 250	16.7	0.437	8.2
399-2-26	BL3-2-26	< 400	< 250	18.3	0.443	8.5
399-2-27	BL3-2-27	< 400	267	17.2	0.434	7.9
399-2-28	BL3-2-28	< 400	1276	17.1	0.448	7.7
399-2-12	BL3-2-12	< 400	< 250	16.4	0.430	8.3
399-2-16	BL3-2-16	< 400	< 250	16.2	0.430	8.2
399-2-15	BL3-2-15	< 400	< 250	16.5	0.428	8.3
399-2-14	BL3-2-14	< 400	< 250	16.8	0.439	8.2
399-2-13	BL3-2-13	< 400	< 250	16.8	0.436	8.3
399-3-23	BL3-3-23	< 400	< 250	17.5	0.422	8.5
399-2-17	BL3-2-17	< 400	< 250	16.6	0.430	8.2
399-2-18	BL3-2-18	< 400	343	16.4	0.430	8.3
399-2-19	BL3-2-19	< 400	< 250	16.2	0.433	8.2
399-2-20	BL3-2-20	< 400	< 250	15.9	0.438	8.3
399-2-22	BL3-2-22	< 400	< 250	15.8	0.429	8.5
399-2-31	BL3-2-31	< 400	745	15.7	0.440	7.6
399-2-29	BL3-2-29	< 400	688	16.1	0.443	8.2
399-2-30	BL3-2-30	< 400	< 250	15.5	0.429	7.6
399-2-21	BL3-2-21	< 400	< 250	16.0	0.429	8.4
399-3-25	BL3-3-25	< 400	400	15.8	0.432	8.2
399-3-31	BL3-3-31	< 400	< 250	15.7	0.421	8.4
399-3-30	BL3-3-30	< 400	< 250	16.1	0.436	8.4
399-3-32	BL3-3-32	< 400	2078	15.3	0.445	7.9
399-3-24	BL3-3-24	< 400	302	15.2	0.427	8.2
399-3-26	BL3-3-26	< 400	< 250	14.4	0.427	8.3
399-3-27	BL3-3-27	< 400	< 250	15.0	0.425	8.2
399-3-28	BL3-3-28	< 400	422	15.0	0.434	8.4
399-3-29	BL3-3-29	< 400	< 250	15.4	0.430	8.5
399-2-23	BL3-2-23	< 400	< 250	14.5	0.431	8.5
399-2-24	BL3-2-24	< 400	< 250	14.4	0.434	8.5
399-2-5	BL3-2-5	< 400	< 250	14.2	0.434	8.7

BL3-300 Area IFC pumped

Well Name	Sample ID	pH	ORP (mv)	purge rate
399-2-9	BL3-2-9	7.5	96	L/min for 5 min
399-2-10	BL3-2-10	7.6	78	L/min for 5 min
399-2-8	BL3-2-8	7.6	89	L/min for 5 min
399-2-7	BL3-2-7	7.6	92	L/min for 5 min
399-2-11	BL3-2-11	7.5	98	L/min for 5 min
399-2-26	BL3-2-26	7.5	95	L/min for 5 min
399-2-27	BL3-2-27	7.6	89	L/min for 5 min
399-2-28	BL3-2-28	7.5	96	L/min for 5 min
399-2-12	BL3-2-12	7.7	93	L/min for 5 min
399-2-16	BL3-2-16	7.7	94	L/min for 5 min
399-2-15	BL3-2-15	7.7	95	L/min for 5 min
399-2-14	BL3-2-14	7.5	104	L/min for 5 min
399-2-13	BL3-2-13	7.5	100	L/min for 5 min
399-3-23	BL3-3-23	7.7	91	L/min for 5 min
399-2-17	BL3-2-17	7.7	91	L/min for 5 min
399-2-18	BL3-2-18	7.6	96	L/min for 5 min
399-2-19	BL3-2-19	7.7	94	L/min for 5 min
399-2-20	BL3-2-20	7.6	94	L/min for 5 min
399-2-22	BL3-2-22	7.7	96	L/min for 5 min
399-2-31	BL3-2-31	7.8	90	L/min for 5 min
399-2-29	BL3-2-29	7.5	98	L/min for 5 min
399-2-30	BL3-2-30	7.7	89	L/min for 5 min
399-2-21	BL3-2-21	7.7	89	L/min for 5 min
399-3-25	BL3-3-25	7.7	93	L/min for 5 min
399-3-31	BL3-3-31	7.7	91	L/min for 5 min
399-3-30	BL3-3-30	7.5	99	L/min for 5 min
399-3-32	BL3-3-32	7.5	99	L/min for 5 min
399-3-24	BL3-3-24	7.6	98	L/min for 5 min
399-3-26	BL3-3-26	7.7	98	L/min for 5 min
399-3-27	BL3-3-27	7.7	99	L/min for 5 min
399-3-28	BL3-3-28	7.7	100	L/min for 5 min
399-3-29	BL3-3-29	7.7	90	L/min for 5 min
399-2-23	BL3-2-23	7.8	88	L/min for 5 min
399-2-24	BL3-2-24	7.7	88	L/min for 5 min
399-2-5	BL3-2-5	7.7	90	L/min for 5 min

Appendix 4: 300-FF-5: Polyphosphate Infiltration Schedule

(Preliminary schedule obtained from Dawn Wellman that is subject to change)

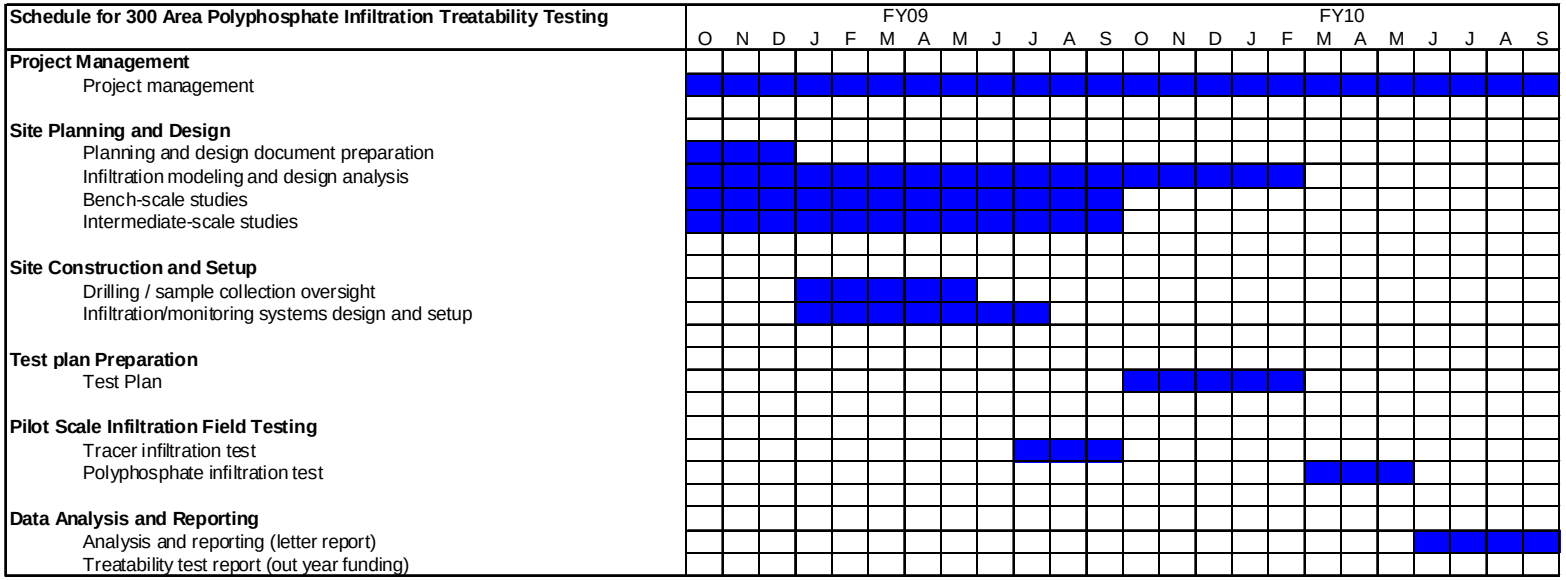

Appendix 5: The Method of Anchored Distributions (MAD)

Our proposed approach includes the following elements: (1) a general statistical theory; (2) a systematic division of the theory into distinct modules, and (3) a systematic data classification scheme that links the statistical elements with the computational tools needed for implementation. We will build a platform around independent modules that can be modified individually without compromising the others. Decisions on assumptions to be implemented or computational tools to be employed are left to the user's discretion. We refer to our approach as the Method of Anchored Distribution, or by the acronym MAD.

We will classify the various kinds of data useful for inverse modeling into two broad types and assimilate each particular dataset in a systematic fashion according to its type in this classification. The two data types relate to anchors in different ways, and play different roles in determining the anchored distributions. In this systematic procedure, simplifying assumptions are easy to implement, and powerful numerical models can be used with just simple modifications.

Data Classification

We consider a spatial variable $Y(\boldsymbol{x})$, where Y is defined continuously in space and x denotes the space coordinate. We denote the entire field in the model domain by $\widetilde{Y}$. Given data Z that relate to the field in some way, the goal is to derive a conditional distribution of the field, $p\left(\widetilde{Y}\middle|Z\right)$, and provide random samples of this distribution.

In practice, the relation between the available data Z and the variable Y ranges from direct measurements to empirical relations, to involved functions, representing natural processes, and formulated using numerical models. We propose a systematic classification of all relevant data based on an abstraction of the data-to-unknown relation. Datasets are then assimilated systematically according to their types in this classification.

Type-A Data: The values of Y at a finite set of unambiguously-defined locations. Type-A data can be written as: $z_a=y(\boldsymbol{x}_a)+\varepsilon$, where ε are zero-mean errors. Uncertainties in the data are described by a joint (Gaussian or non-Gaussian) distribution of ε. These data may be direct measurements of Y, or measurements of covariates that can provide point Y values by empirical relations, i.e., statistical regression. Hence, Type-A data can include direct and indirect measurements. These relations between z_a and Y may be stationary or non-stationary. In hydrogeological studies with Y being the hydraulic conductivity, examples of covariates include grain-size distributions, core-scale geophysical properties, and slug-tests that can be interpreted on a sufficiently small support.

Type-B Data: This category covers all data that are not of Type-A. Type-B data can be written as: $z_b = \mathrm{M}\left(\widetilde{y}\right)+\varepsilon$, where M is a known function of the Y field. The function M can be given analytically or numerically. This type of data represent quantities that are influenced by all the Y values in a spatial domain, be it part or the entirety of the model domain. In other words, type-B data are the outcomes of non-local processes (or field functions). Typical examples for

Type-B data include non-local processes, including head measurements in pumping tests and concentration measurements in tracer tests. In such examples, the function *M* is represented by a numerical model that computes the outcomes of the experiments given any conductivity field. The function *M* is also called a forward model in the context of inversion. The forward process may be steady-state or transient. With this classification, we will be able to present a framework for inverse modeling that is independent of the source of data or the modeling tools associated with it.

Using Anchors for Inverse Modeling

A common goal of inverse modeling is to create conditional simulations of the field $\widetilde{Y}$, which in turn can be used to predict physical processes of interest. Conditional simulations start with a geostatistical description of the general statistical behavior of the unknown field. Such a description, sometimes referred to as a Space Random Function (SRF), may include "structural" parameters such as the expected value of *Y* and its covariance. It is important because it provides a parsimonious description of the field $\widetilde{Y}$. We recognize that the parameters of the SRF need to be inferred from all available data. We also recognize that conditioning on data cannot be achieved solely by accurate estimates of the structural parameters of the SRF. The SRF provides unconditional simulations of the field $\widetilde{Y}$. These simulations need to be further conditioned on the data via "controlling points" in the field.

We will refer to these controlling points as ***anchors***. Conceptually, the structural parameters describe regular trends and spatial associations, whereas the anchors capture local features that actually exist in reality.

One may immediately identify anchors with type-A data, which provide values of *Y* at specific locations. Indeed, Type-A data identify "measured" anchors. These anchors are collocated with the measurements, and are in the form of *Y* values plus measurement and modeling (regression) errors.

Anchors are more than type-A data by another name. For type-B data, we "plant" a number of anchors in the field as agents for these indirect data. We call them "inverted" anchors. These anchors are intended to capture the information in the Type-B data that is relevant to the *Y* field. This is achieved by transforming the type-B information into the form of *Y* values at the chosen anchor locations, drawing upon our knowledge of the random field of *Y* and the non-local process *M* that generates the observed data (see Section 3). The result of this transformation will be distributions of the *Y* values at the anchors. Subsequently, simulations conditioned on these anchors are in effect conditioned on the type-B data.

MAD views both structural parameters and anchors as parameters of the model. Denote the vector of structural parameters by θ and the vector of anchor values by υ, the goal is to define the joint statistical distribution of the vector $\Theta=(\theta,\upsilon)$.

The parameters in the vector $\Theta=(\theta,\upsilon)$ are model devices that establish the connections between the unknown continuous field $\widetilde{Y}$ and the data $z=(z_a, z_b)$. The SRF described by θ characterizes $\widetilde{Y}$ statistically. The anchors υ provide information on local features of the

particular realization of the field that is observed. These local features are respected, in the sense of conditioning, in each of the realizations of the *Y* field. The anchors "anchor" the realizations with local information.

Anchors can assume various forms, depending on the measurements or physical processes they represent. Type-A data provide anchors, collocated with the measurement locations, in the form of *Y* values plus errors, representing measurement and modeling (e.g., regression) errors. For Type-B data, MAD will create multiple anchors, with the *Y* values at each anchor represented by a statistical distribution that intends to reflect spatial variability *as well as* measurement and modeling errors.

The multiple anchors associated with Type-B data are intended to capture the Type-B information relevant to *Y*. For example, if the Type-B information is in the form of breakthrough curves from a tracer experiment, we will have a network of anchors in the form of conductivity values that are physically and statistically in agreement with the observations. The Physical agreement would be obtained from physically-based modeling, using the model *M*, whereas the statistical agreement will follow the statistical formulation of the inference problem. The extent of the anchor network would depend on the spatial extent of the experiment and on the form of averaging used to compute the breakthrough curve. These anchors, once inferred, will be used for inference of the *Y* field as well as for conditioning realizations of the *Y* field. In order to generate conditional simulations, we will need to obtain the distribution of the model parameters based on the data, that is, conditional simulations of $p(\boldsymbol{\theta}, \boldsymbol{\upsilon}|z)$.

Type-A anchors are collocated with the actual measurements. For Type-B data we will create anchors and transfer information from data to anchors. Type-A data will thus provide either *measured* or *regressed* anchors or anchors by *regression,* whereas Type-B data provides *inverted* anchors or anchors by *inversion.* The inversion with Type-B data thus results in a transformation of information. This procedure requires knowledge of the random field of *Y* as well as of the process *M* that generates the observed data. The field *Y* and the process *M* together provide the link between the observations and the anchor values.

MAD is similar to the pilot point method in the sense that both use implanted points as a bridge for moving information from Type-B data to the field $\widetilde{Y}$. However, this is where the similarity ends. MAD is a totally different concept, primarily because it avoids the problematic optimization step used by the pilot point method. Anchors are model parameters to be estimated; in a Bayesian approach the estimation provides their distribution. They are not intermediate devices to help with optimization. As such, they do not alter the statistical distributions of the SRF through subjective considerations (e.g., optimization).

A Schematic Presentation of MAD

In this section we give a schematic presentation of MAD in order to show how it accommodates the principles discussed in earlier sections. Denote the Type-A and Type-B data by z_a and z_b, respectively, where z_a and z_b are general symbols for the data, and can be either single values or distributions. In addition, denote measured anchors by υ_a and inverted anchors by υ_b. The

corresponding anchor locations are $\boldsymbol{x}_a$ and $\boldsymbol{x}_b$. All anchors are collectively denoted by $\boldsymbol{\upsilon}$ at locations $\boldsymbol{x}_\upsilon$. With this notation, we can state the joint distribution of the structural parameters and the anchors as follows:

(1)

$$\begin{aligned} p(\boldsymbol{\theta}, \boldsymbol{\nu} \mid \boldsymbol{z}_{\mathrm{a}}, \boldsymbol{z}_{\mathrm{b}}) &\propto p(\boldsymbol{\theta}, \boldsymbol{\nu} \mid \boldsymbol{z}_{\mathrm{a}}) \times p(\boldsymbol{z}_{\mathrm{b}} \mid \boldsymbol{\theta}, \boldsymbol{\nu}, \boldsymbol{z}_{\mathrm{a}}) \\ &= p(\boldsymbol{\nu}_{\mathrm{a}} \mid \boldsymbol{z}_{\mathrm{a}}) \cdot p(\boldsymbol{\theta} \mid \boldsymbol{\nu}_{\mathrm{a}}, \boldsymbol{z}_{\mathrm{a}}) \cdot p(\boldsymbol{\nu}_{\mathrm{b}} \mid \boldsymbol{\theta}, \boldsymbol{\nu}_{\mathrm{a}}, \boldsymbol{z}_{\mathrm{a}}) \times p(\boldsymbol{z}_{\mathrm{b}} \mid \boldsymbol{\theta}, \boldsymbol{\nu}, \boldsymbol{z}_{\mathrm{a}}) \\ &= p(\boldsymbol{\nu}_{\mathrm{a}} \mid \boldsymbol{z}_{\mathrm{a}}) \cdot c(\boldsymbol{\nu}_{\mathrm{a}})\, p(\boldsymbol{\theta})\, p(\boldsymbol{\nu}_{\mathrm{a}} \mid \boldsymbol{\theta}) \cdot p(\boldsymbol{\nu}_{\mathrm{b}} \mid \boldsymbol{\theta}, \boldsymbol{\nu}_{\mathrm{a}}) \times p(\boldsymbol{z}_{\mathrm{b}} \mid \boldsymbol{\theta}, \boldsymbol{\nu}) \end{aligned}$$

In this formula, p($\boldsymbol{\theta}$) is the prior distribution of $\boldsymbol{\theta}$ and $c(\upsilon_a)$ is a normalizing constant. An important simplification employed in (1) is that the information contained in z_a is captured by the corresponding anchors υ_a, such that whenever they (υ_a) appear as conditions, z_a can be dropped off from the conditioning terms, because the information it carries is already contained in υ_a.

Equation (1) is represented schematically in **Figure 1**. This figure shows the modular structure of the MAD approach. There are three modules, or blocks, in MAD, labeled as Block I, II and III, respectively.

Block I is focused on the Type-A data. It computes the joint distribution of structural parameters ($\boldsymbol{\theta}$) and anchors ($\boldsymbol{\upsilon}$)**,** based on the Type-A data as well as any prior knowledge on the parameter vector $\boldsymbol{\theta}$. There is a wide range of ideas on how to deal with prior information. One concept that has gained some acceptance in hydrology is the minimum relative entropy. There are other concepts that can be used in this context, such as the Reference Prior method. The important point is that the approach to modeling the prior is not hard-wired into MAD.

The output of Block I is the conditional distribution $p(\boldsymbol{\theta}, \boldsymbol{\upsilon} \mid z_a)$, which is the posterior pdf of $\boldsymbol{\theta}$ with respect to z_a. If we view z_b as the "main" data, then this provides a prior of ($\boldsymbol{\theta}, \boldsymbol{\upsilon}$) for the Bayesian analysis of z_b in Block II.

Block II incorporates Type-B data through the likelihood function $p(z_b \mid \boldsymbol{\theta}, \boldsymbol{\upsilon})$. When combined with the Block I product, $p(\boldsymbol{\theta}, \boldsymbol{\upsilon} \mid z_a)$, where $\boldsymbol{\upsilon}$ are the anchor values at locations $\mathbf{x}_{\boldsymbol{\upsilon}}$, it yields the posterior $p(\boldsymbol{\theta}, \boldsymbol{\upsilon} \mid z_a, z_b)$. The likelihood function $p(z_b \mid \boldsymbol{\theta}, \boldsymbol{\upsilon})$ is linked to observations by a forward model *M*, through the relationship $z_b = \mathrm{M}(\tilde{y}) + \varepsilon$. This relationship is comprised of two elements: random field generation and forward simulation. The joint distribution of $\boldsymbol{\upsilon}$ and $\boldsymbol{\theta}$ from Block I is used to generate conditional realizations of the *Y* field, $\tilde{y}$. With each realization, the forward *M* generates the Type-B data that would then be compared with Type-B observations in order to evaluate the likelihood function. Several forward models can be employed simultaneously, depending on the number of different Type-B data employed in the inversion process. Examples for *M* functions include flow models, solute fate and transport models and geophysical models.